OPEN FILE RECORD

OFR 20

THE UNDERWATER LIGHT CLIMATE OF BILLABONGS OF THE ALLIGATOR RIVERS REGION, NORTHERN TERRITORY (FINAL REPORT)

prepared by

T.D. Walker[1], J.T.O. Kirk[2] and P.A. Tyler[1]

[1]Department of Botany, University of Tasmania, Hobart
[2]CSIRO Division of Plant Industry, Canberra

3 May 1982

Supervising Scientist for the Alligator Rivers Region

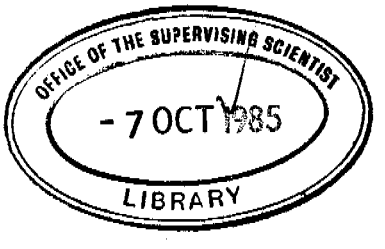

SSR 46

THE UNDERWATER LIGHT CLIMATE OF BILLABONGS OF THE ALLIGATOR RIVERS REGION, NORTHERN TERRITORY

by

T. D. Walker[1]

J. T. O. Kirk[2]

and

P. A. Tyler[1]

[1]Department of Botany,
University of Tasmania, Hobart.

[2]C.S.I.R.O. Division of Plant Industry,
Canberra.

CONTENTS

SUMMARY

The distribution of photosynthetically-active radiation (PAR) underwater has been investigated for a number of Alligator Rivers billabongs, together with the physical, chemical and biological conditions of the waters which determine this underwater light climate. Of the three parameters most likely to affect light conditions, namely dissolved organic colour (gilvin), turbidity and chlorophyll, turbidity was shown to be the dominant influence. Gilvin concentrations were always low and only seldom did chlorophyll modify the spectral properties of the underwater PAR. The presence of finely-divided sediments, turbidity, so characteristic of many of the billabongs, specifies a blue and green-deficient spectrum and a shallow euphotic zone. Laboratory studies indicate that turbidity exerts its influence through absorption rather than scattering. The greater the turbidity, the greater the limitation of PAR to a narrow band of red wavelengths. The resulting spectrum resembles closely that of non-turbid but highly humic waters in other parts of the world. In the clearest billabongs there is a transmission peak in the yellow, as in oligotrophic lakes and in the ocean.

In most billabongs, turbidity increases markedly through the Dry with consequent contraction of both the spectral bandpass of PAR and the euphotic depth. Other billabongs show capricious fluctuations in optical conditions. Noarlanga is unique in that its clarity improves as the Dry progresses. For most of the billabongs the Wet is a time of fluctuating water clarity, with the euphotic depth reaching an annual maximum at the Dry/Wet interchange.

There was high correlation between Secchi depth and the euphotic depth determined from PAR measurements. There was no relationship between Secchi depth and chlorophyll concentrations and the Secchi disk cannot

be used as an indicator of trophic conditions as it often is elsewhere in the world. Nonetheless, with its close correlation with euphotic depth and with its simplicity and ease of operation, it becomes an excellent routine monitoring tool if used with care.

1. INTRODUCTION

Light is a major limiting factor for photosynthesis, and to understand primary production in any given water body, it is necessary to measure, at appropriate depths, the intensity of photosynthetically-active radiation (henceforth PAR). PAR is that waveband of solar radiation which can be used for photosynthesis by plants. Generally, it is taken to be from 400 to 700nm, roughly corresponding to the spectrum of visible light. Additional information on the underwater light field is obtained if the spectral distribution of the penetrating radiation can be measured. Since the attenuation of sunlight with depth in natural waters is brought about by a combination of absorption and scattering processes, characterization of these optical properties of the water is necessary for an understanding of the underwater light climate.

As part of a comprehensive limnological investigation of billabongs (small riverine lakes) in the uranium-rich Alligator Rivers Region, Northern Territory, a study of both the underwater light field available for photosynthesis, and the optical properties of the water which determine this light field, has been carried out. Characterization of the former was accomplished *in situ*, with attendant measurements of turbidity, phytoplankton chlorophyll and gilvin (dissolved yellow humic substances) being made in the nearby Jabiru laboratory of the Office of the Supervising Scientist. Further examination of the optical properties of water from seven billabongs was carried out in the Canberra laboratories of the C.S.I.R.O. Division of Plant Industry.

This report is the second in a series. The first report on stratification behaviour of the billabongs (Walker, Waterhouse and Tyler, 1982), contains geographical, climatic and hydrological details of the study area and descriptions of the billabongs, which are summarised in Figure 1.1 and Table 1.1.

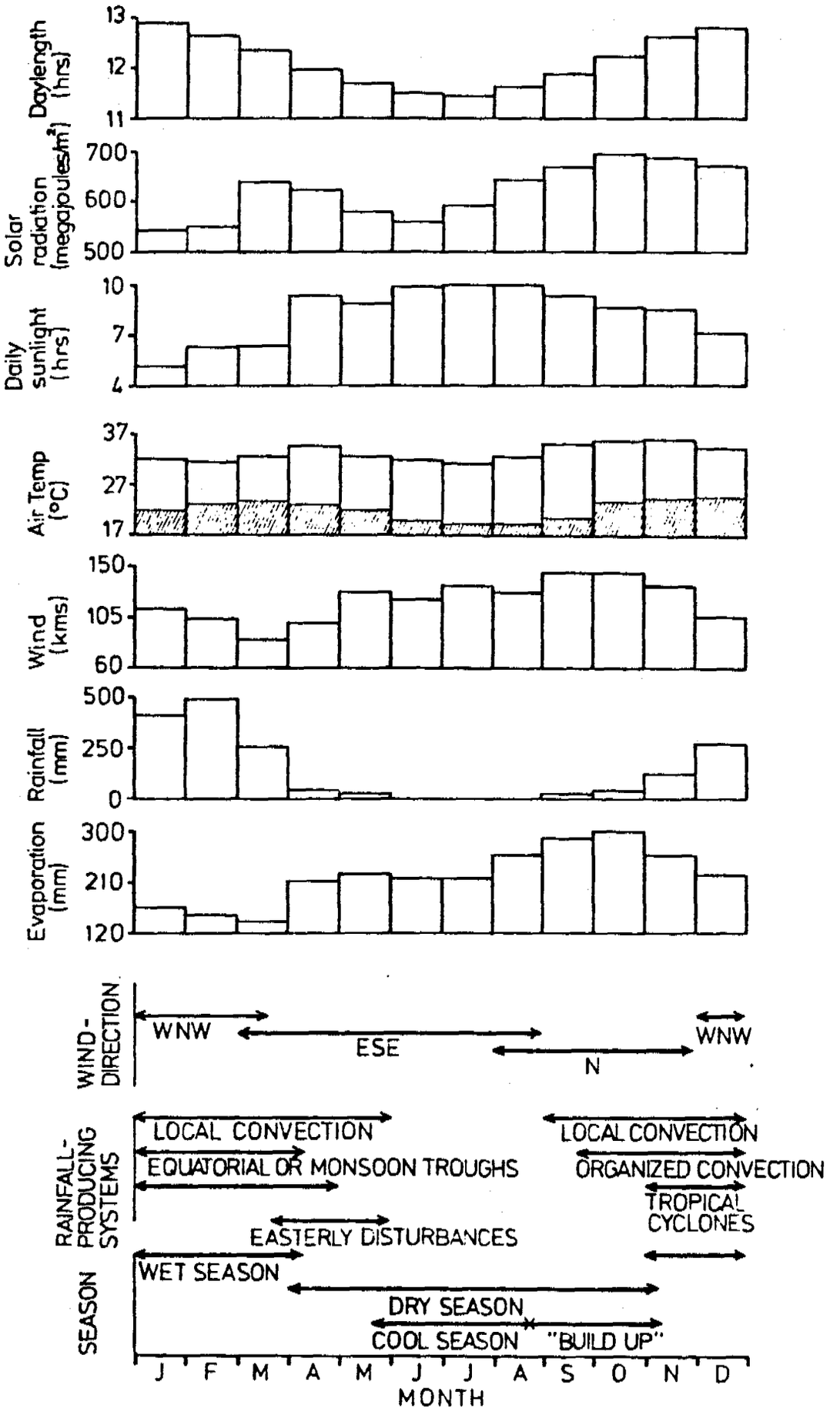

Fig 1.1. Synopsis of seasonal meteorological attributes of the Alligator Rivers Region. (After Walker, Winterhouse and Tyler, 1982).

Table 1.1 A classification of the billabongs investigated in this study. (After Walker, Waterhouse and Tyler, 1982).

Billabong Classification	Catchment	Billabong Name
Channel	Magela	Mudginberri
	Nourlangie	Noarlanga
" /Escarpment rockpool	Magela	Bowerbird
" /Backflow	Baroalba/ Magela	Goanna
" /Floodplain	Magela	Island
	Nourlangie	Kulukuluku
Backflow	Magela	Georgetown
		Gulungul
Floodplain	Magela	Ja Ja
		Leichhardt
		Jabiluka
		Nankeen

2. THEORETICAL CONSIDERATIONS

2.1 CHARACTERISTICS OF THE INCIDENT LIGHT FIELD

The intensity, or irradiance, of a light beam incident on a water surface is generally expressed in terms of energy units (e.g. ergs per second, calories per second, or watts). However, a light beam can also be considered as a stream of particle-like "wave packets" or quanta. The amount of radiant energy in one quantum is inversely proportional to the wavelength of that energy, so that a quantum of short wavelength (e.g. blue light) contains more energy than a quantum of long wavelength (e.g. red light). Put the other way around, a given amount of radiant energy of long wavelength will contain more quanta than an equivalent amount of energy of short wavelength. Since photosynthesis is a photochemical process and, as such, one absorbed quantum of light is as good as another regardless of wavelength*, a given quantity of light energy is of more value if it contains red quanta rather than blue. It is apparent, then, that in the context of photosynthesis, it is of more benefit to express irradiance in quantum units - quanta per square centimetre per second.

Under clear, sunny conditions, about 80% of the incident light is parallel, direct from the sun (Kirk, 1977b), at an angle determined by the solar altitude. The other 20% is diffuse, principally blue light from the sky, but this proportion increases in hazy or overcast conditions as a result of increased atmospheric scattering (Kirk, 1977b). The spectral distribution of sunlight varies with the solar altitude, there being relatively more red light than blue when the sun is low in the sky (Jerlov, 1976) because of differential absorption and scattering in the atmosphere.

* Of course, wavelength of the light is important to the extent that it can greatly affect the probability that a quantum of light will be absorbed.

As light strikes a water surface, some of it is lost by reflection at the air-water interface, and, to a lesser extent, by back-scattering from subsurface particles and bubbles (Strickland, 1958; Cox, 1974; Jerlov, 1976). Losses from these sources may range from a few per cent at noon of a fine, calm day in the tropics, to over 30% under conditions of strong winds, overcast sky and turbulent water. Light penetrating the water surface is refracted downwards, so that the apparent solar altitude is α, where α is related to the real solar altitude α' by the relation:-

$$\cos\alpha = \frac{1}{1.33} \cos\alpha' \quad \ldots\ldots\ldots\ldots (1)$$

Consequently just below a calm water surface under conditions of direct sunlight, most of the light will be parallel, at an angle α to the horizontal.

2.2 INHERENT OPTICAL PROPERTIES OF NATURAL WATER BODIES .

Following penetration of a natural water surface, the light is affected in two fundamental ways. Firstly, some of the light is converted from radiant energy to some other form such as heat or photosynthetic energy, a process known as absorption, and secondly, the directional quality of the light, or its angular distribution, is altered as a result of scattering within the water. These effects are described and quantified by three of the so-called "inherent optical properties" of water (Jerlov, 1976; Kirk, 1977b), namely:-

1. The absorption coefficient (a), which quantifies the proportion of incident light which is absorbed.
2. The scattering coefficient (b), which quantifies the proportion of incident light which is scattered.
3. The volume scattering function $\beta(\theta)$, which describes the angular distribution the light scattered from the point of incidence of a light beam. In most natural waters, the volume

scattering function is in a forward direction, within a narrow angle relative to the incident light beam (Jerlov, 1970, 1976). In any natural water, the inherent optical properties are determined by a number of different factors, some contributing to absorption alone, and others to both scattering and absorption.

2.3 COMPONENTS OF NATURAL WATERS CONTRIBUTING TO ABSORPTION

Natural water can be considered as a four-component filter comprising pure water, dissolved organic colour (gilvin), phytoplankton, and suspended non-living particles (tripton). These four components will be examined in turn.

1. Although pure water absorbs light throughout the visible spectrum, it acts as a monochromator for blue light (Jerlov, 1976) by its preferential absorption of the longer (red) wavelengths.
2. Dissolved yellow humic substances in the water (= gilvin (Kirk, 1976)), preferentially absorb in the blue end of the spectrum. Gilvin is a complex mixture of products of plant decomposition, mostly polymerised oxidised phenolics (Kirk, 1977b). The gilvin content of any given water may exhibit considerable seasonal or erratic variation due to fluctuations in rainfall or runoff, or to changes in land use in the catchment.
3. Phytoplankton may contribute significantly to light absorption in productive waters. The type of photosynthetic pigments present determine the effect on the spectral distribution of underwater light, whilst the size and shape of the colonies or cells will influence the quantity of light absorbed per unit biomass (Kirk, 1975).
4. The contribution of tripton-mineral particles, plant debris etc. - to the total absorption coefficient is difficult to

determine given the difficulty of distinguishing in the laboratory the effects of intense scattering and those of true absorption by the scattering particles (Kirk, 1979). One effect of such particles is that by scattering the light they increase its pathlength and therefore also its chances of being absorbed by gilvin, phytoplankton or water itself within a given depth. However, in highly turbid waters, tripton may absorb most of the quanta, preferentially absorbing shorter (blue) wavelengths (Kirk, 1980b).

2.4 COMPONENTS OF NATURAL WATERS CONTRIBUTION TO SCATTERING

The main contributors to scattering are the suspended particles; primarily mineral particles from soil erosion, but also plankton (Jerlov, 1976; Kirk, 1977b). Molecular scattering by water itself plays a relatively small part, even in waters of very low turbidity. Scattering by particles greater than about 1μm in diameter (including phytoplankton) is more or less independent of wavelength (Jerlov, 1976), though for smaller particles a certain amount of preferential scattering of the shorter wavelengths may occur (cf. Halldal and Halldal, 1973). Most particulate scattering is at small angles, but the amount of high angle scattering, which is also wavelength selective, increases as the particulate size approaches the wavelength of light (<1μm).

2.5 THE VERTICAL ATTENUATION COEFFICIENT FOR PAR

Monochromatic light is absorbed in an exponential manner by clear, non-scattering water. Linear increases in concentration of pure coloured substances in pure water also produce exponential absorbtion of monochromatic light. The penetration of light under these conditions is given by the Beer-Lambert Law. Thus,

$$I_z = I_o e^{-K_\lambda z} \quad \ldots\ldots(1)$$

or

$$I_z = I_o 10^{-E_\lambda z} \quad \ldots\ldots(2)$$

where I_z is the intensity at depth z metres

I_o is the surface intensity, and

K_λ and E_λ are respectively the natural logarithm and base 10 logarithm vertical attenuation coefficients for light of wavelength λ in the water; $K_\lambda = 2.303\ E_\lambda$.

Rearrangement of equation (2) gives:-

$$E_\lambda = \frac{1}{z} \log_{10} \left(\frac{I_o}{I_z}\right) \text{.....(3)}$$

Thus a plot of $\log_{10} \left(\frac{I_o}{I_z}\right)$ against z will have a slope of E_λ. Alternatively, a plot of $\log_{10} \left(\frac{I_z}{I_o}\right)$ against z will have a slope of $-E_\lambda$. Using base 10 logarithms instead of natural logarithms can be of advantage since a value of $E_\lambda = 1$ corresponds to a 10% transmission per metre depth, $E_\lambda = 2$ corresponds to a 1% transmission per metre depth, and so on (Kirk, 1977b).

Although the Beer-Lambert Law applies to monochromatic light in clear, non-scattering water, and though different wavelengths are attenuated at different rates in any given water, Kirk (1977a) indicates that, in practice, the attenuation of the whole PAR spectral band approximates equations (1) and (2). Thus:-

$$Q_z = Q_0 10^{-Ez} \text{.....(4)}$$

where Q_z is the irradiance for the whole photosynthetic waveband at depth z metres

Q_0 is the irradiance at the surface, and

E is the (base 10 logarithm) vertical attenuation coefficient for PAR. K (Natural logs) = 2.303E.

I and E have units m^{-1}.

The depth at which light intensities are just sufficient for a day's photosynthesis to balance a day's respiration is known as the compensation level, or euphotic depth. A value of 1% of surface irradiation is commonly used as the compensation intensity. By rearranging equation (4) and substituting values we can calculate the euphotic depth, z_{eu}.

Thus $$E = \frac{1}{z} \log_{10} \left(\frac{Q_0}{Q_z}\right) \quad \ldots\ldots\ldots\ldots\ldots (5)$$

and $$z_{eu} = \frac{1}{E} \log_{10} \frac{100}{1}$$

$$= \frac{2}{E} \quad \ldots\ldots\ldots\ldots\ldots\ldots\ldots (6).$$

For clear waters under direct sunlight, E is dependent to some extent on solar altitude, because of the shorter path light travels through the water at high solar altitudes, but in turbid waters, the directional quality of the light is quickly lost with increasing depth, and there is less dependence on E on solar altitude. Nevertheless, time of measurement should be specified when quoting values of E.

2.6 REFLECTANCE

In addition to the downwards penetration of light, there is always a much smaller flux of quanta in an upwards direction, originating from multiple scattering of the incident light beam. This upwards quantum irradiance is also available for photosynthetic utilization. The proportion of upward to downward irradiance, denoted as the reflectance, R, (Jerlov, 1976; Kirk, 1977a), provides some indication of the light scattering characteristics of the water. Thus:-

$$R = \frac{Q_u}{Q_d} \quad \ldots\ldots\ldots\ldots (7)$$

where R is the reflectance

Q_u is the upward irradiance, and

Q_d is the downward irradiance.

Reflectance increases initially with increasing depth as the angular distribution of the light within the water becomes proportionally enriched at lower angles to the horizontal - a cumulative result of multiple scattering of the downwelling quanta. Eventually the angular distribution ceases to change with depth, at which stage it is known as the asymptotic radiance distribution, and is characterised by a constant reflectance

known as the asymptotic reflectance, R_a. In highly scattering waters, R_a is reached at relatively shallow depths.

3. METHODS

Intensity of downwelling PAR in the range 400-700nm was measured at various depths with a Lambda Li-Cor LI-185 (1978-79) or Li-188 (1980-81) quantameter combined with the LI-192S underwater quantum sensor (Fig. 3.1). The vertical attenuation coefficients for downwelling irradiance, E_d (base-10 logs) and K_d (natural logs) were calculated by plotting $\log_{10}(\frac{Q_z}{Q_0}.100)$ (= $\log_{10}(\%\ Q_0)$) against z giving a line of slope $-E_d$ (see section 2.5); then $K_d = 2.303\ E_d$. The plots of $\log_{10}(\%\ Q_0)$ against $\frac{z}{z_m}$ are illustrated for Jabiluka only (Fig. 4.10-1 in section 4.10). For other billabongs, the derived E_d values are tabulated. The depth of the euphotic zone (z_m) was calculated using equation (6) of section 2.5. Upwelling irradiance was measured by reversing the sensor. Reflectance, R, (upwards over downwards irradiance), was determined for the midpoint of the euphotic zone ($=R_{(z_m)}$, where z_m = 10% Q_0).

Transparency was measured with a 25 cm black and white quartered Secchi disk. Turbidity was measured in the Jabiru laboratory with a Hach 2100 turbidimeter, which gives a measure of the proportion of light scattered by the water at right angles to the incident beam. Phytoplankton chlorophyll was determined by filtration of samples through GF/C glass fibre filters, followed by spectrophotometric analysis of either acetone extracts (Jeffrey and Humphrey, 1975) (Jabiru laboratory) or methanolic extracts (Talling, 1969) (Canberra laboratory).

The natural colour of freshwaters, caused by dissolved organic acids (gelbstoff), has traditionally been measured with a colorimetric comparator against a platinum standard, the Hazen scale (APHA 19th). Kirk (1976) introduced the term gilvin to refer to organic colour and recommended as a

more precise measure of its concentration, the optical absorbance of the filtered sample (0.22μm pore size) at 440nm ($=G_{440}$, m^{-1}). Good correlation between the two methods was found for Tasmanian waters (... and Tyler, unpublished data) and for this study the latter was adopted.

The absorption spectra of the particulate and soluble fractions (the material retained, and not retained, respectively, by a 0.22μm filter) of the water samples were measured with an integrating sphere spectrophotometer, and the absorption coefficients (as defined by I.A.P.S.O., 1979) due to these components in the original water body calculated, as described previously (Kirk, 1976; 1980). The total absorption spectra of the water due to all components were, as before (Kirk, 1981a), obtained by adding, at each wavelength, the absorption coefficients due to particulate and soluble colour to the value of the coefficient for pure water, taken from the literature (Morel and Prieur, 1977). Calculation of the proportion of the absorbed quanta that are captured by the individual absorbing components was carried out in the manner described previously (Kirk, 1976; 1980).

Spectral distribution of downward quantum irradiance was measured at various depths with a Techtum QSM 2500 submersible quantaspectrometer (Fig. 3.1) which scans between 400 and 740 nm in either direction. The sensor was lowered in a waterproof housing from a derrick projecting about 1.5 m outwards from the side of the boat, and the spectral distribution of quantum flux recorded on a constant speed chart recorder.

Kirk (1979) and Steane (1979) encountered an apparent hysteresis effect in the resultant quantum irradiance vs wavelength curves plotted from scans in the 400→740 direction compared with scans in the opposite direction. Examination of the supposed "mirror image" traces showed that whilst the spectrometer wavelength indicator needle correctly indicated the start of each scan, it reached the other end of the wavelength scale some time before the quantum output had ceased to operate. Kirk (1979)

ensured any error remained constant by scanning in the 400→740 nm direction only. However Steane (1979) rectified the situation by doing mirror image scans at each depth and then superimposing the charts, face to face, so that the two traces coincided. The start of one run could then be marked on the opposing chart as the finish of the other. This was the method adopted here.

From among the depths at which spectral distribution scans were made, those depths approximating to Qo, 50%Qo, 10%Qo (z_m) and 1%Qo (z_e)* were chosen for plotting. The attenuation spectrum of a billabong (= spectral distribution of vertical attenuation coefficient) was determined at 10 nm intervals from the traces for those depths where all PAR wavelengths were present (i.e. the upper part of the euphotic zone).

4.0 FIELD RESULTS

The light transmission characteristics of the waters of twelve billabongs have been studied. In general, measurements have been confined to the dry season, although a few observations from the wet are reported. In addition, diurnal variation of the incident light field was investigated on one occasion. Since water clarity in the billabongs presents a continuum, both geographically and temporally, for ease of reporting, the billabongs have been assigned a position on this continuum on the basis of their vertical attenuation coefficients in May/June.

The standard method for measurement of colour (Anon. 1974) recommends centrifugation to remove turbidity. Kirk (1976), on the other hand, recommends filtration through 0.22 μm membranes for his G_{440} measurement. Throughout 1979, 0.22 μm membranes were used but their slow filtration rates made analyses tedious and time consuming, often involving sequential prefiltration and frequent changing of expensive membranes. In addition, centrifugation does not totally clear the supernatent of very finely divided clay particles. For this reason, filtration through the faster

* as determined by the Li-Cor quantameter.

Figure 4.0-2 shows how important the choice of filter pore size can be in the measurement of G_{440} or any other absorbance measurement.

0.45 µm membranes was later adopted.

Since any residual particulate material would affect the G_{440} measurement, the performance of the various membranes was compared. Figure 4.0-1 shows that in May 1979, for all billabongs except Georgetown, the 0.45 µm membrane was adequate. For Georgetown, however, the 0.22 µm filter removed greatly more suspended material than the 0.45 µm filters, but in order to reduce the turbidity to levels achieved by 0.45 µm filter in other billabongs, an 0.1 µm filter was necessary. From 1980 onwards G_{440} was measured only for those billabongs for which 0.45 µm filters were satisfactory.

At the time of the May 1979 measurements Jabiluka and Gulungul were not noticeably turbid (Fig. 4.0-1). Later in the year, however, turbidity in these, and some other, billabongs may exceed the May 1979 value for Georgetown and then the 0.45 µm filters would be inadequate. Apparently, major increases in turbidity in these billabongs during the Dry are brought about by very finely divided material (<0.45µm). It is simple, from visual observation alone, to know which billabongs carry these fine suspensions and on this basis the billabongs were divided into two groups, turbid and non-turbid (Table 4.0.1). This division coincides in large measure with the classification of sediment type by Hart and Thomas (1981).

4.1 The incident light field

The characteristics of the incident light field were examined on one day (27/6/79); a day of clear blue skies with no signs of cloud, heat or smoke haze. Measurements commenced mid-morning and ceased at sunset.

Figure 4.1-1, depicting the intensity of PAR over the seven and a half hour study period, indicates that maximum intensity was reached between 1230 and 1300 hours, about the time of maximum solar altitude. The situation shown is one of rapid change in intensity for most of the solar day, except for a two hour period of little change around the daily maximum.

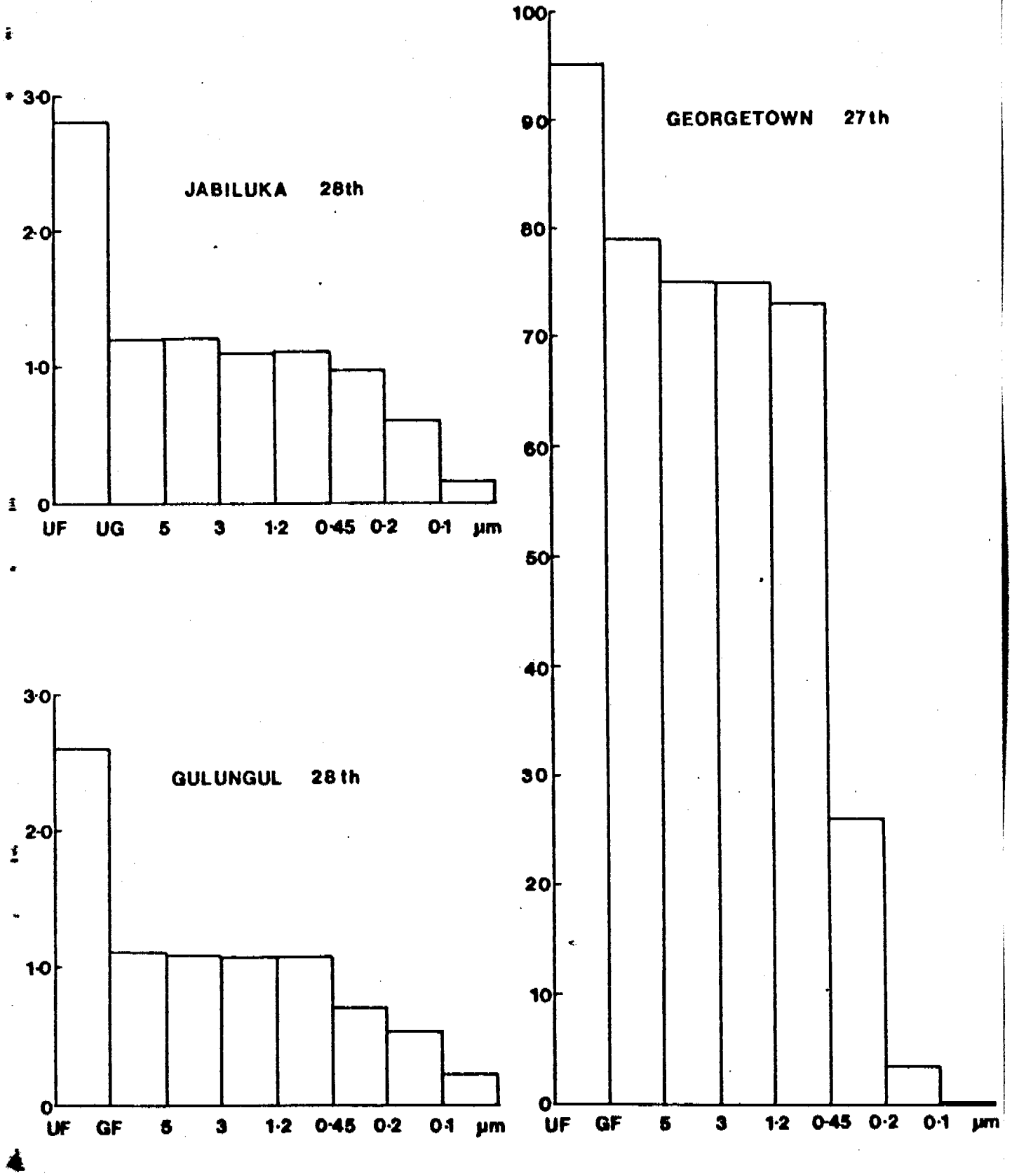

Fig. 4.0.1 The effect of sequential filtration, through filters of various pore sizes, on turbidity values for selected billabongs, May 1979.

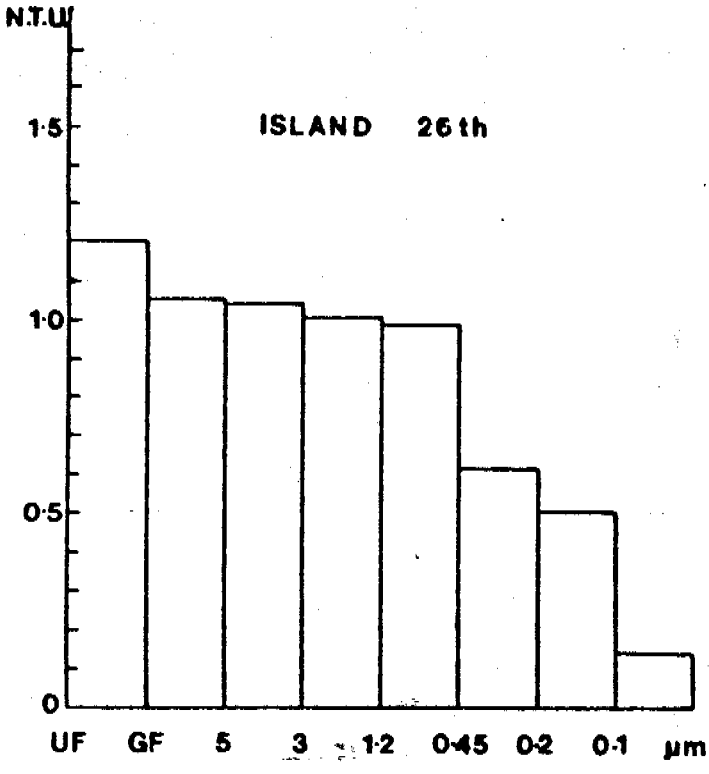
N.T.U
1·5
1·0
0·5
0
ISLAND 26th
UF GF 5 3 1·2 0·45 0·2 0·1 µm

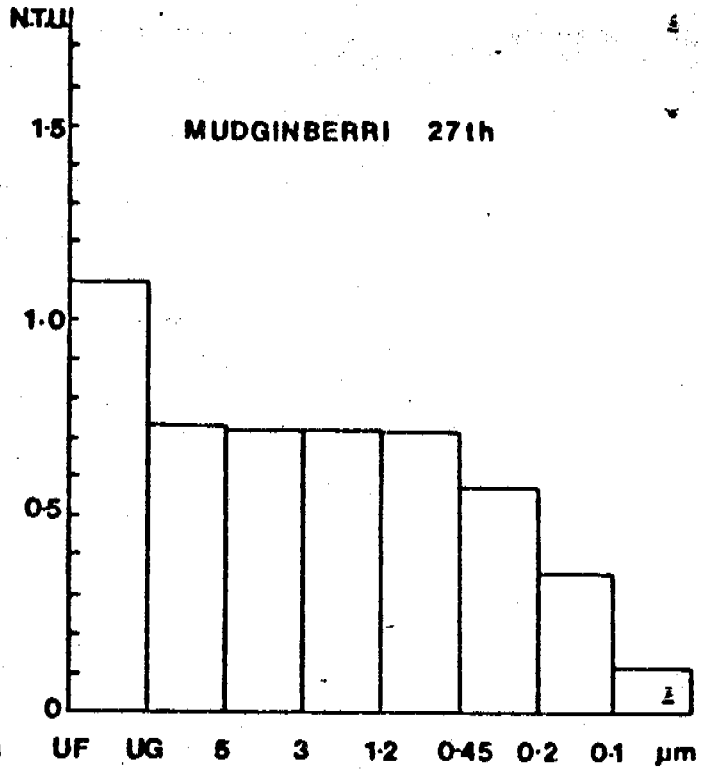
N.T.U
1·5
1·0
0·5
0
MUDGINBERRI 27th
UF UG 5 3 1·2 0·45 0·2 0·1 µm

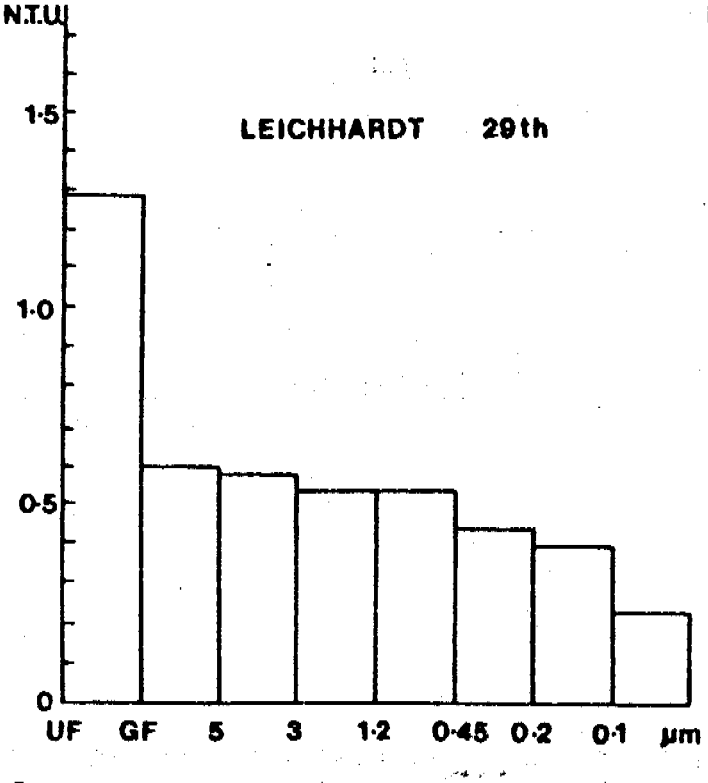
N.T.U
1·5
1·0
0·5
0
LEICHHARDT 29th
UF GF 5 3 1·2 0·45 0·2 0·1 µm

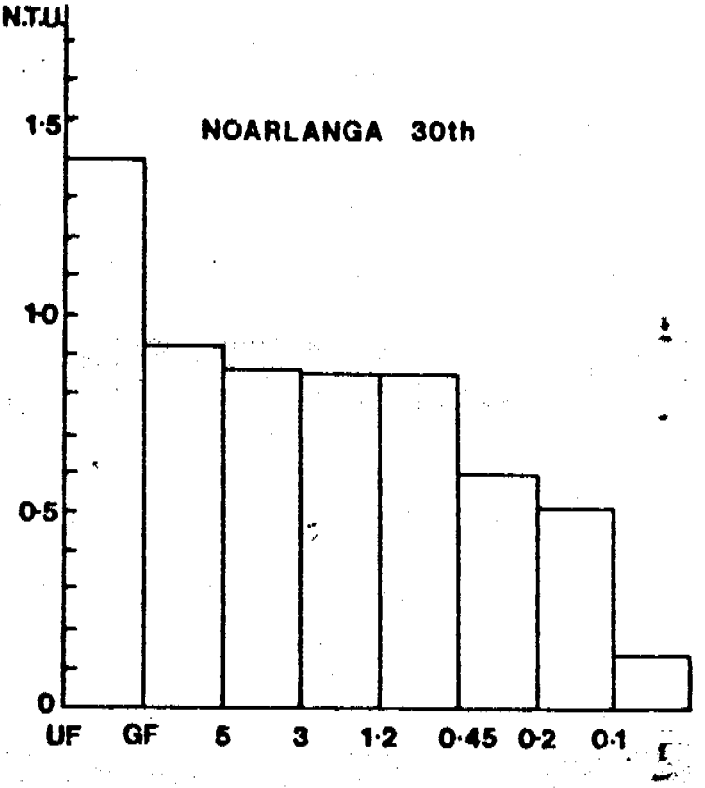
N.T.U
1·5
1·0
0·5
0
NOARLANGA 30th
UF GF 5 3 1·2 0·45 0·2 0·1

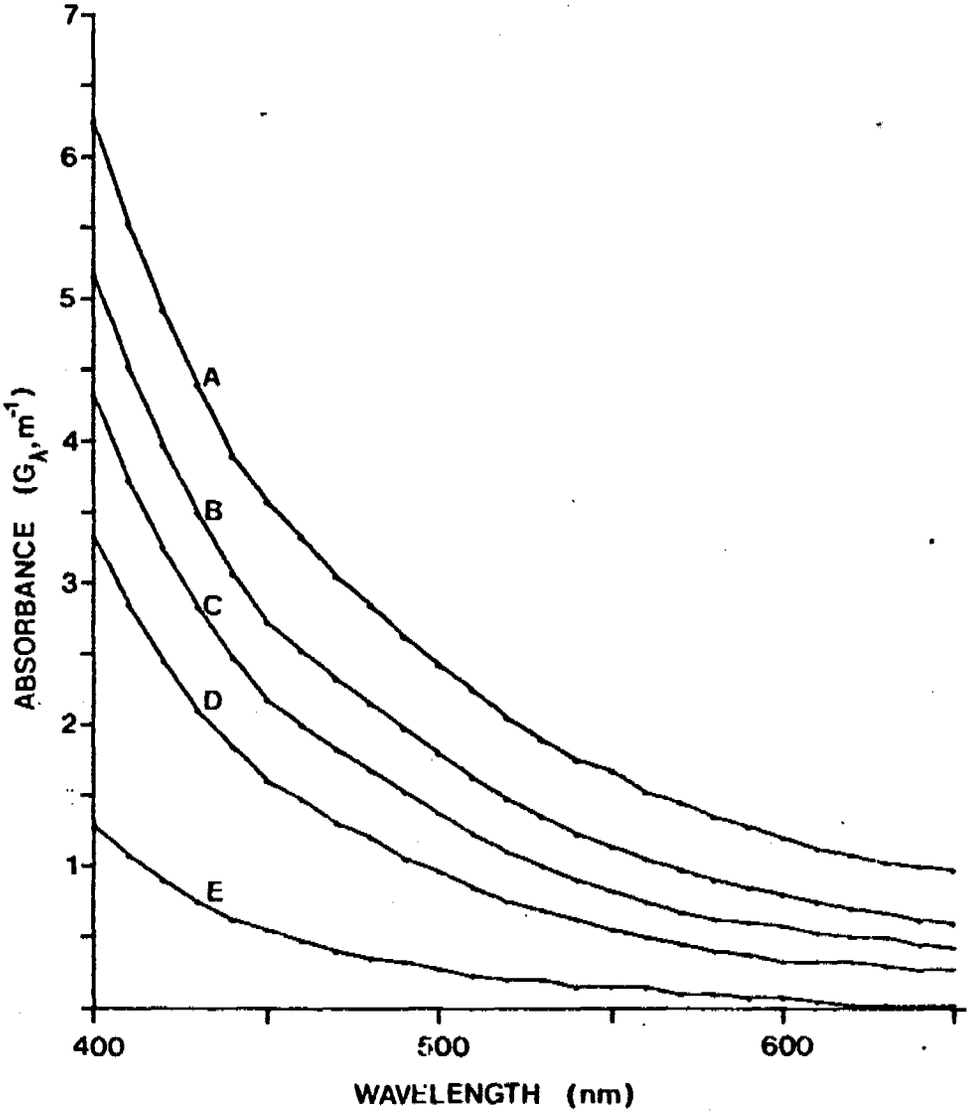

Fig 4.0-2. Spectrophotometric scans, against a distilled water blank, of water from turbid Tooms Lake, Tasmania, showing the effects of filtration through filters of various pore size.

A = unfiltered
B = 1.2μm
C = 0.45μm
D = 0.22μm
E = 0.1μm.

Table 4.0-1

Turbid	Non-turbid
Georgetown	Bowerbird
Gulungul	Mudginberri
Goanna	Island
Ja Ja	Leichardt
Jabiluka	Noarlanga
Nankeen	Kulukuluku
Mine Valley	Red Lily
Umbungbung	Nimbawah
Jingalla	

Table 4.0.1 Billabongs of the Alligator Rivers region classified as turbid or non-turbid from visual observation during the Dry.

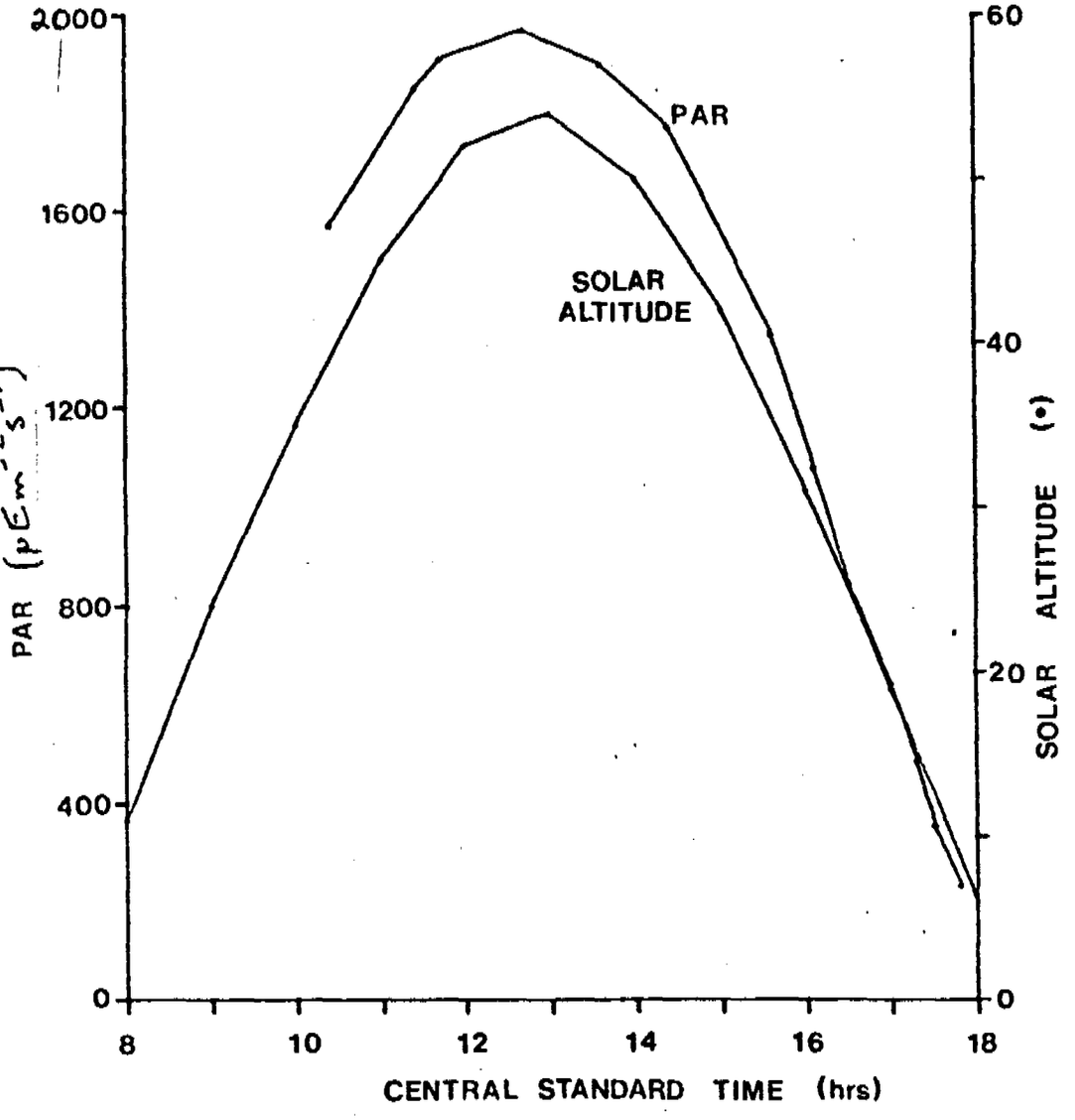

Fig. 4.1.1 Temporal variation of solar altitude and incoming photosynthetically active radiation (PAR) at Jabiru on 27/6/79.

Spectral analysis of the incident PAR (Figs. 4.1-2,3) indicates considerable variation in spectral distribution with solar altitude. The variation is one of relatively more blue light and less red at higher solar altitudes, and the converse at low solar altitudes. This finding is in agreement with Jerlov (1976) and Kirk (1977) who ascribe such variation to the effect of solar altitude on the path length of sunlight through the atmosphere. Blue light scatters much more strongly than does the longer wavelengths, so the lower the solar altitude, the longer the pathlength, and higher the relative proportion of red light reaching the ground.

4.2 The underwater light field in Bowerbird billabong.

Secchi transparency data (Fig. 4.2-1) show Bowerbird to be a clear billabong for most of the year, a supposition borne out by the E values (Table 4.2-). Light penetration appears to be generally sufficient to allow the depth of the euphotic zone to extend to or beyond the maximum depth of this escarpment rockpool. The optical clarity of these waters is hardly surprising given the low concentrations of three light absorbing components in the water - tripton (measured as turbidity), gilvin and chlorophyll (Figs. 4.2-1B,2A,B). From the limited data available, it appears that the highest turbidity and lowest transparency coincide during the wet season as sediment and detritus is introduced by the creek in spate. Maximum transparency occurs at the Wet/Dry interchange when gilvin values are at a minimum. Thus, the maximum euphotic depth occurs at the Wet/Dry interchange, but increases in the value of E lead to a contraction of the euphotic zone as the Dry progresses (Table 4.2-1).

Spectral irradiance data from early June (Fig. 4.2-3) indicates the elimination of the 400-450 nm blue waveband by the midpoint of the euphotic zone (z...), a flat peak at 590 nm, and a shoulder in the 630-650 nm region. Calculation of the attenuation spectrum (Fig. 4.2-4) discloses that the blue and red wavelengths are attenuated equally strongly, whereas

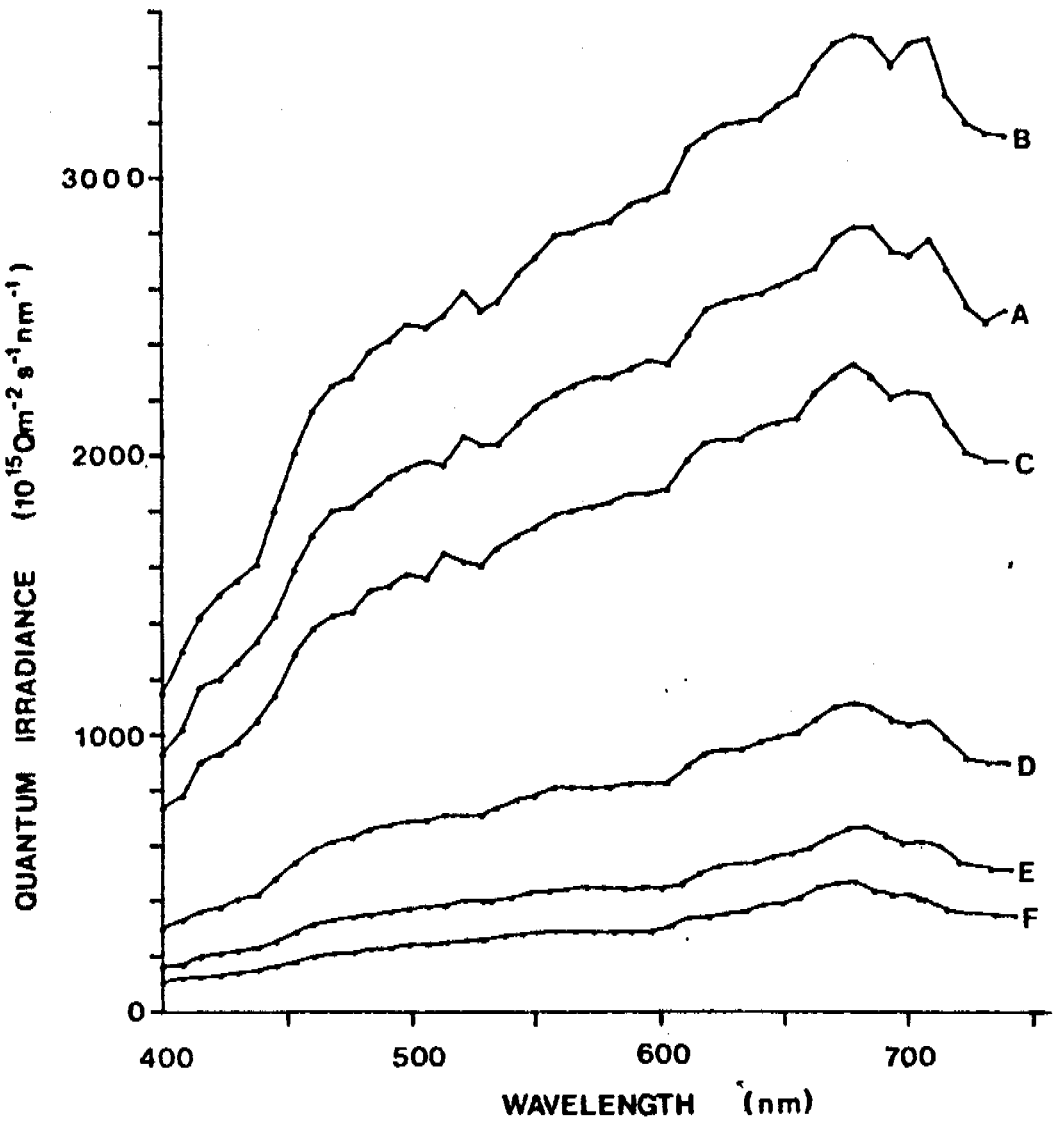

Fig. 4.1.2 Temporal variation in spectral composition of incoming PAR at Jabiru on 27/6/79. α^1 = solar angle.

A = 10.23 hrs. : $\alpha^1 = 40^0$

B = 12.40 hrs. : $\alpha^1 = 52^0$

C = 15.30 hrs. : $\alpha^1 = 40^0$

D = 17.00 hrs. : $\alpha^1 = 19^0$

E = 17.30 hrs. : $\alpha^1 = 12^0$

F = 17.45 hrs. : α^1 9^0

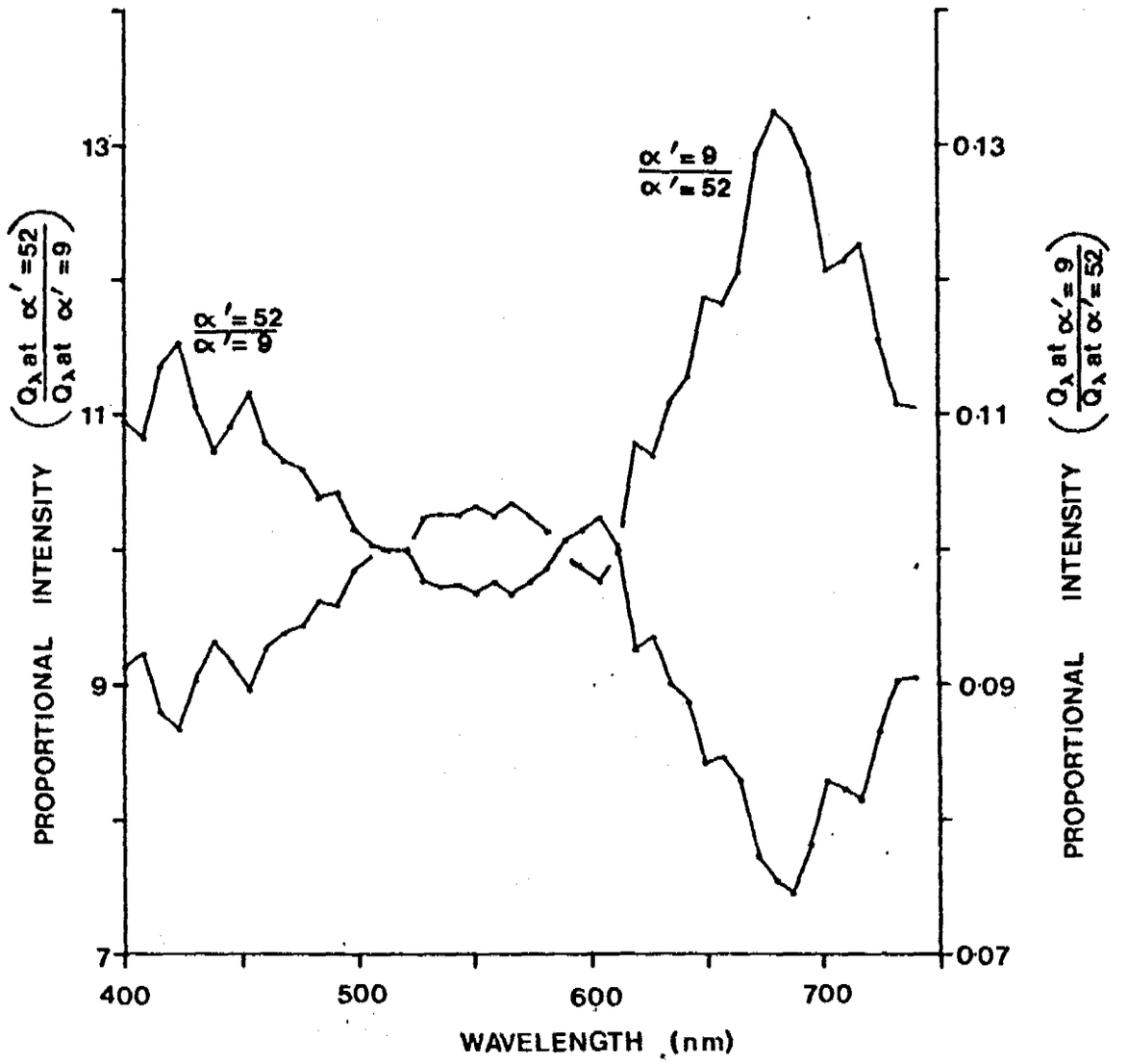

Fig. 4.1.3 Relative spectral distribution of PAR at high ($\alpha^1 = 52^0$) and low ($\alpha^1 = 9^0$) solar altitude at Jabiru on 27/6/79.

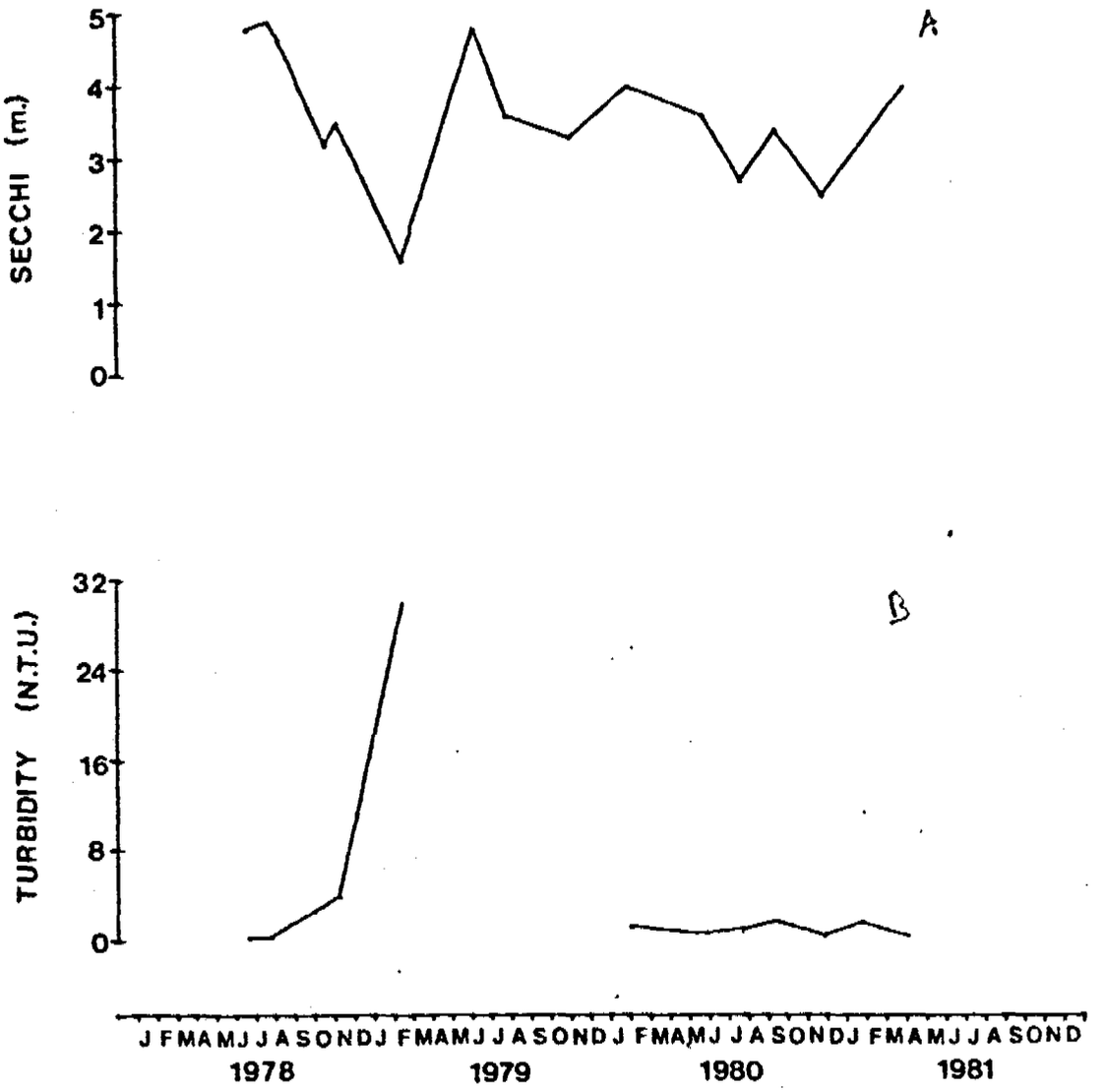

Fig. 4.2.1 Seasonal variations in Secchi transparency (A) and turbidity (B) in Bowerbird billabong.

Table 4.10A

Date	Time (hrs)	E_d (m^{-1})	z_{eu} (m)	$z_{S.D.}$ (m)
7/ 4/81	0900	0.65	3.1	2.3
28/ 5/79	1430	1.07	1.9	
11/ 7/79	0830	1.39	1.4	0.6
12/ 6/79	0840	1.41	1.4	0.45
9/ 8/79	0845	1.59	1.3	0.5
30/ 8/80	1245	1.81	1.1	0.4
24/10/80	1530	3.39	0.6	0.3
25/11/80	0820	5.09	0.4	0.08
13/11/79	1115	6.84	0.3	0.15

Table 4.10A Optical characteristics of Jabiluka billabong. Symbols as for Table 4.2A.

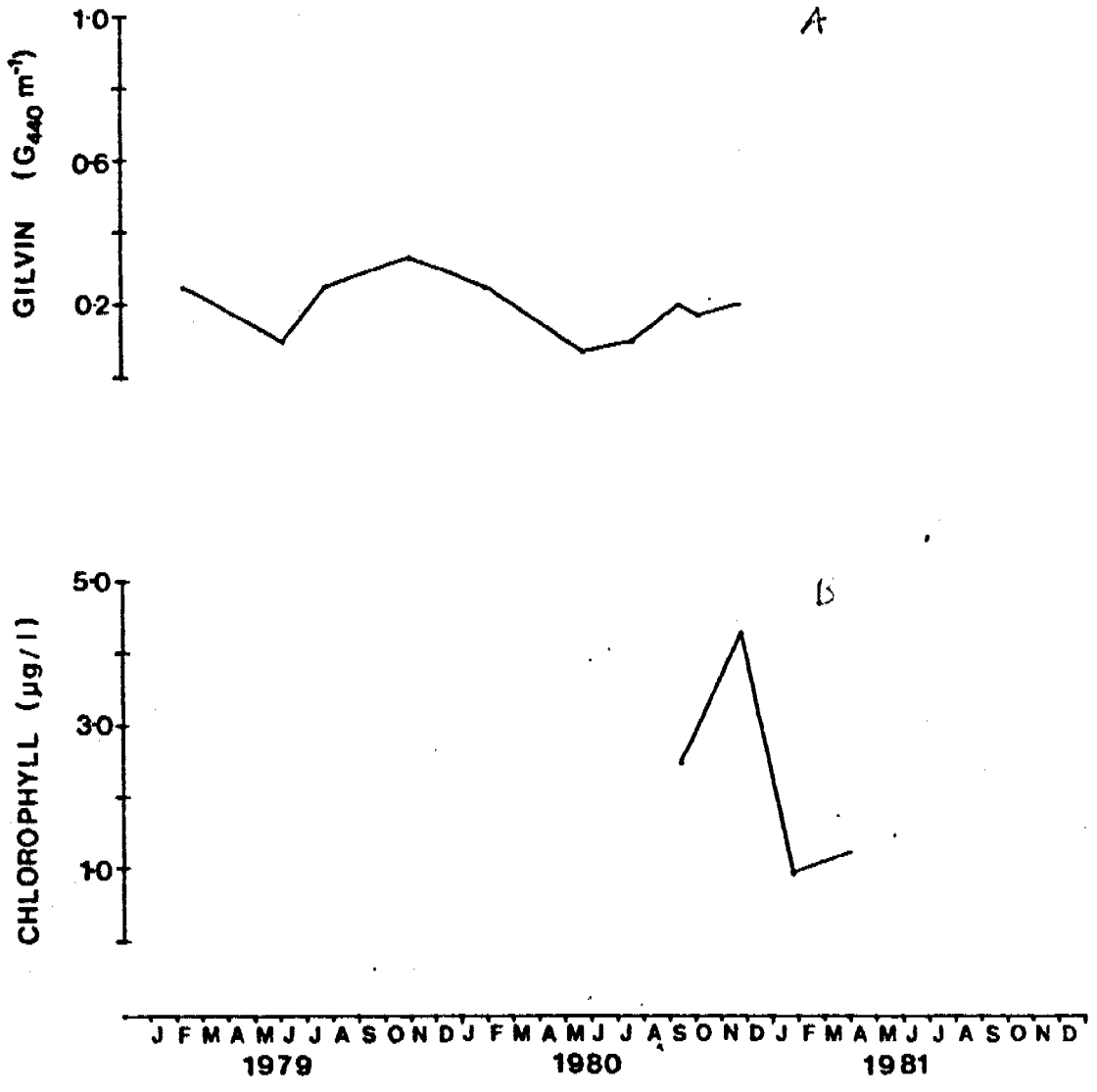

Fig. 4.2.2 Seasonal variations in gilvin (G_{440}) (A) and chlorophyll (B) in Bowerbird billabong.

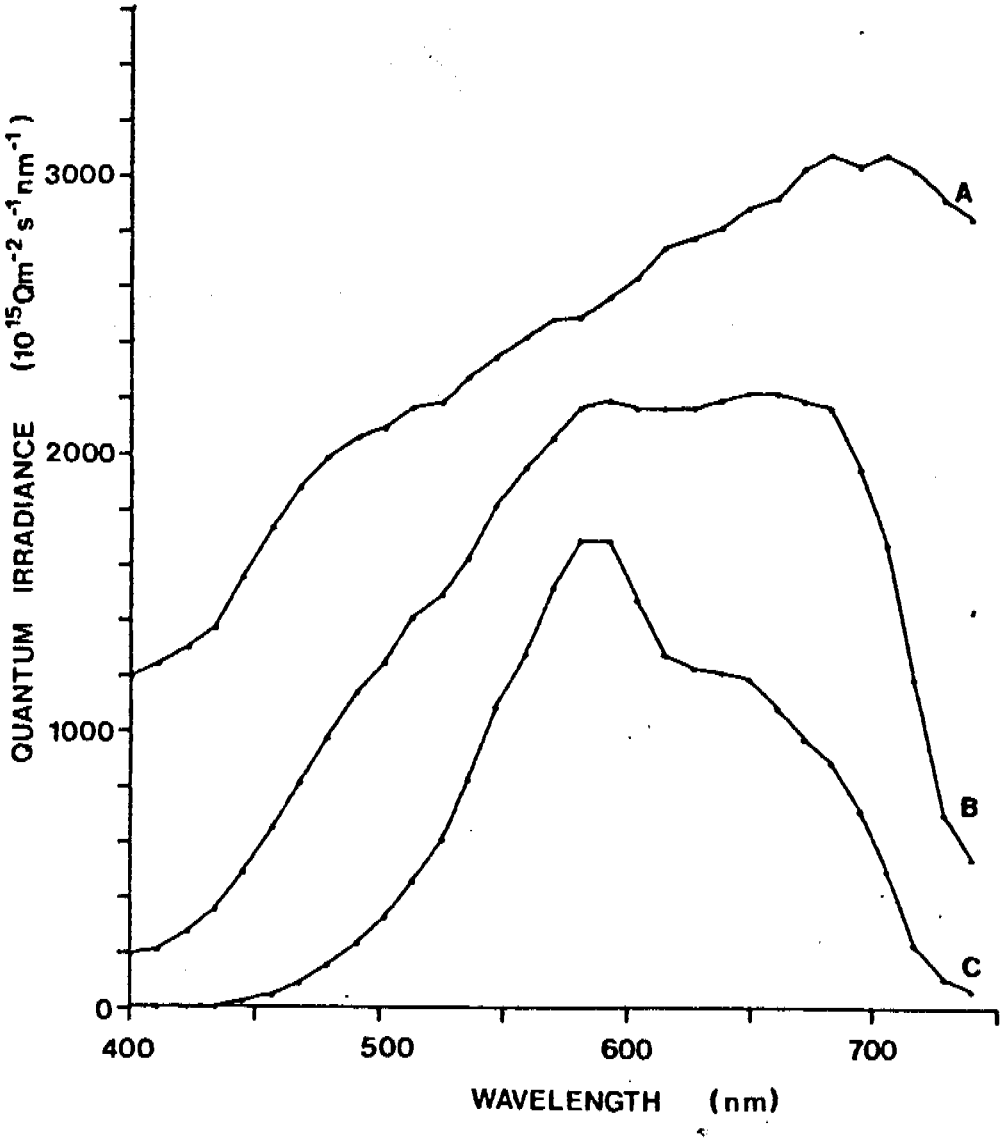

Fig. 4.2.3 *In situ* quantaspectrometric measurements at selected depths in Bowerbird billabong on 7/6/79.

A = 0.01 m : 100% Q_0

B = 1.0 m (x1.5) : 50% Q_0

C = 4.0 m (x6) : 7% $Q_0 \approx z_m$

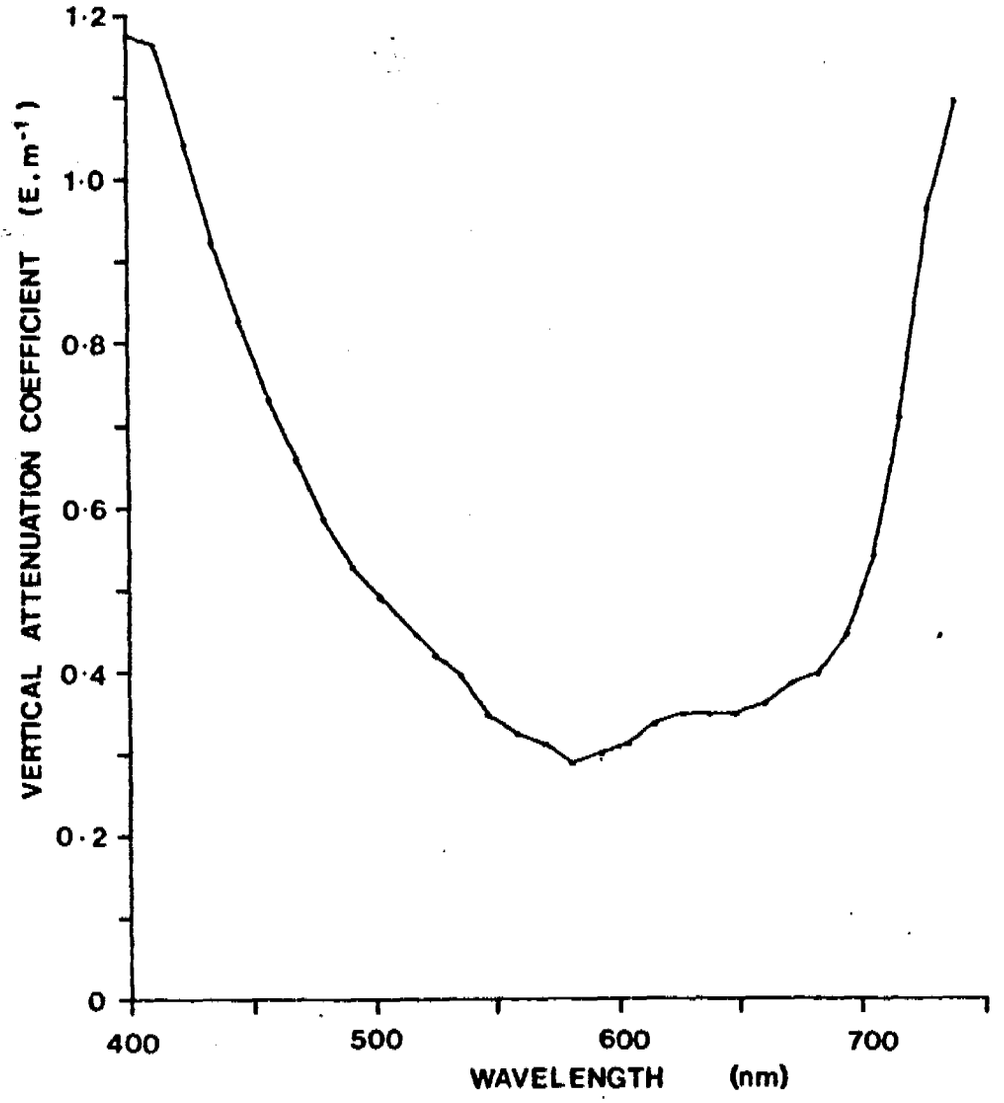

Fig. 4.2.4 The attenuation spectrum of Bowerbird billabong on 7/6/79. Vertical attenuation coefficients have been calculated, at 10 nm intervals, from the *in situ* quantaspectrometric data.

the middle waveband experiences comparatively little diminution of intensity with depth. Attenuation of the blue wavelengths is attributable to absorption by gilvin and tripton, whereas attenuation of long wavelengths is primarily due to absorption by water itself. The absorptive power of the gilvin and tripton combination on the one hand, and water itself on the other, are of approximately the same magnitude (Fig. 4.2-4).

4.3 The underwater light field in Noarlanga billabong

In contrast to the situation in Bowerbird, where the euphotic zone contracted as the Dry progressed, the converse occurred in Noarlanga in 1979, where euphotic depth increased 160% between May and Movember (Table 4.3). This increase is consistent with concomitant changes in turbidity, gilvin and transparency.

Turbidity of surface waters peaks during the Wet with corresponding minima* of transparency (Fig. 4.3-1A,B). Following the Wet/Dry interchange, a decrease in turbidity occurs, mirrored by a dramatic increase in transparency, and these trends are maintained throughout the Dry. These seasonal responses of turbidity and transparency are contrary to those experienced in Bowerbird and most other billabongs. There, the transparency is maximal at the Wet-Dry interchange because suspended particles, which have previously been maintained in suspension by turbulent flow, sediment. Thereafter, as water levels fall, resuspension of sediments by wind-induced turbulence, and increasing algal crops, cause rises in turbidity and a corresponding decline in water clarity. Why the situation differs in Noarlanga is not entirely known. Certainly the abrupt morphometry of the billabong, its sandy sediments, and the considerable protection afforded by surrounding vegetation, are not conducive to the resuspension of sediments.

* (any reading of transparency during the Wet is likely to be an overestimate due to the influence on the Secchi disk of the strong currents which course through this billabong).

Table 4.3.4

Date	Time (hrs)	E_d (m^{-1})	z_{eu} (m)	$z_{S.D.}$ (m)
14/11/79	0930	0.37	5.4	2.8
22/8/79	0850	0.41	4.9	3.3
24/7/79	0915	0.43	4.7	2.6
28/6/79	0850	0.46	4.3	2.9
30/5/79	1155	0.58	3.4	2.1

Table 4.3A Optical characteristics of Noarlanga billabong. Symbols as for Table 4.2A.

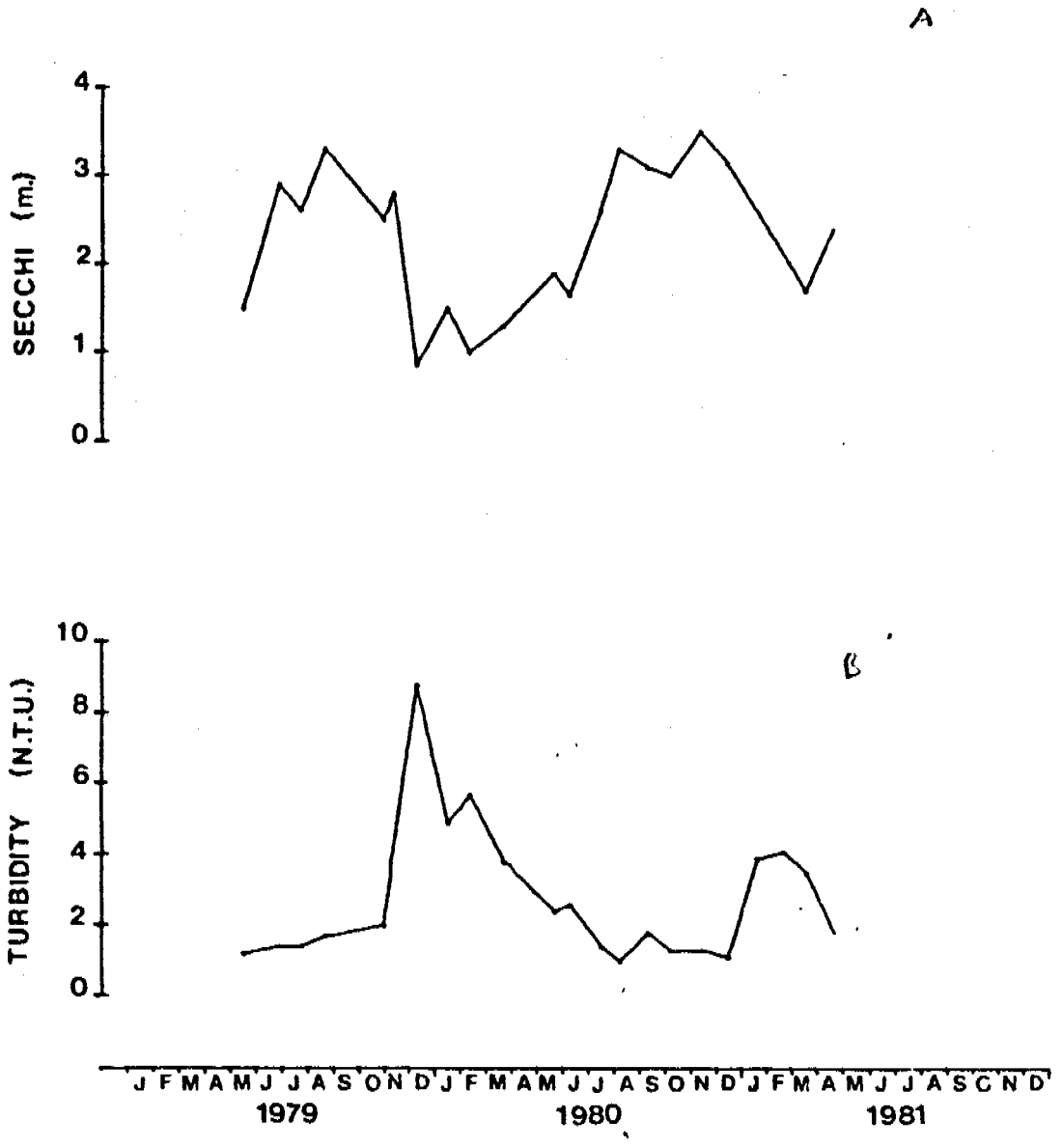

Fig. 4.3.1 Seasonal variations in Secchi transparency (A) and turbidity (B) in Noarlanga billabong.

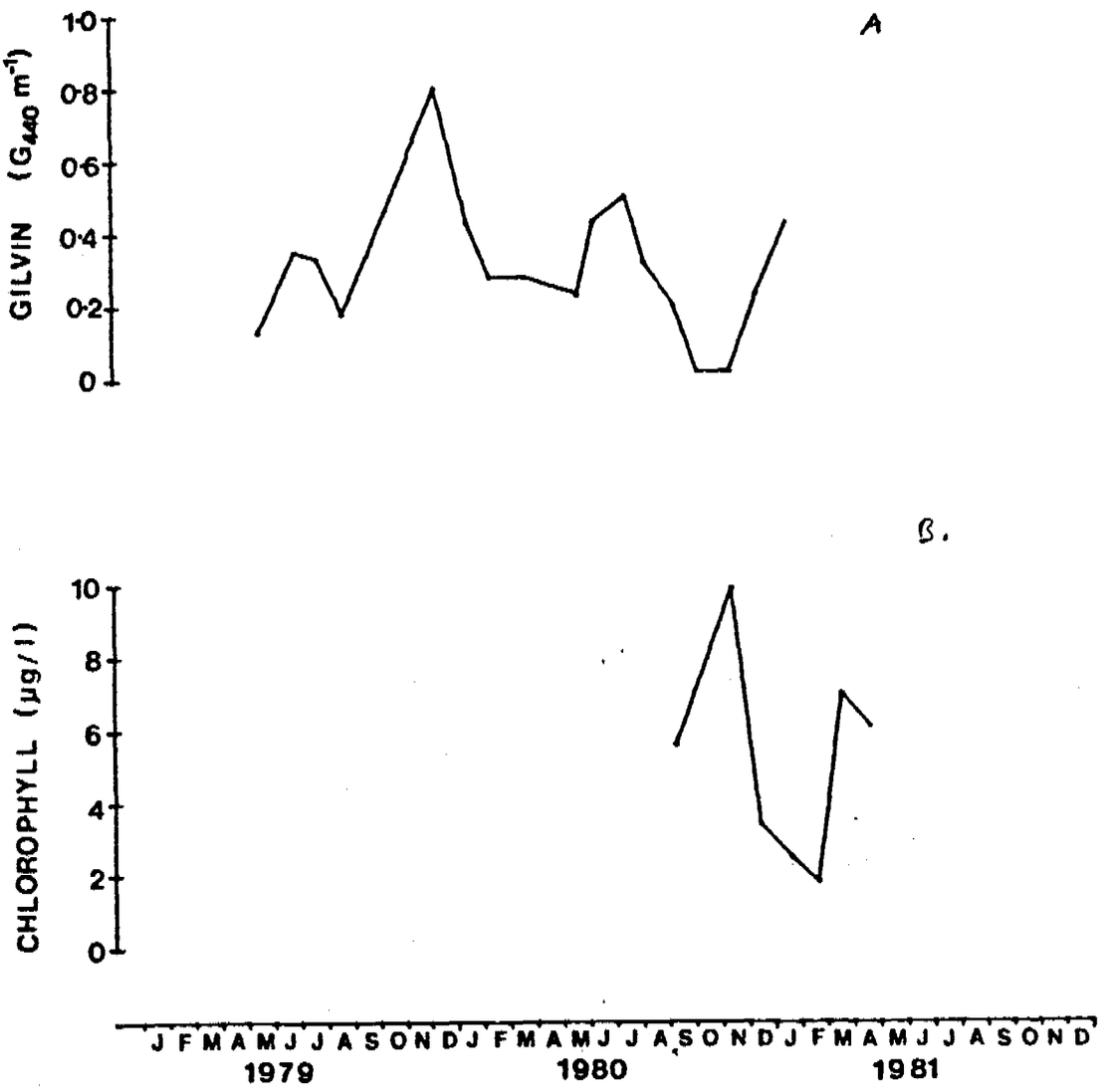

Fig. 4.3.2 Seasonal variations in gilvin (G_{440}) (A) and chlorophyll (B) in Noarlanga billabong.

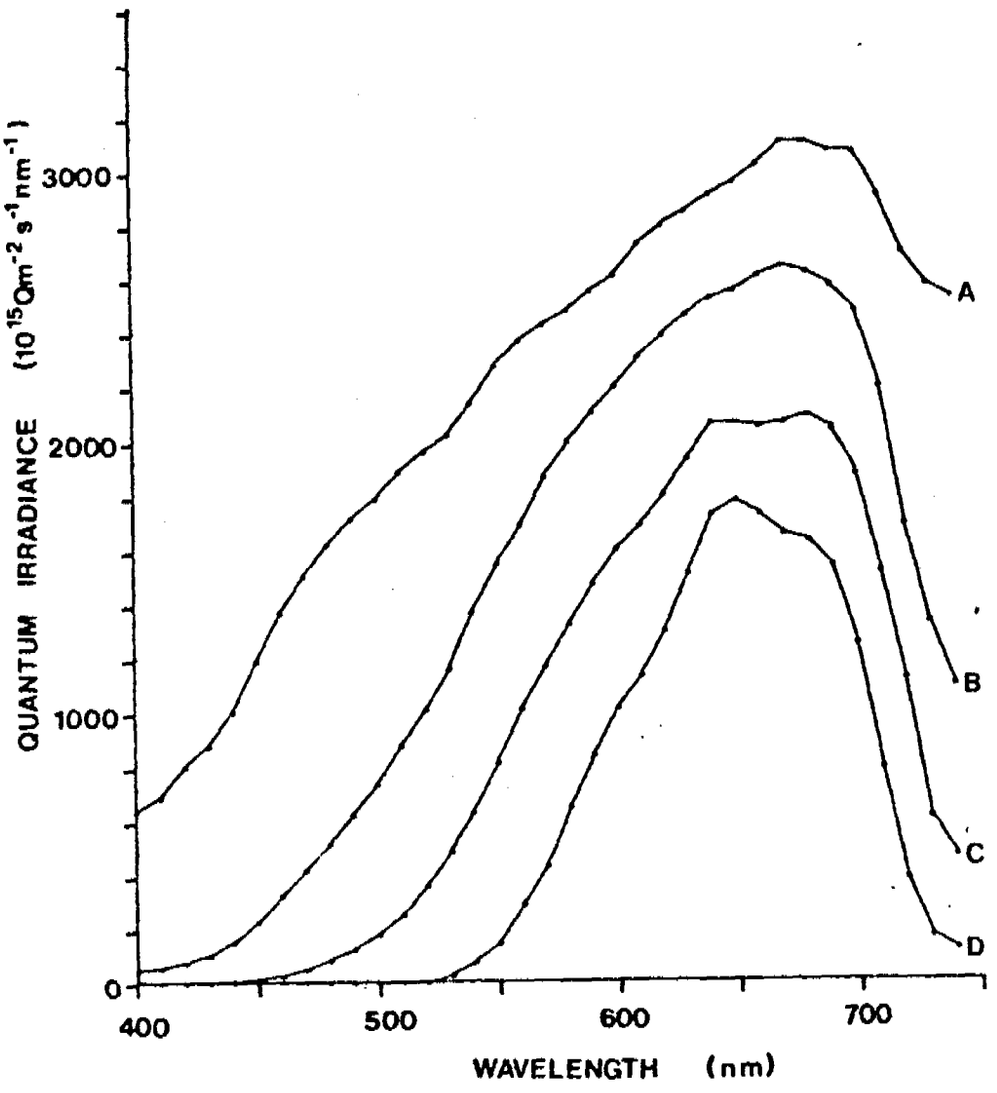

Fig. 4.3.3. *In situ* quantaspectrometric measurements at selected depths in Noarlanga billabong on 30/5/79.

A = 0.1 m : 80% Q_o

B = 0.5 m (x1.3)

C = 1.0 m (x2) : 20% $Q_o \approx z_m$

D = 3.0 m (x20) : 1% $Q_o = z_{eu}$

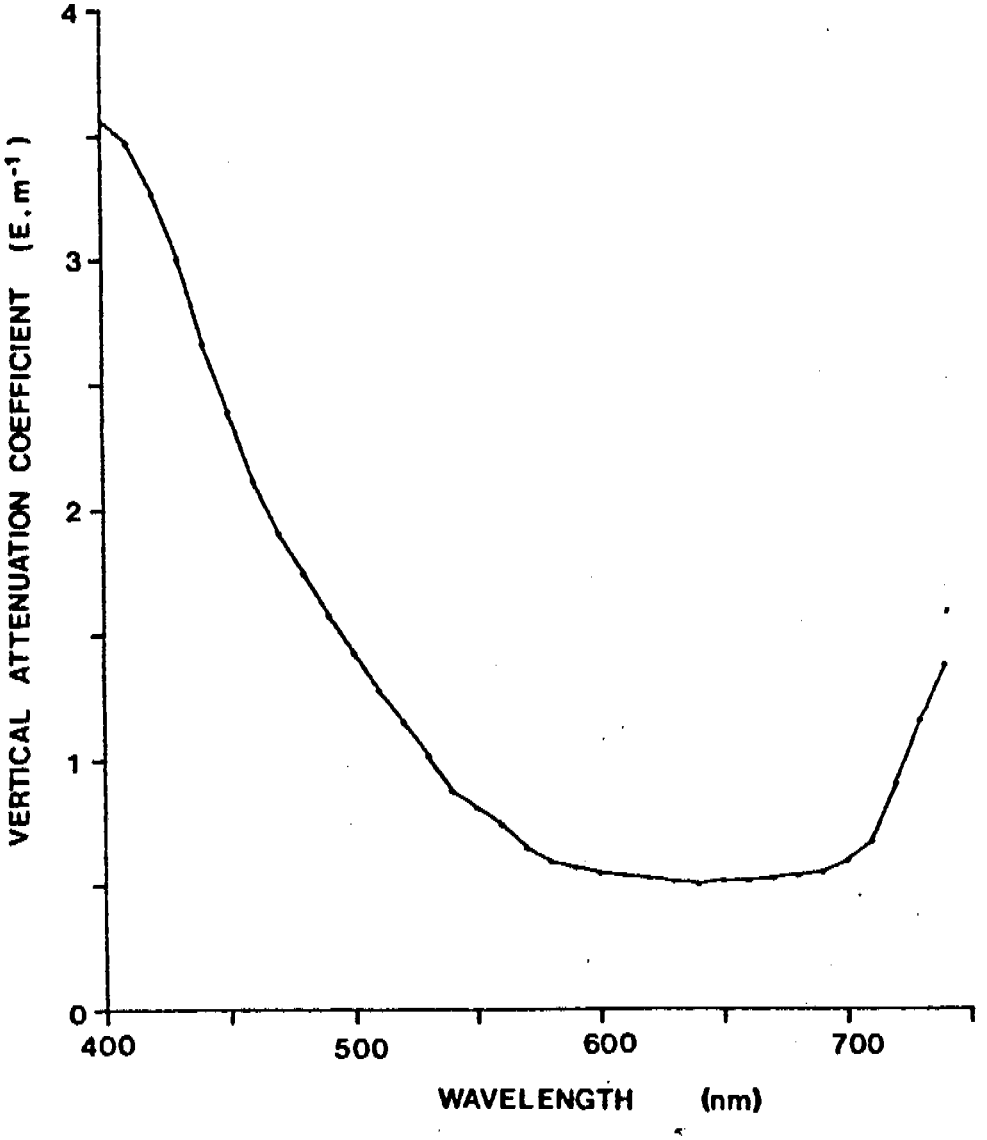

Fig. 4.3.4 The attenuation spectrum of Noarlanga billabong on 30/5/79.

The increase in euphotic depth during the Dry would also be favoured by declining gilvin values over the same period. This was the case for the 1980 Dry; data is lacking for the late Dry of 1979, but there is no reason to suspect that that year was different (Fig. 4.2-3A). The overall picture is that of two yearly maxima in gilvin, one in the early to mid-Wet, as products of terrestial plant decomposition are washed into the billabong, and one during the early Dry.

Spectral irradiance data from late May, 1979 (Fig. 4.3-3) reveal that by [illegible], the 400-450 nm waveband had been extinguished, and the remainder of the spectrum was dominated by a broad, fairly flat peak from 640 to 690 nm. By [illegible], this peak was resolved into a maximum at 650 nm and a shoulder at 680 nm, probably resulting from slight absorption at around 660-670 nm by low concentrations of chlorophyll-a. The strong attenuation of the shorter wavelengths is also illustrated by the spectral attenuation data (Fig. 4.3-4), with a less marked maximum affecting wavelengths exceeding 710 nm. A broad band of low, relatively constant attenuation covered the wavelengths 580-700 nm, which includes the slight chlorophyll-a absorption peak (660-670 nm), which would be obscured by the logarithmic nature of the vertical attenuation coefficient. The predominance of short wavelength absorption over that of the red wavelengths, in contrast to the situation described above for Bowerbird, is largely due to the seasonally higher gilvin content and turbidity.

4.4 The underwater light field in Mudginberri billabong

The limited number of PAR attenuation data (Table 4.4) suggest that slight contraction of the euphotic zone occurs during the first half of the Dry. Transparency evidence (Fig. 4.4-1A) supports the notion of a general deterioration in water clarity through the Dry. In 1978 and 1980, maximum dry season transparency occurred in April/May as surface inflows reduced to a trickle, and suspended particles settled to the bottom in the

Table 4.4.4

Date	Time (hrs)	E_d (m^{-1})	z_{eu} (m)	$z_{S.D.}$ (m)
2/5/79	1245	0.53	3.8	1.7
2/6/78	1010	0.53	3.8	2.3
16/9/78	1100	0.57	3.5	

Table 4.4.5 Optical characteristics of Mudginberri billabong. Symbols as for Table 4.2.1.

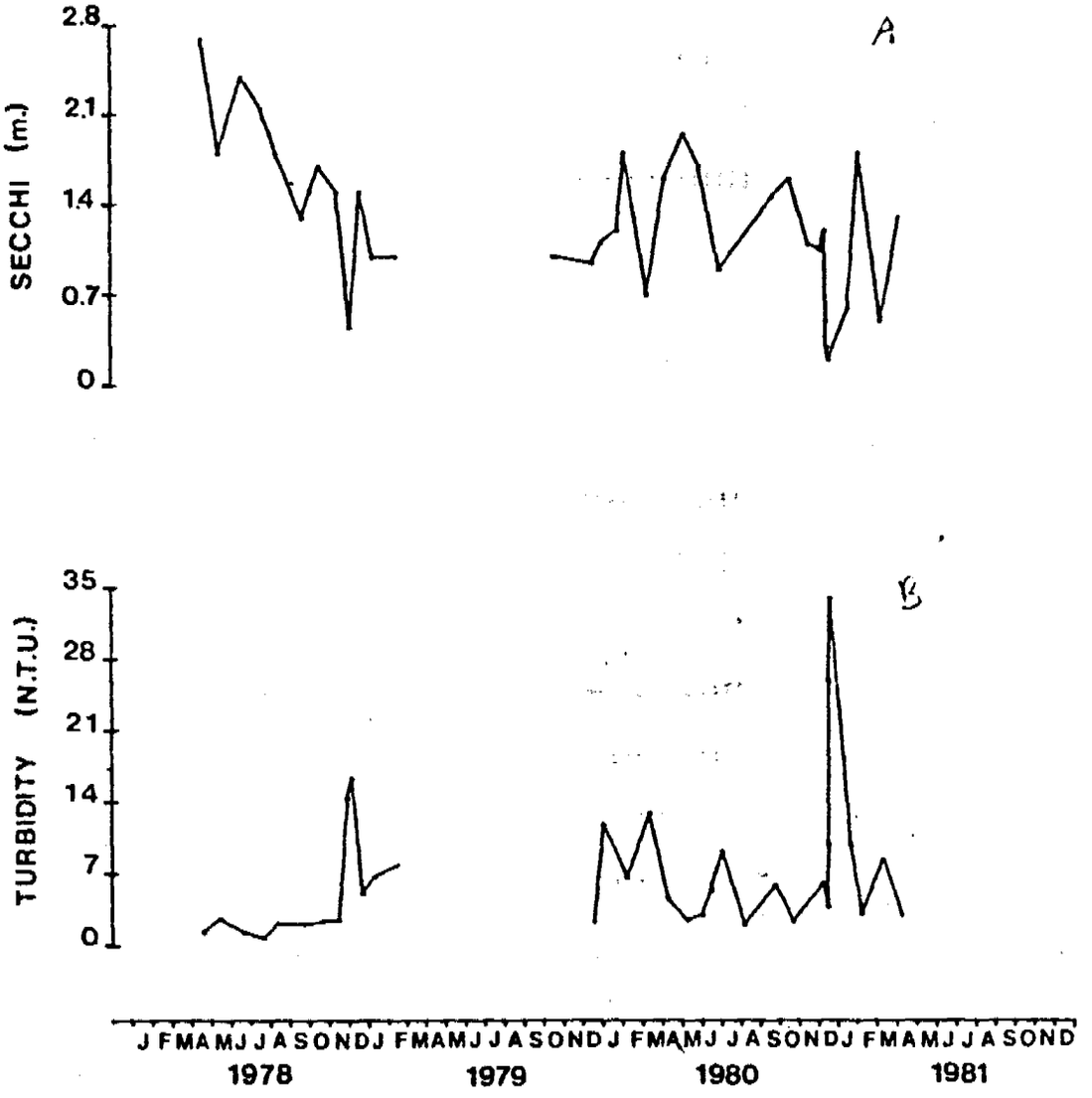

Fig. 4.4.1 Seasonal variations in Secchi transparency (A) and turbidity (B) in Mudginberri billabong.

now standing water. However, the 1978 maximum of 2.7 metres was considerably greater than that in 1980 of 1.95 metres. By late October in both years, transparency had fallen to around 1.6 metres. The July 1980 transparency minimum, mirrored by the dry season maximum in turbidity, can possibly be ascribed to the phytoplankton bloom, indicated qualitatively by the distinct greenish hue of the water. That chlorophyll data which is available (Fig. 4.4-2B) suggests a general rise in trophic status over the Dry. By contrast, gilvin (Fig. 4.4-3A) fluctuated widely during the early Dry, 1980, but stabilized over the August to November period.

The heavy rains at the commencement of the Wet, produce strong increases in both gilvin and chlorophyll (Fig. 4.4-2A,B) as detrital and other material of terrestial origin washes into the billabong. Following establishment of creek flow, sudden deterioration of water clarity occurs (Fig. 4.4-1A) as turbidity increases nearly tenfold (Fig. 4.4-1B) even though chlorophyll concentrations decline precipitously (Fig. 4.4-2B); sand mining at the southern end of Mudginberri during July 1980 is probably the cause of higher turbidity values during the first flush of 1981 compared with 1978. Soon after the first flush, gilvin and turbidity values decline.

In situ spectroradiometric measurements on three dates showed considerable similarities in the spectral distribution of the underwater light. Elimination of the 400-450 nm waveband, leaving a spectrum dominated by a broad peak in the 580-660 region, with a shoulder around 690-700 nm, occurred by the midpoint of the euphotic zone (Figs. 4.4-3,4,5). By z_{eu}, the peak is resolved into two distinct maxima (≈590 nm and 640 nm) of equal magnitude on the May and June dates but with the 590 nm peak in the September sample distinctly superior.

The intervening trough (around 630 nm) may be ascribable to absorption by chlorophyll a satellite band (perhaps reinforced by chlorophyll c at 630 nm) the trough (660-670 nm) by chlorophyll a.

The spectral attenuation characteristics for the May and June investigations are, except for the 400-440 nm waveband, virtually identical

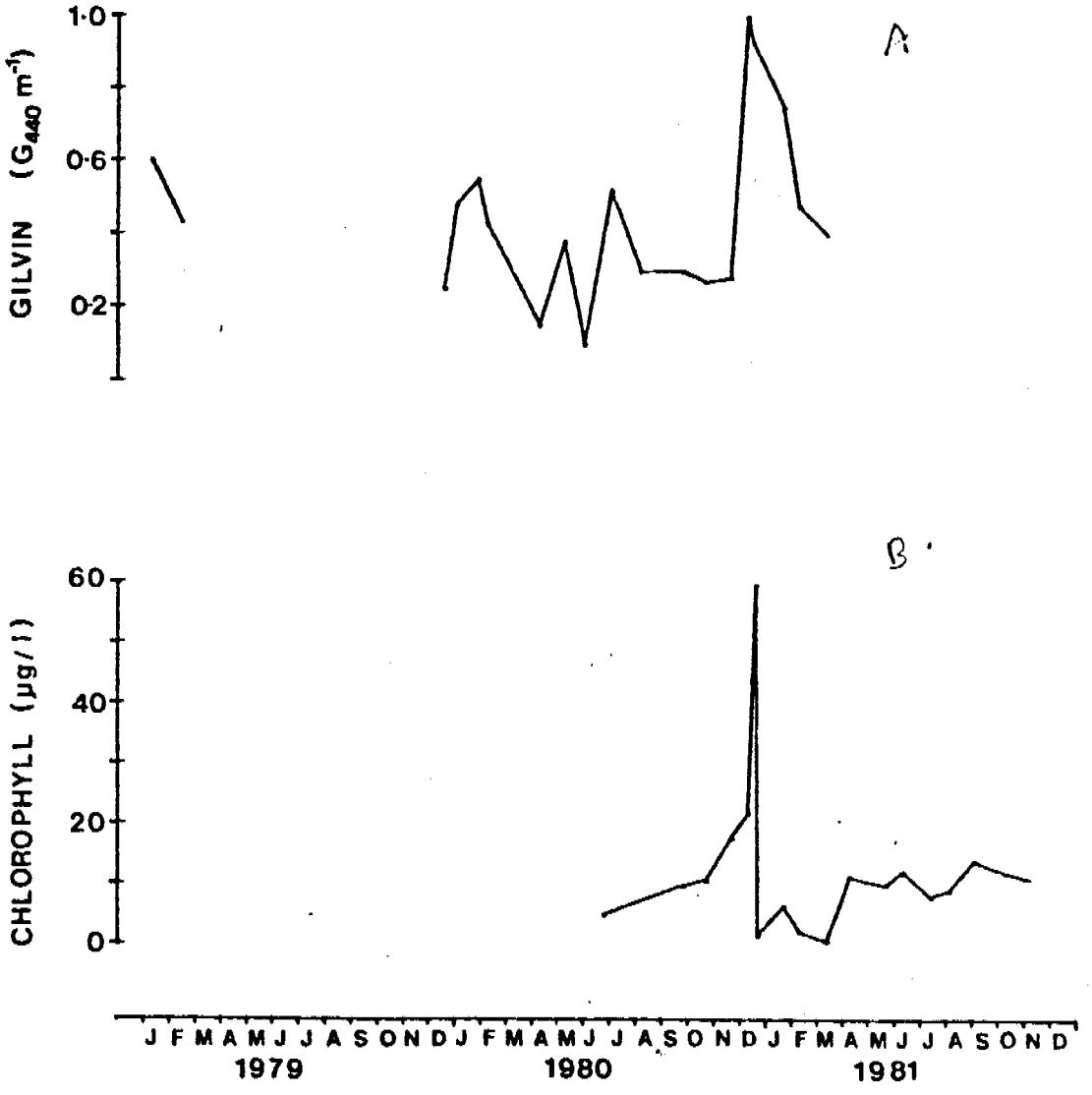

Fig. 4.4.2 Seasonal variations in gilvin (G_{440}) (A) and chlorophyll (B) in Mudginberri billabong.

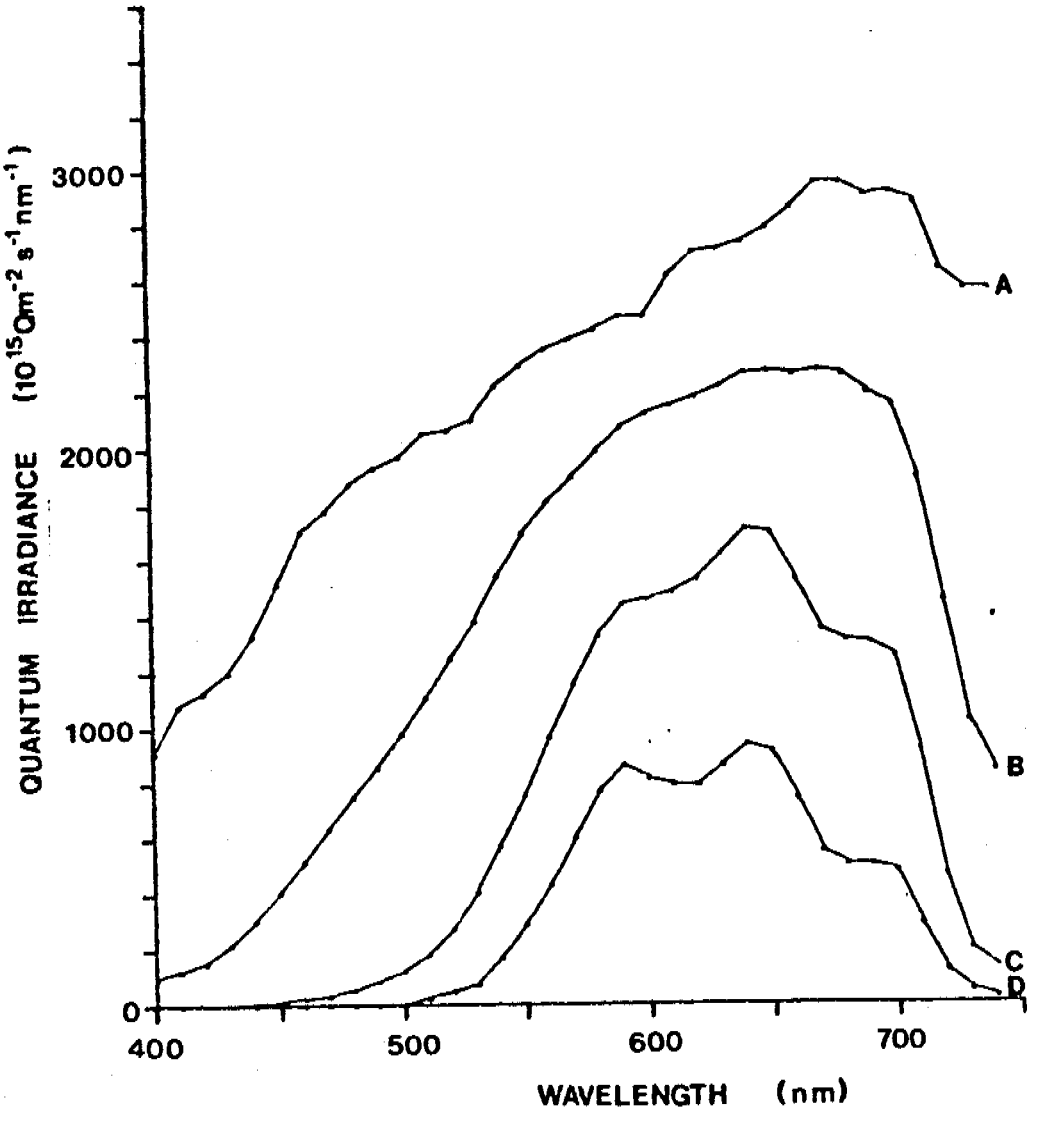

Fig. 4.4.3 *In situ* quantaspectrometric measurements at selected depths in Mudginberri billabong on 1/6/78.

A = 0.01 m : 100% Q_o

B = 0.5 m (x1.3) : 53% Q_o

C = 2.0 m (x5) : 8% $Q_o \approx z_m$

D = 4.0 m (x20) : 1% $Q_o = z_{eu}$

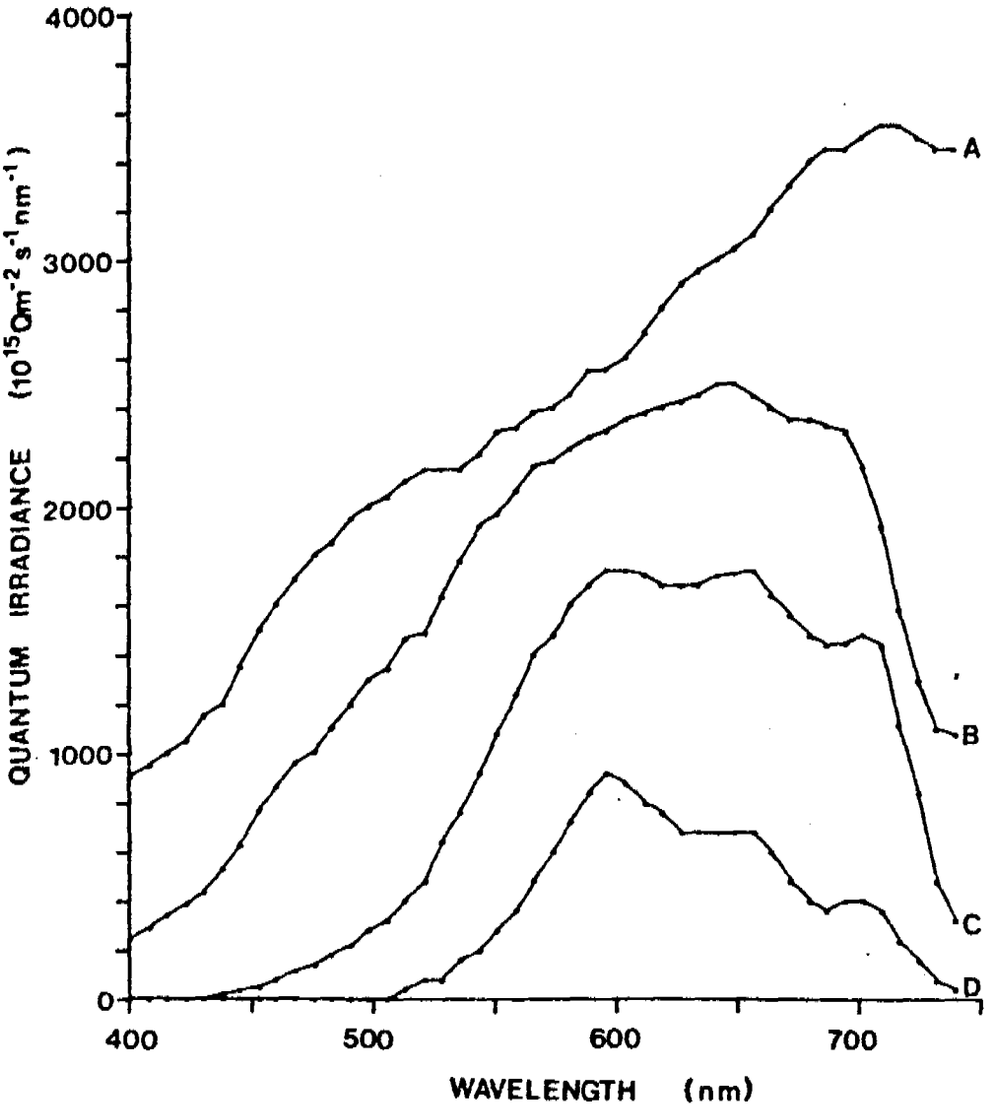

Fig. 4.4.4 *In situ* quantaspectrometric measurements at selected depths in Mudginberri billabong on 16/9/78.

A = Aerial : 100% Q_o

B = 0.05 (x1.3) : 54% Q_o

C = 1.5 m (x3.3) : 15% $Q_o \approx z_m$

D = 4.0 m (x33) : 0.7% $Q_o \approx z_{eu}$

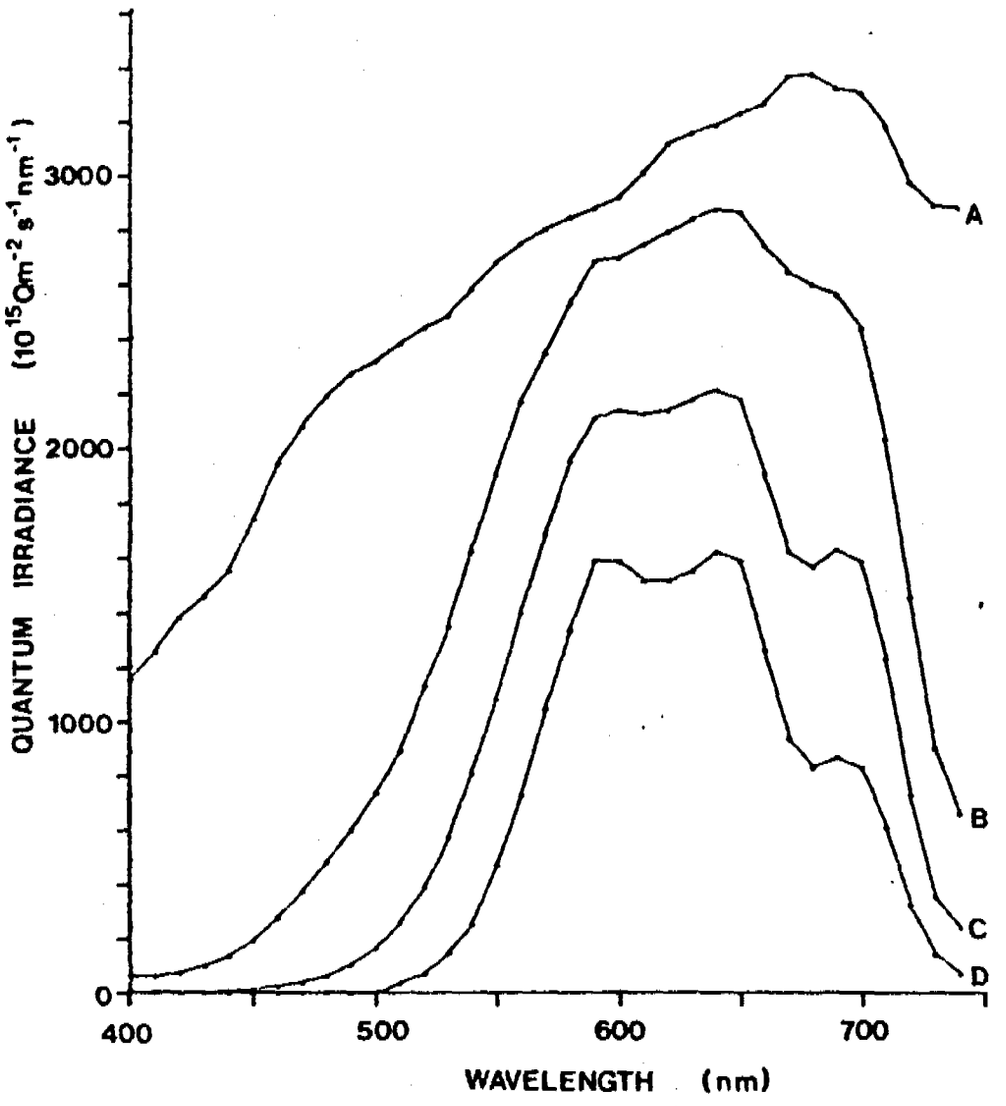

Fig. 4.4.5 *In situ* quantaspectrometric measurements at selected depths in Mudginberri billabong on 27/5/79.

A = 0.1 m : 94% Q_o

B = 1.0 m (x2) : 31% Q_o

C = 2.0 m (x5) : 9% $Q_o \approx z_m$

D = 4.0 m (x30) : 0.8% $Q_o \simeq z_{eu}$

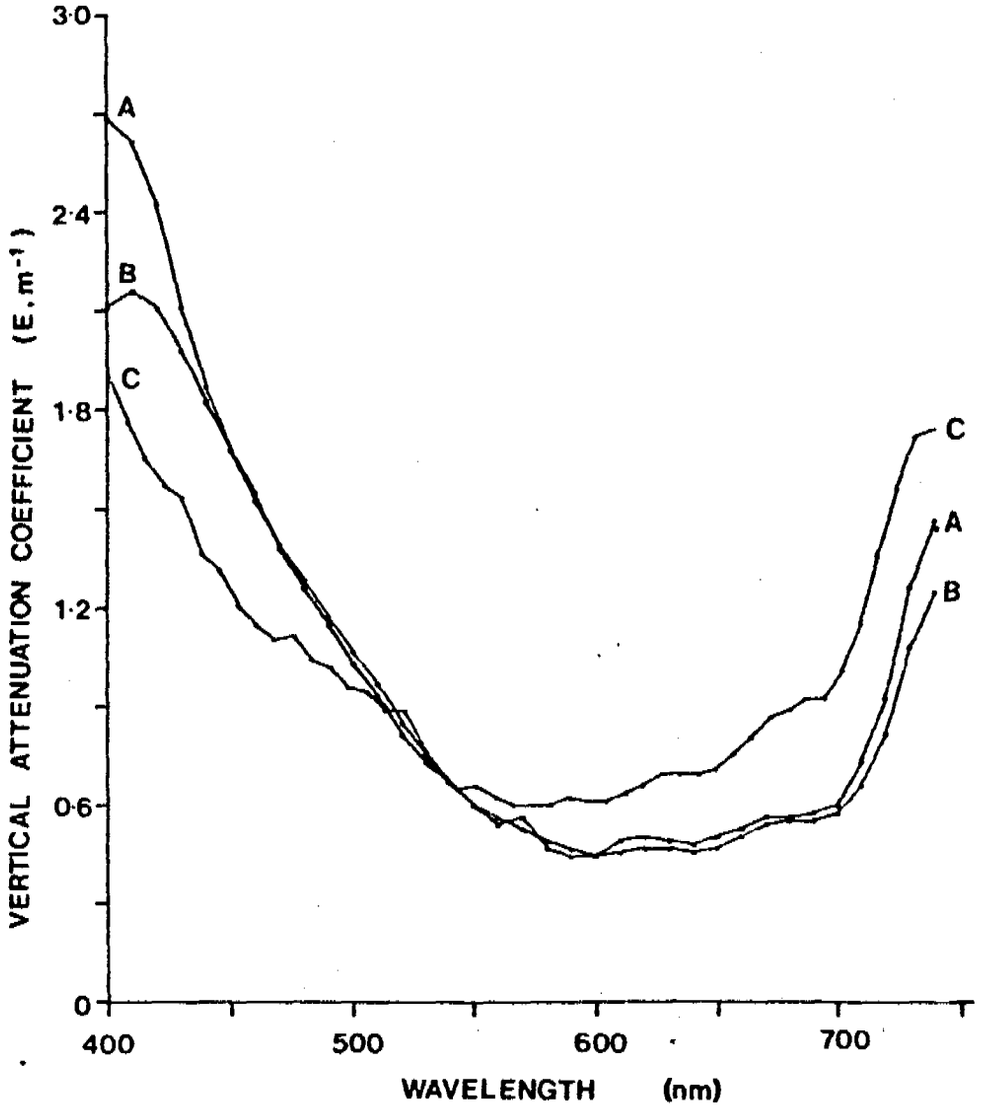

Fig. 4.4.6 The attenuation spectra of Mudginberri billabong on [illegible] (A), [illegible] (B) and [illegible] (C).

(Fig. 4.4-6), and very similar in shape to that obtained for Noarlanga in May (Fig. 4.3-4). However, the September attenuation spectrum bears resemblance to that reported for Bowerbird (Fig. 4.2-4), where blue and red wavelengths are attenuated equally strongly, indicating low tripton and gilvin concentrations.

4.5 The underwater light field in Kulukuluku billabong

The single PAR attenuation profile in August, 1981 (Table 4.5) indicated a euphotic depth of 3.6 metres, 50% of the maximum depth of the water column, and comparable to that expected for Mudginberri for the same time of year. Seasonal trends in water clarity are suggested by variation in transparency (Fig. 4.5-1A), which reaches it lowest levels during the early Dry, and has maxima during the late Dry and at various periods during the Wet, a situation somewhat reminiscent of Noarlanga (section 4.2). By contrast, turbidity (Fig. 4.5-1B) increases over the late Dry, although the range of variation is very small (1.3-3.1 N.T.U.). It appears that the highest gilvin values occur during the Wet and the lowest during the late Dry (Fig. 4.5-2A). Chlorophyll data (Fig. 4.5-2B) suggest a mid-Dry maximum in trophic status.

The spectral irradiance in August at [illegible]lukuluku (Fig. 4.5-3) was almost identical to that for Mudginberri in June (Fig. 4.4-3), with elimination of short wavelengths and troughs at the chlorophyll a (~670 nm) and its satellite band (~625nm) absorption wavelengths, leaving an irradiance peak at 650 nm. The attenuation spectrum (Fig. 4.5-4) confirms the preferential absorption of the shorter wavelengths.

4.6 The underwater light field in Island billabong

In this, the largest of the study billabongs, an annual range of 2.0-3.6 metres in euphotic depth is indicated by the vertical attenuation coefficients (Table 4.6), for which a virtually complete seasonal coverage is available. No definite seasonal patterns are apparent; instead, euphotic depth (z_{eu}) fluctuates capriciously, though only within the narrow 2-3 metre zone, indicating a relatively constant light climate for most of the year. The dramatic and unexpected increase in water clarity during late October, 1980, is an exception.

The transparency data (Fig. 4.6-1A) give a different impression, with distinct seasonal trends of maxima at the Wet/Dry interchange followed

Table 4.5

Date	Time (hrs)	E_d (m^{-1})	z_{eu} (m)	$z_{S.D.}$ (m)
16/8/78	0900	0.56	3.6	2.4

Table 4.5 Optical characteristics of Kulukuluku billabong. Symbols as for Table 4.2.

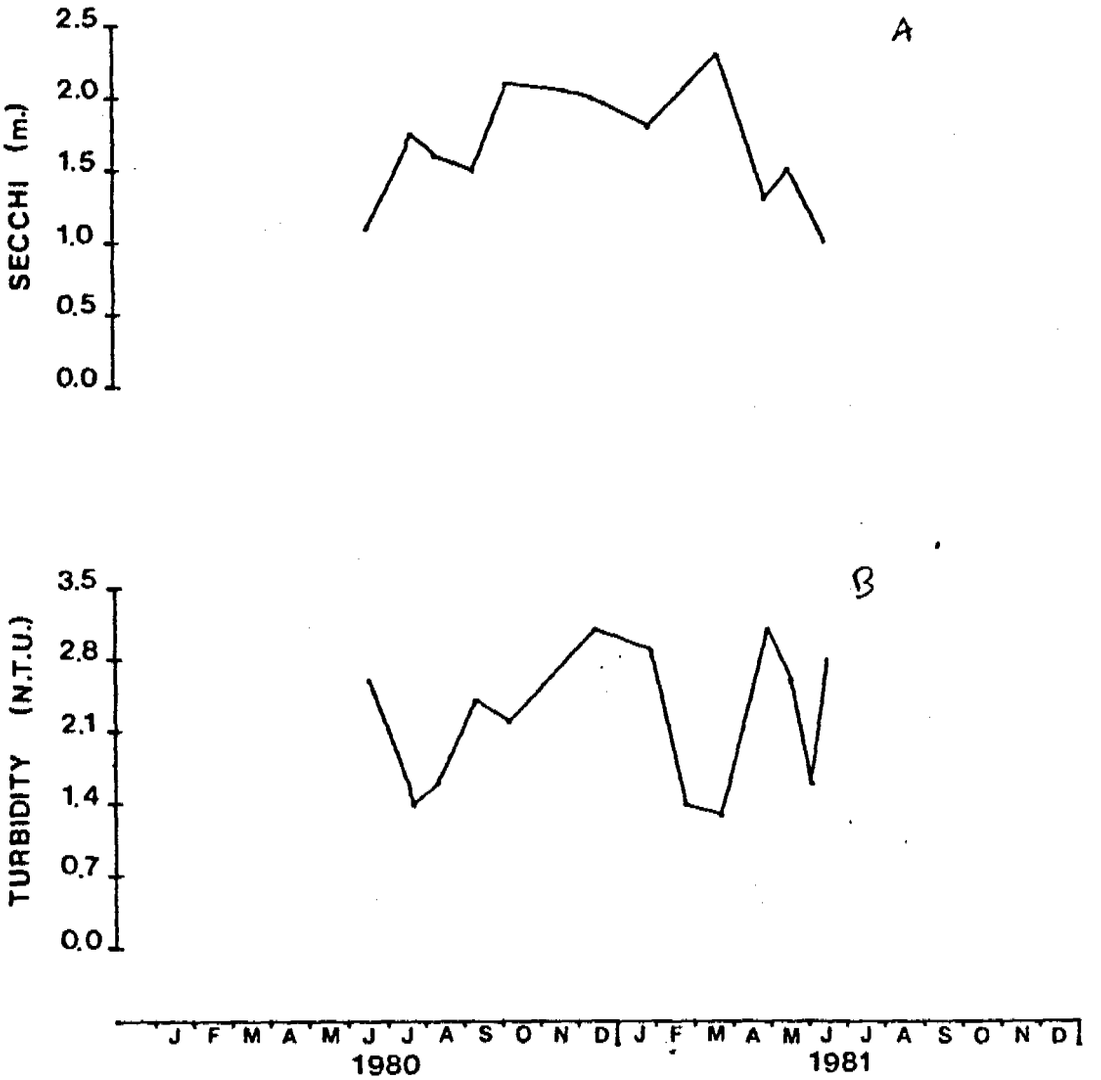

Fig. 4.5.1 Seasonal variations in Secchi transparency (A) and turbidity (B) in Kulukuluku billagong.

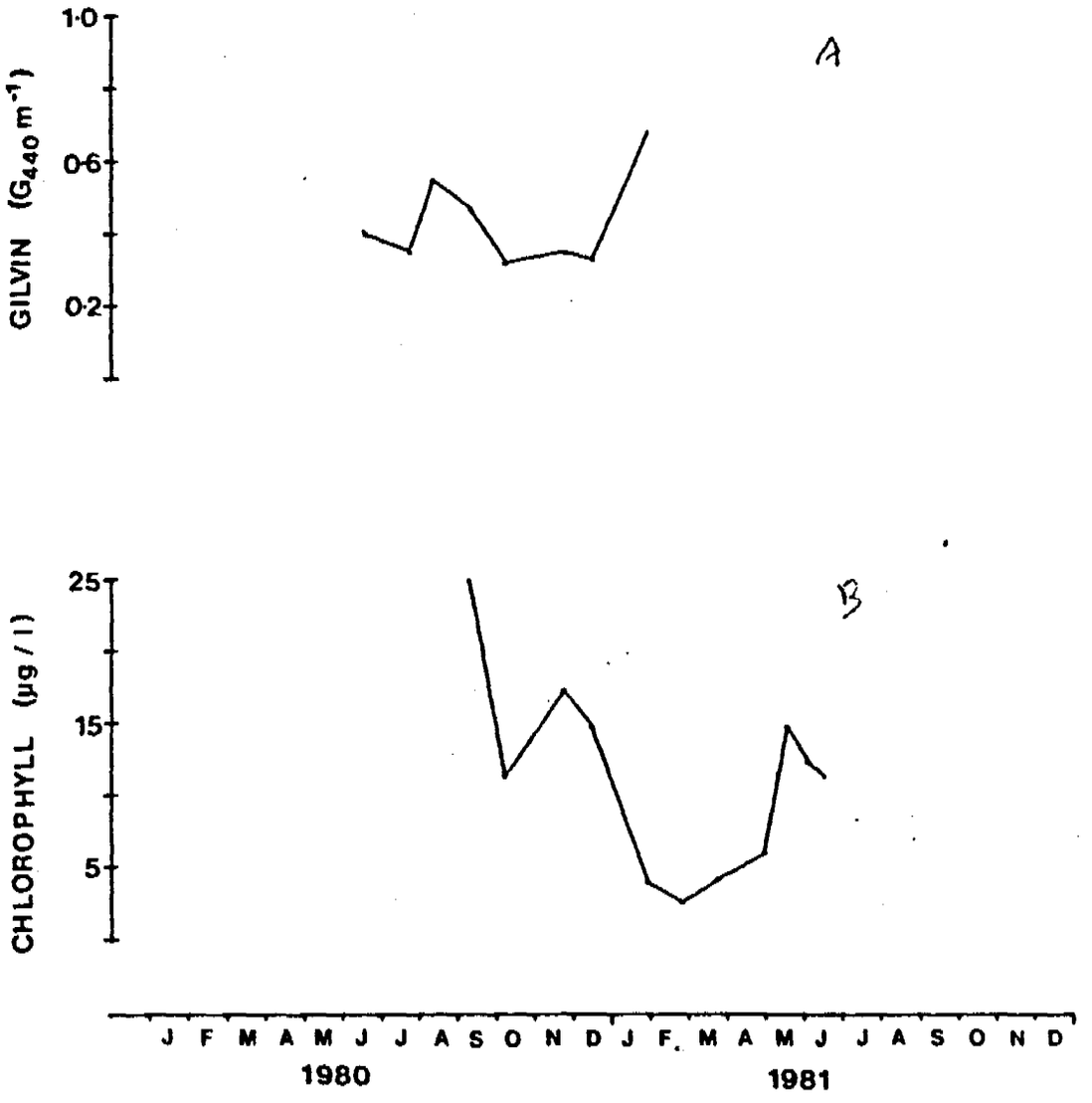

Fig. 4.5.2 Seasonal variations in gilvin (G_{440}) (A) and chlorophyll (B) in Kulukuluku billabong.

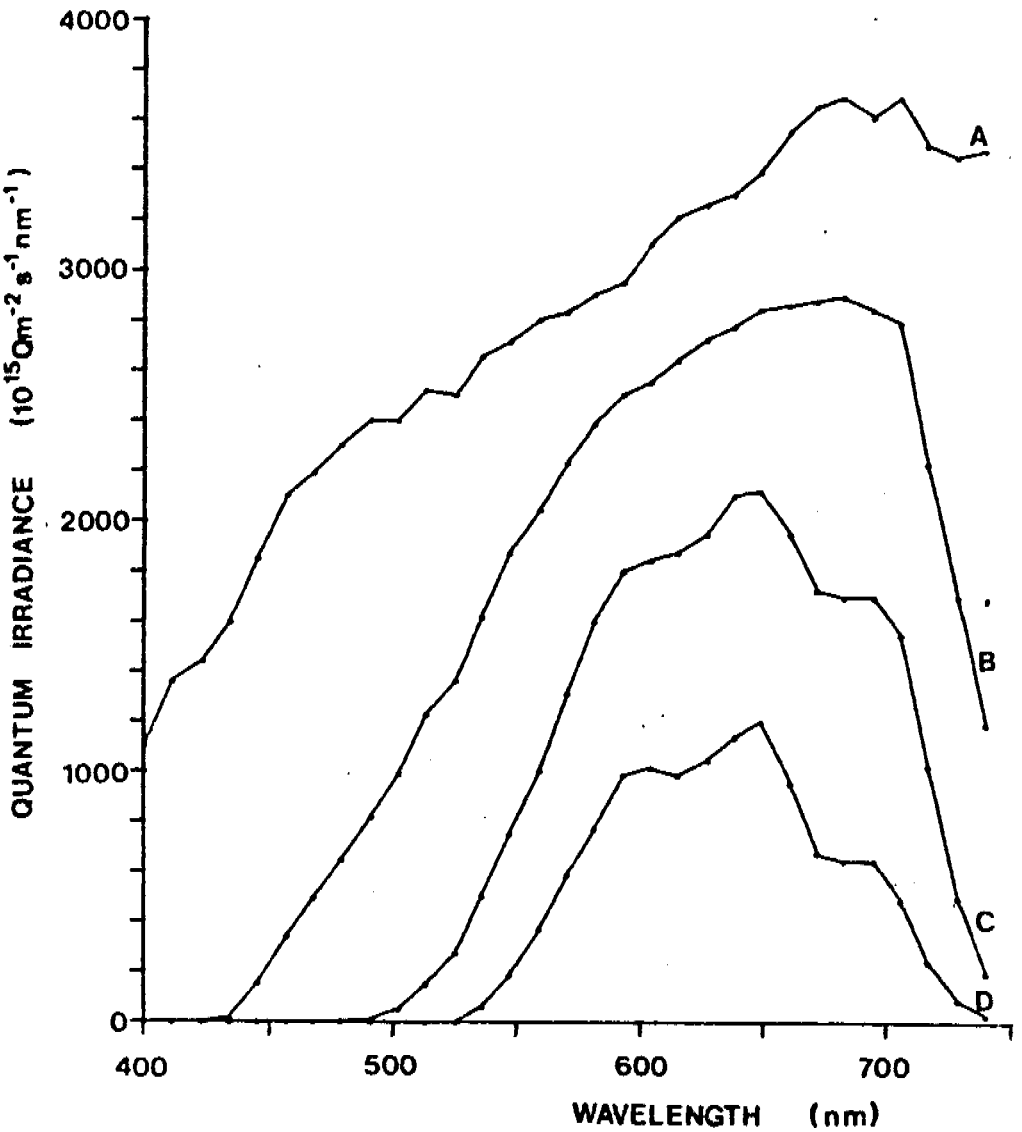

Fig. 4.5.3 *In situ* quantaspectrometric measurements at selected depths in Kulukuluku billabong on 14/8/81.

A = Aerial : 100% Q_o

B = 0.5 m (x1.4) : 45% Q_o

C = 2.0 m (x4.2) : 8% $Q_o \approx z_m$

D = 4.0 m (x25) : 0.6% $Q_o \approx z_{eu}$

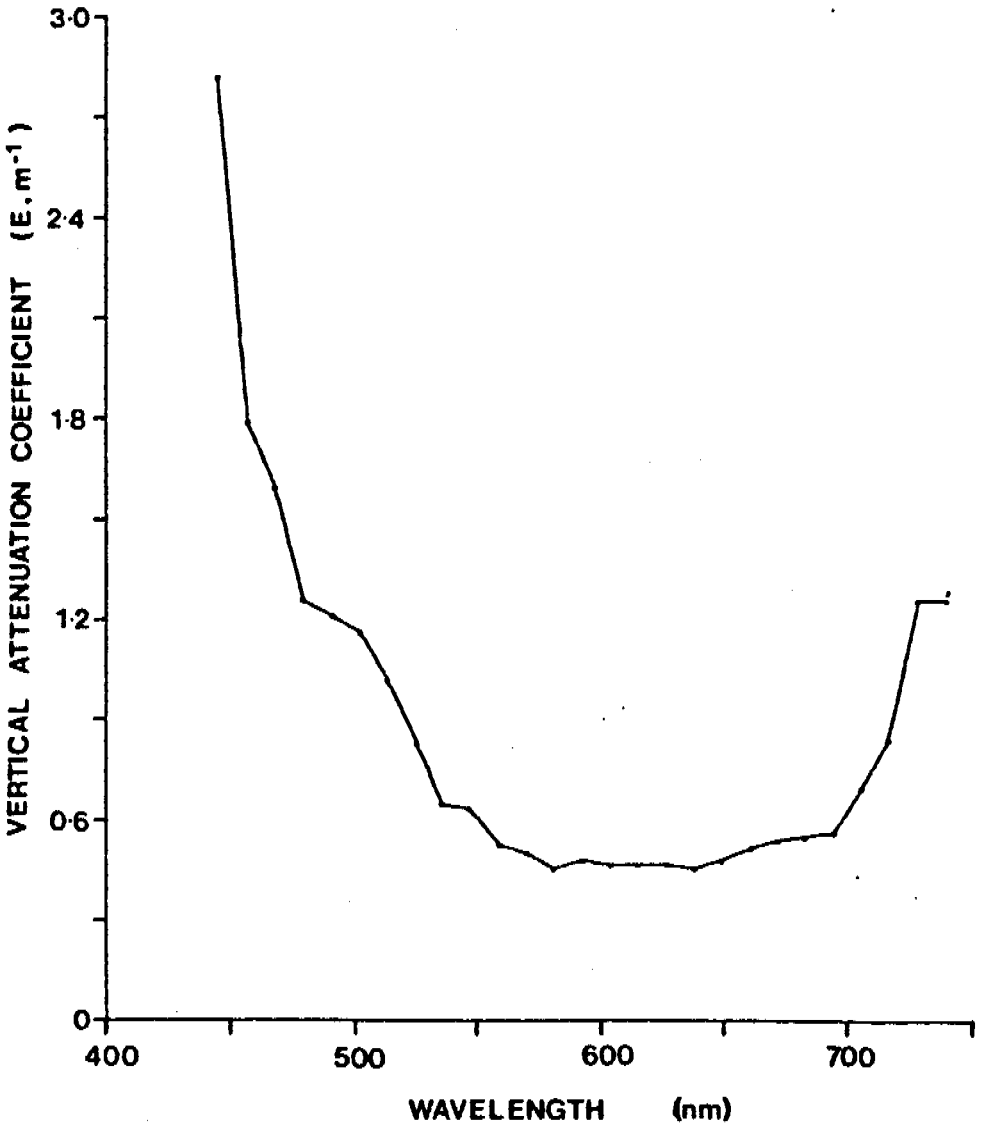

Fig. 4.5.4 The attenuation spectrum of Kulukuluku billabong on 14/8/81.

Table 4.6B

Date	Time (hrs)	E_d (m^{-1})	z_{eu} (m)	$z_{S.D.}$ (m)
30/10/80	1200	0.55	3.6	
26/ 3/81	0755	0.62	3.2	1.5
28/ 4/81	0915	0.67	3.0	2.0
13/11/79	0945	0.68	2.9	0.8
5/ 6/78	1100	0.69	2.9	1.4
26/ 8/80	1600	0.70	2.9	1.2
19/ 7/79	0815	0.72	2.8	1.3
24/ 5/79	0855	0.72	2.8	1.55
26/ 2/81	0810	0.78	2.6	1.9
15/ 8/79	0900	0.81	2.5	1.2
8/12/80	1530	0.84	2.4	1.1
21/ 6/79	1345	0.98	2.0	

Table 4.6A Optical characteristics of Island billabong. Symbols as for Table 4.2A.

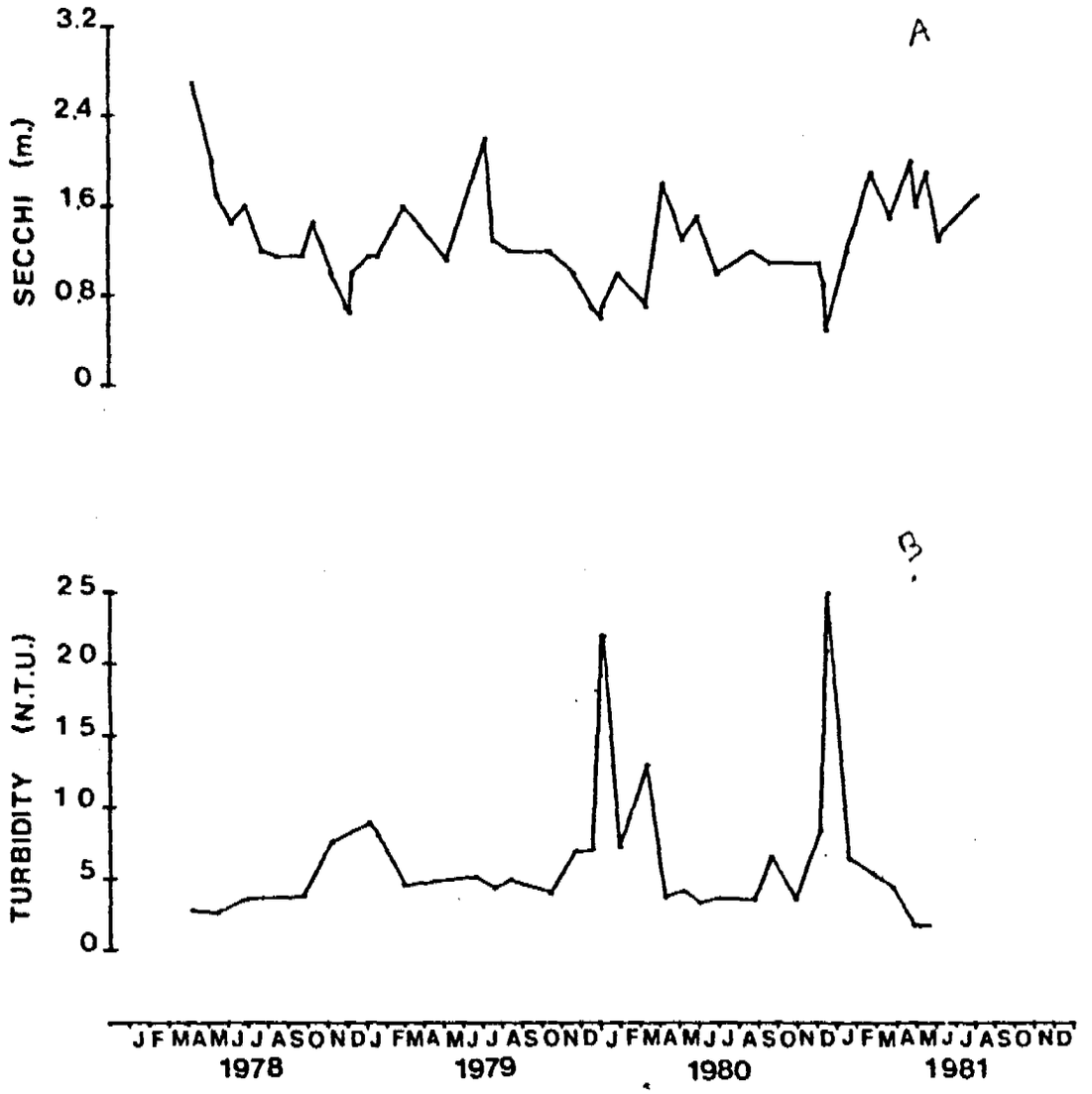

Fig. 4.6.1 Seasonal variations in Secchi transparency (A) and turbidity (B) in Island billabong.

by a decline for the remainder of the Dry. Minima of transparency, coincident with pulses of turbidity (Fig. 4.6-1B), indicate the first flushes of the Wet. Over the Dry, the turbidity remains almost constantly low.

Although the range of variation of gilvin concentrations differs from year to year, the pattern of seasonal fluctuation appears to be similar (Fig. 4.6-2A), with an annual maximum during the first weeks of the Wet. By the Wet/Dry interchange a considerable fall in gilvin levels has occurred, but an early Dry maximum soon follows. For the remainder of the Dry, whilst no rain falls, gilvin values decline until the onset of the first rains.

Chlorophyll levels during the Dry (Fig. 4.6-2B) indicate that Island attains a higher trophic status than all the other billabongs previously described. The annual minimum occurs early in the Wet, rising to a maxima in the early Dry. The remainder of the Dry is characterized by capricious fluctuations. For much of the Dry, phytoplankton populations are suspected to be the major contributor to turbidity, but, as they are swept out by the first flush, tripton becomes the major component of turbidity. It seems likely that the fluctuations in chlorophyll concentrations through the Dry are the main cause of the random changes in euphotic depth.

Given Island's higher trophic status during the Dry, it is not surprising that on both occasions for which *in situ* spectroradiometric data is available (Fig. 4.6-3,4), strong absorption occurred at the chlorophyll-a wavelength of 660-670 nm. However, as for other billabongs, the dominant feature of the spectrum is the rapid disappearance of the 400-500 nm waveband, an event highlighted by the attenuation spectrum (Fig. 4.6-5). This is hardly surprising given that both sets of data were obtained at the time when gilvin achieves its early Dry maximum.

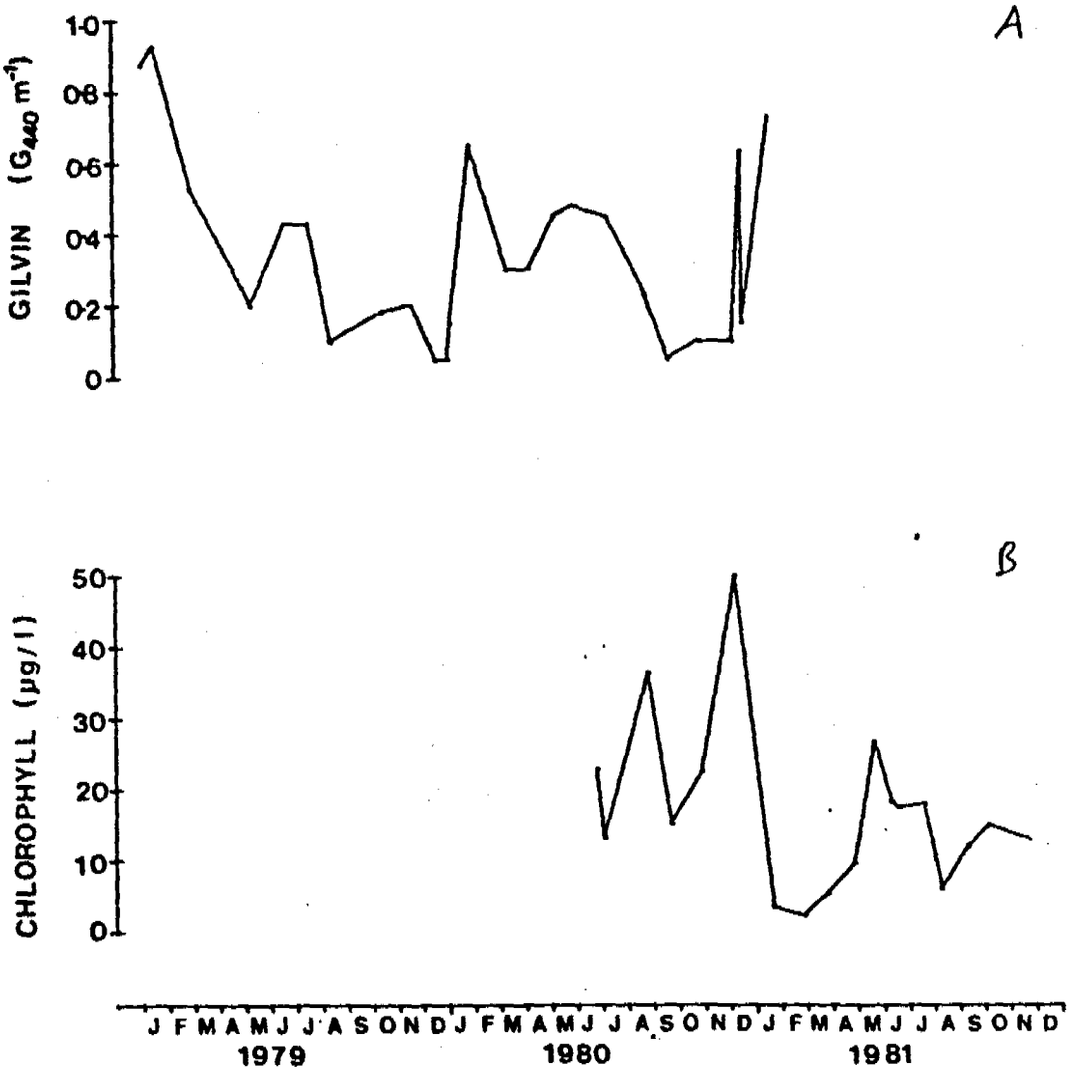

Fig. 4.6.2 Seasonal variations in gilvin (G_{440}) (A) and chlorophyll (B) in Island billabong.

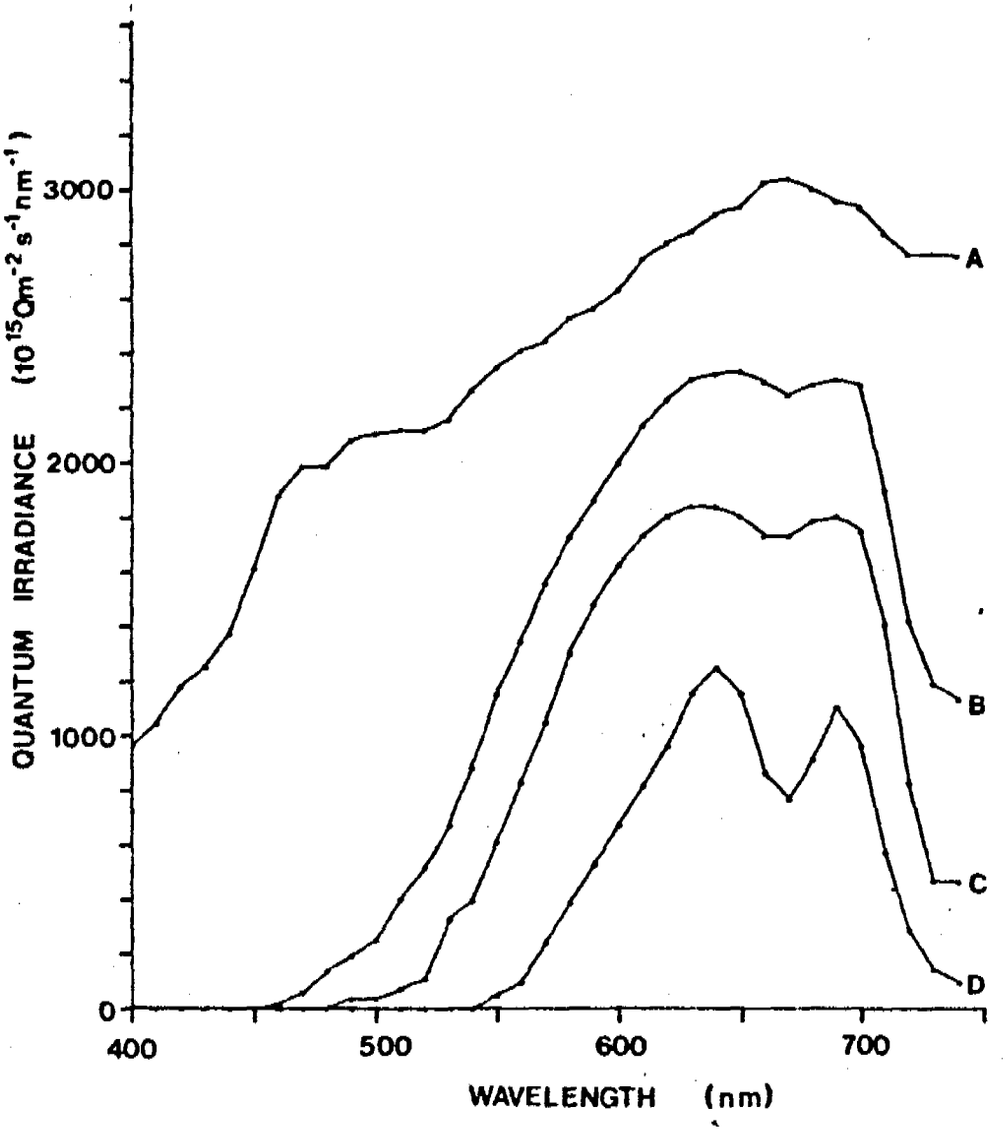

Fig. 4.6.3 *In situ* quantaspectrometric measurements at selected depths in Island billabong on 7/6/78.

A = 0.02 m : ~ 100% Q_o

B = 0.5 m (x1.6) : 37% Q_o

C = 1.0 m (x3) : 14% $Q_o \approx z_m$

D = 3.0 m (x40) : 0.7% $Q_o \approx z_{eu}$

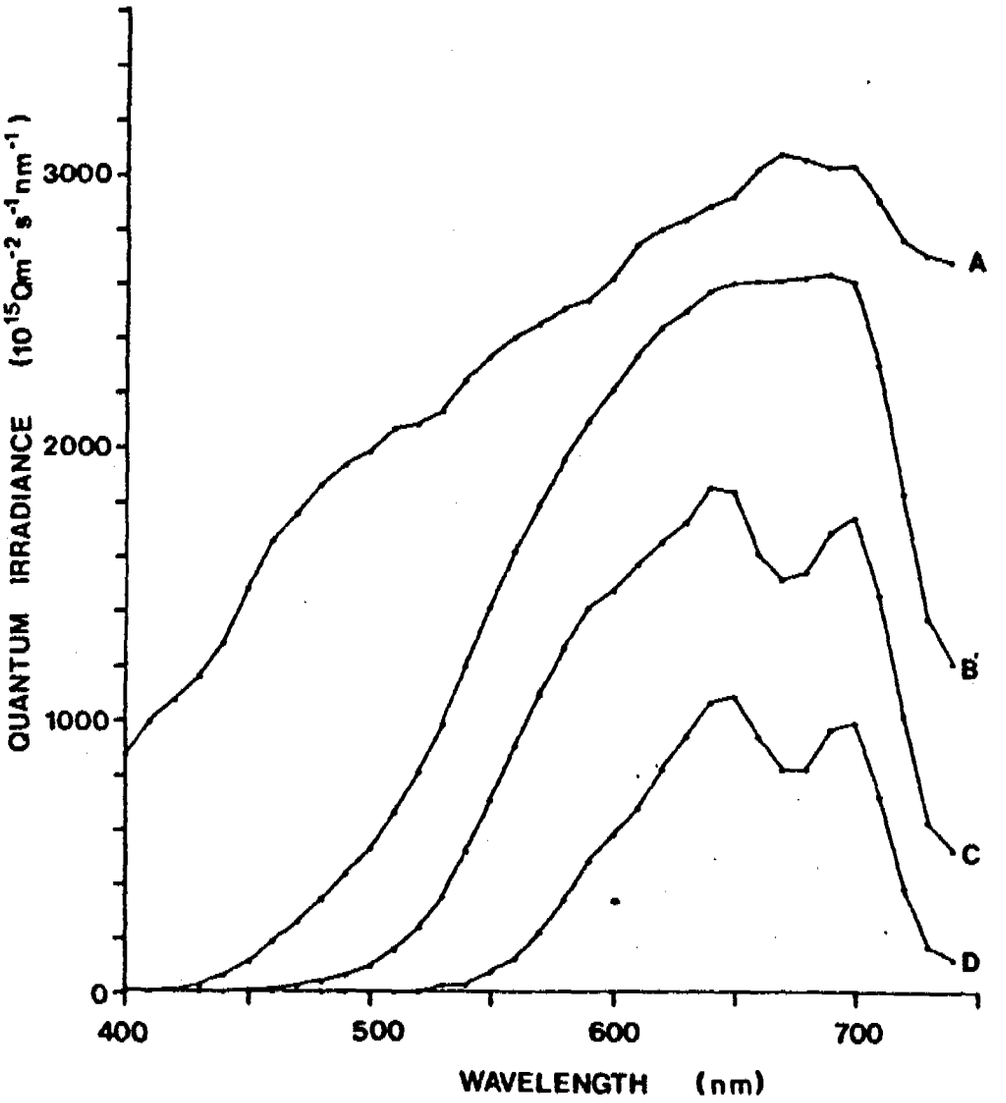

Fig. 4.6.4 *In situ* quantaspectrometric measurements at selected depths in Island billabong on 26/5/79.

A = 0.1 m : 71% Q_o

B = 0.5 m (x1.5)

C = 1.0 m (x2) : 12% $Q_o \approx z_m$

D = 3.0 m (x20) : 0.5% $Q_o \approx z_{eu}$

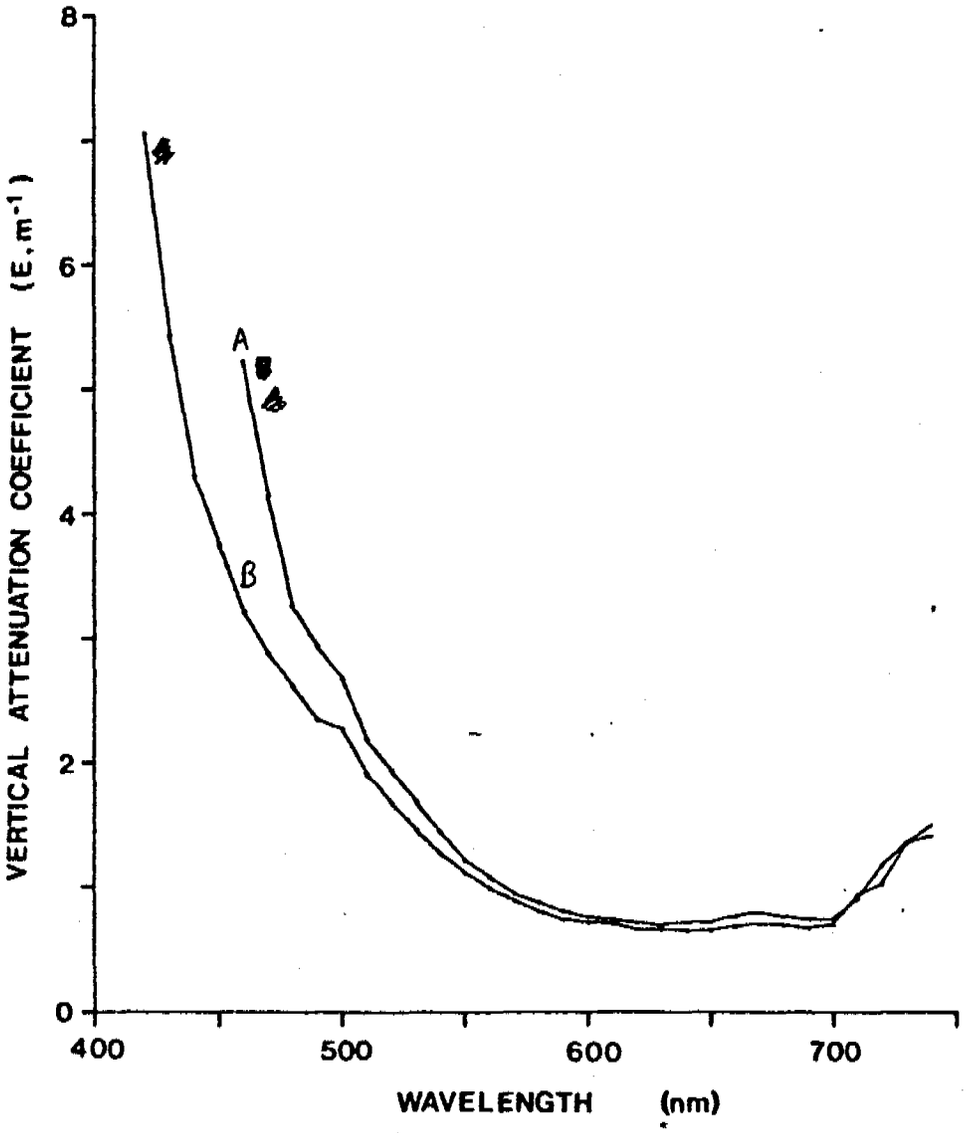

Fig. 4.6.5 The attenuation spectra of Island billabong on 7/6/78 (A) and 26/5/79 (B).

4.7 The underwater light climate in Leichhardt billabong

PAR attenuation coefficients (Table 4.7) provide strong evidence for a progressive contraction of the euphotic zone during the Dry, from a maximum during the weeks just after the Wet/Dry interchange. There is a 2 metre range in z_{eu} over this period, with a minimum depth of about 1 metre. Unfortunately PAR profile data for the Dry/Wet interchange is unavailable, but transparency data (Fig. 4.7-1A) indicate minimal water clarity during the first flush, as incoming floodwaters wash debris into the billabong from the flood plain. Subsequently, there is a general improvement in transparency over the Wet and Wet/Dry interchange until its peak in the early Dry.*

Complementary seasonal trends in turbidity (Fig. 4.7-1B) occur. Turbidity increases through the middle and late Dry to a maximum at the first flush. Thereafter it decreases as the Wet progresses except during unusually high floodpeaks. Contrary to turbidity, gilvin values (Fig. 4.7-2A) decreased during the Dry.

Chlorophyll results (Fig. 4.7-2B) demonstrate both the capricious nature of fluctuations in phytoplankton populations throughout the Dry, as well as the very high levels which may be attained, the highest of all billabongs examined in the Region. Chlorophyll concentrations are at a minimum throughout the Wet.

The only spectral irradiance data available is from a time of low chlorophyll concentrations, yet there was apparently some absorption at the chlorophyll-a wavelength (Fig. 4.7-3). Again, there was rapid attenuation of short wavelengths, the 400-520 nm waveband being eliminated by z_{eu} (Fig. 4.7-3), with relatively constant attenuation over the 550-700

* Sudden, short-lived minima around the time of this peak occurred in May 1979 and June 1981, an event possibly attributable to a minor phytoplankton bloom (see below). The 1.5-2.0 m decline in transparency as the Dry progresses correlates strongly with the diminishing euphotic depth over the same period.

Table 4.7A.

Date	Time (hrs)	E_d (m^{-1})	z_{eu} (m)	$z_{S.D.}$ (m)
8/ 6/79	0830	0.62	3.2	1.4
10/ 7/79	0835	0.78	2.6	2.0
7/ 4/81	0740	0.82	2.4	
15/ 8/80	1000	0.89	2.2	1.1
5/ 9/80	1220	1.03	1.9	0.8
16/10/80	1300	1.06	1.9	0.7
1/ 8/79	0905	1.10	1.8	1.0
10/11/80	1300	1.54	1.3	0.35
13/11/80	1215	1.79	1.1	0.45

Table 4.7A Optical characteristics of Leichardt billabong. Symbols as for Table 4.2A.

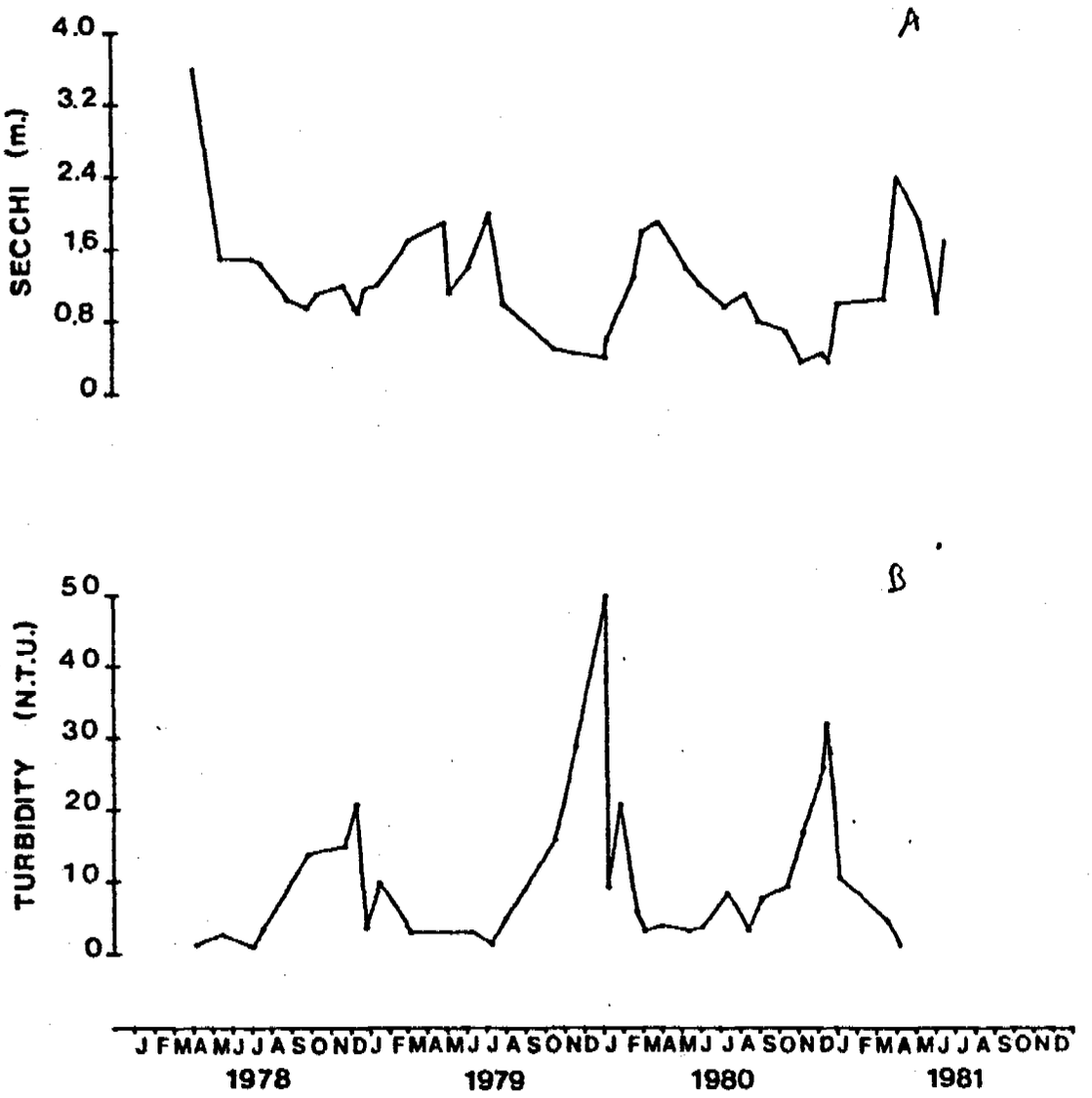

Fig. 4.7.1 Seasonal variations in Secchi transparency (A) and turbidity (B) in Leichardt billabong.

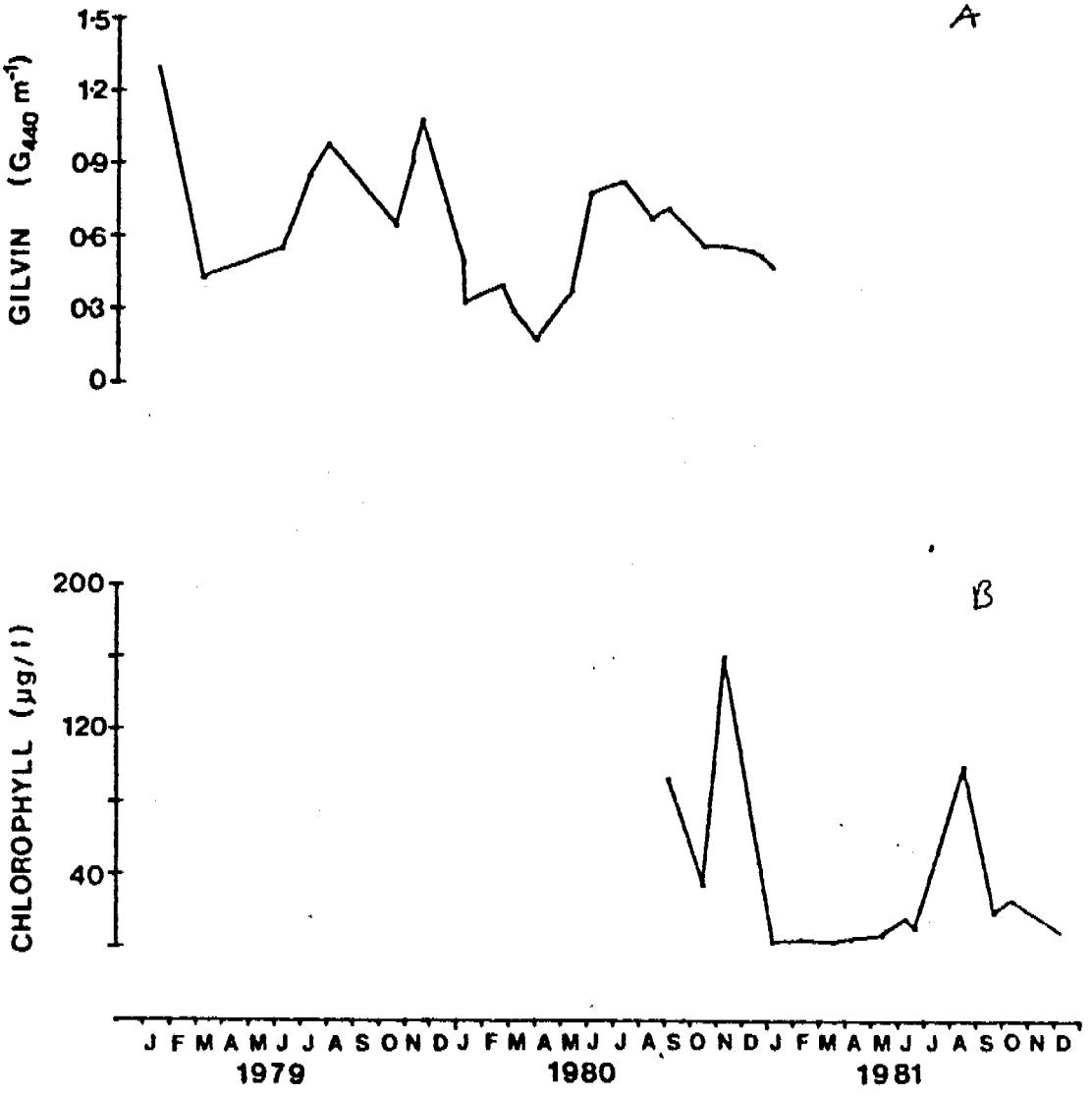

Fig. 4.7.2 Seasonal variations in gilvin (G_{440}) (A) and chlorophyll (B) in Leichardt billabong.

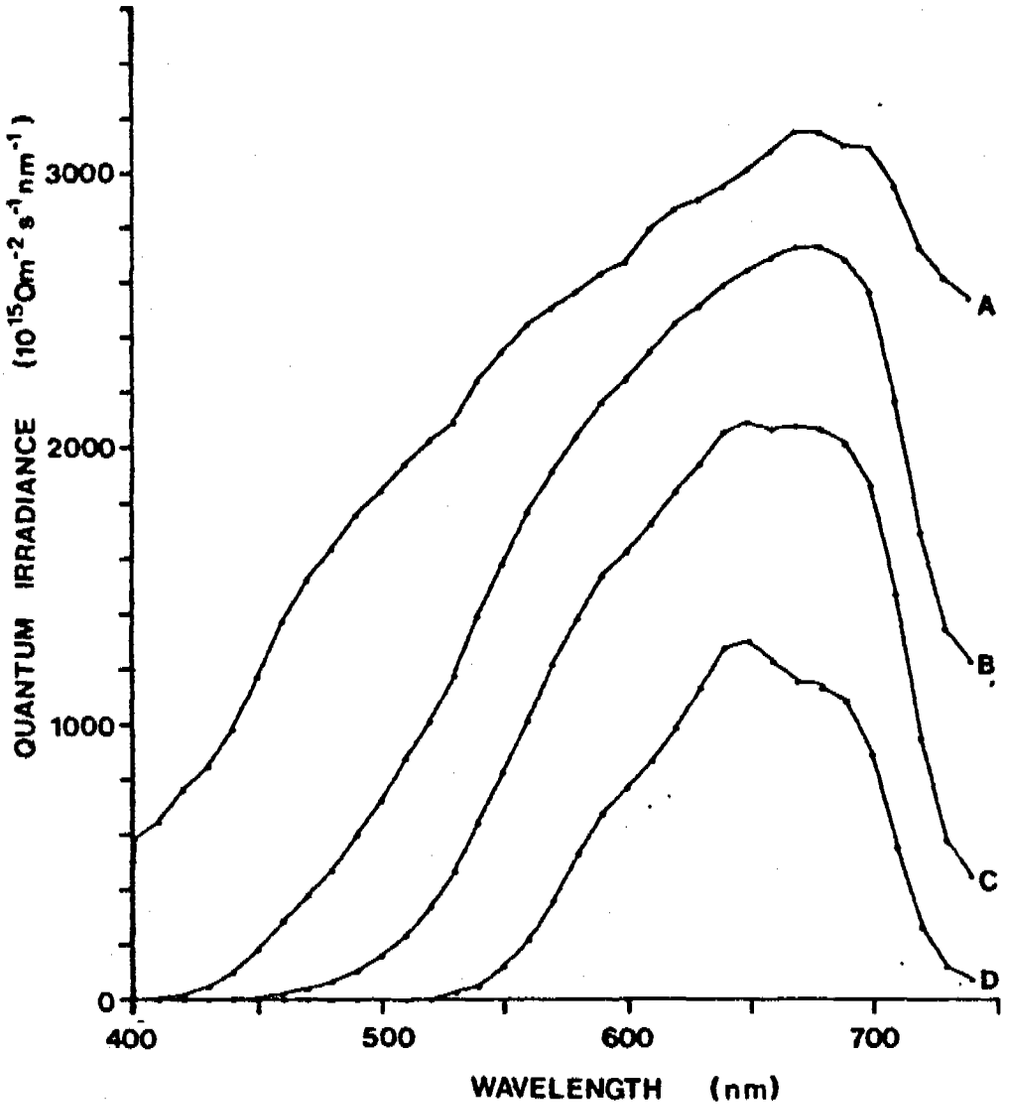

Fig. 4.7.3 *In situ* quantaspectrometric measurements at selected depths in Leichardt billabong on 29/5 /79.

A = 0.1 m : 89% Q_o

B = 0.5 m (x1.5)

C = 1.0 m (x2.5) : 18% $Q_o \approx z_m$

D = 3.0 m (x20) : 0.7% $Q_o \approx z_{eu}$

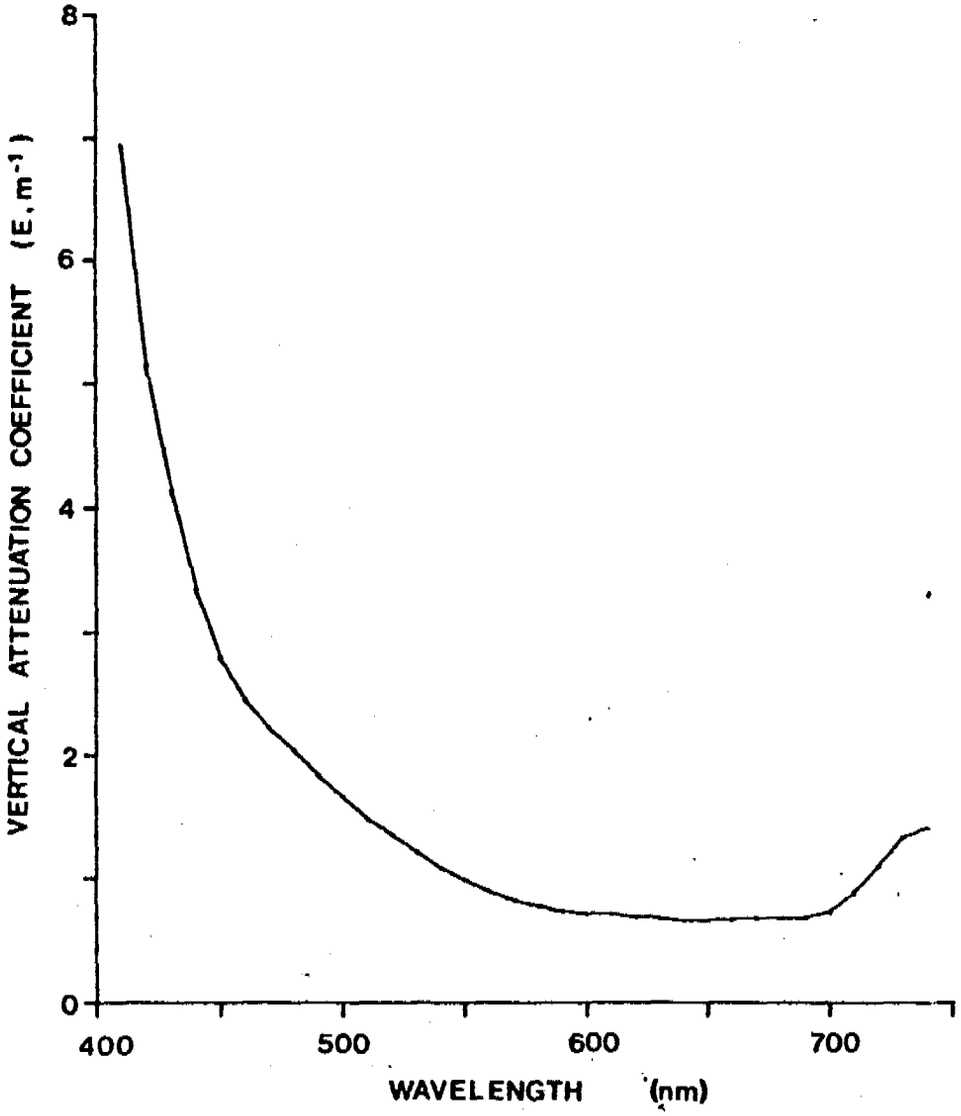

Fig. 4.7.4 The attenuation spectrum of Leichardt billabong on 29/5/79.

nm waveband (Fig. 4.7-4).

4.8 The underwater light field in Ja Ja billabong

Although only two PAR attenuation profiles were taken in Ja Ja, three months apart, it is apparent (Table 4.8) that a severe contraction of the euphotic zone occurs during the Dry season. Transparency (Fig. 4.8-1A) and turbidity (Fig. 4.8-1B) data bear out this conclusion. Transparencies ranged from 3.9 to 0.1 m from April to November, 1978, whilst turbidity soared from 2-140 NTU in the same period.

Chlorophyll levels, (Fig. 4.8-2), low in the Wet, increase to a maximum by the mid Dry, then decline as turbidity increases, limiting algal populations.

The irradiance spectra for June and September (Fig. 4.8-3,4) clearly show the considerable effects of the heavy tripton load, both in comparison with non-turbid billabongs and within the one billabong with a large seasonal range of turbidity. Not only is attenuation extremely rapid, but also transmission is limited to a very narrow waveband at the red end. Comparison of the June spectrum with those of other, non-turbid billabongs, reveals that the transmission peak has been shifted from about 650 nm to around 700 nm. By September, with a twentyfold increase in turbidity, the transmission band is further narrowed, with its peak shifted still more into the red. The attenuation spectra (Fig. 4.8-5) clearly show the changes brought about by the increasing turbidity.

4.9 The underwater light field in Goanna billabong

PAR attenuation data (Table 4.9) indicate that within the space of two months the euphotic zone in this shallow billabong may contract by a metre, to a depth of only 0.4 metres by early August. Transparency data (Fig. 4.9-1A) indicate that further decrease of euphotic depth may be expected during the remainder of the Dry, as surface turbidities (Fig. 4.9-1B) reach exceptionally high levels (300 N.T.U.). By the late Dry,

Table 4.8A

Date	Time (hrs)	E_d (m^{-1})	z_{eu} (m)	$z_{S.D.}$ (m)
7/ 6/78	1400	1.01	2.0	0.75
18/ 9/78	1330	2.04	1.0	

Table 4.8B Optical characteristics of Ja Ja billabong. Symbols as for Table 4.2A.

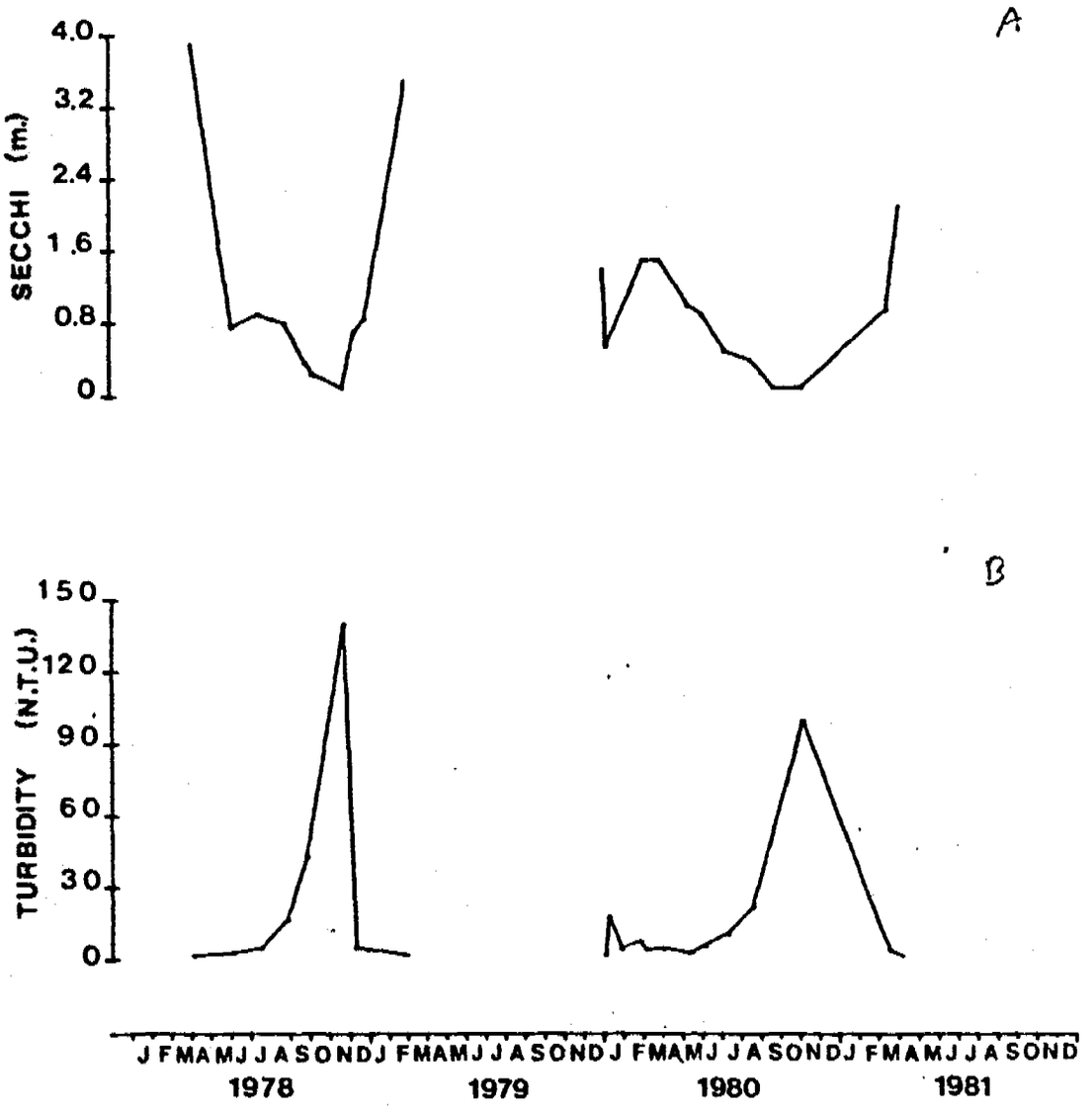

Fig. 4.8.1 Seasonal variations in Secchi transparency (A) and turbidity (B) in Ja Ja billabong.

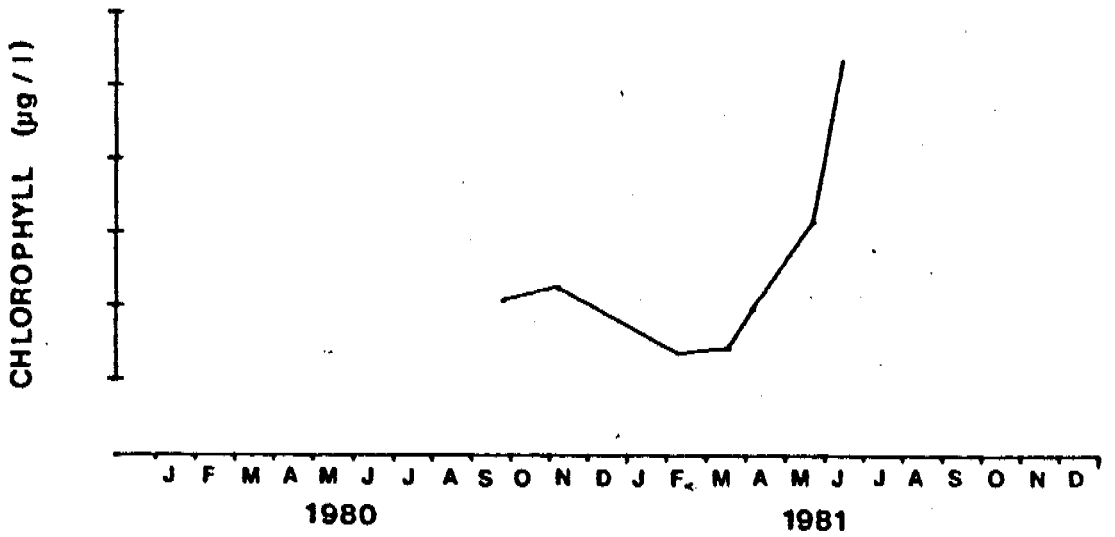

Fig. 4.8.2 Seasonal variations in chlorophyll in Ja Ja billabong.

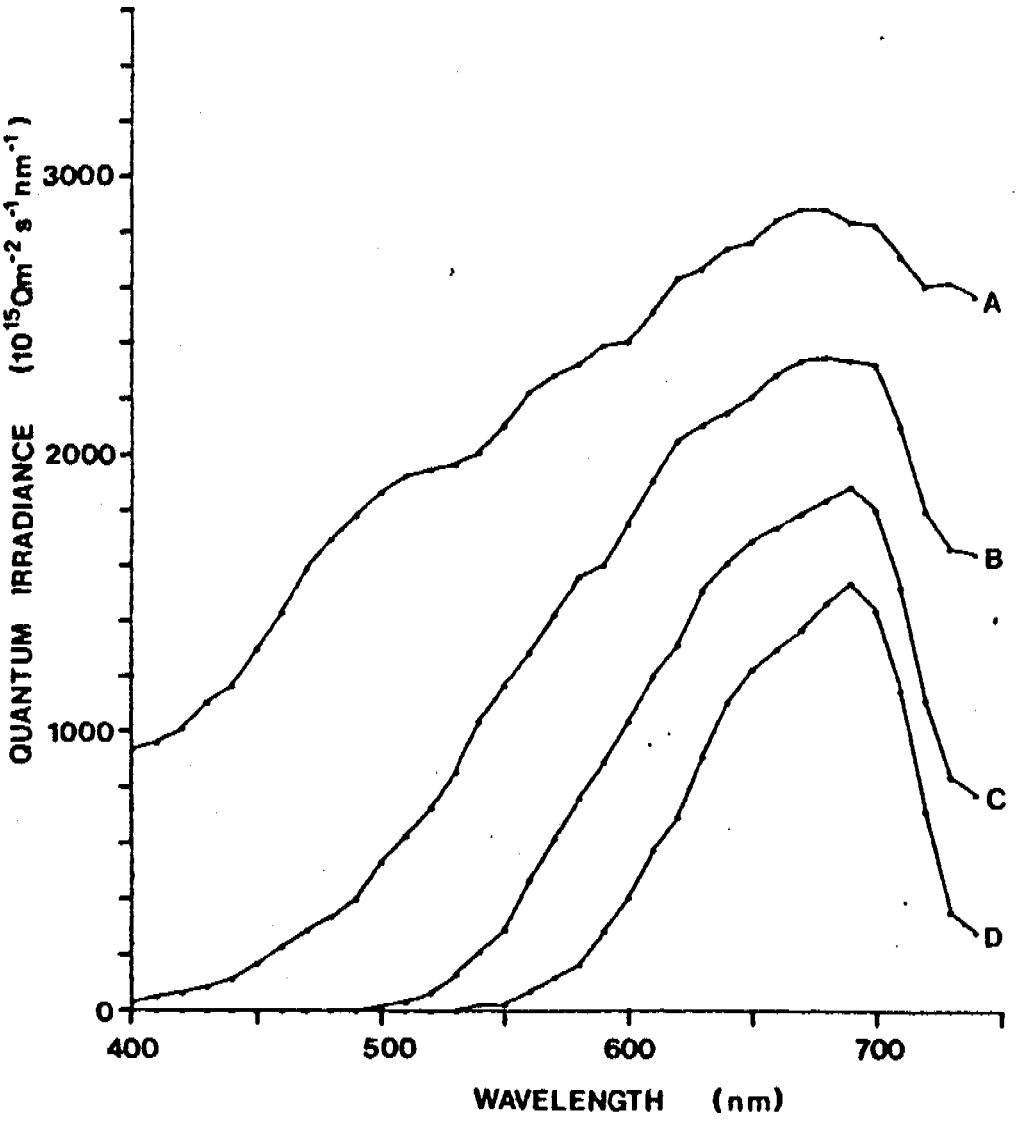

Fig. 4.8.3 *In situ* quantaspectrometric measurements at selected depths in Ja Ja billabong on 7/6/78.

A = 0.02 m : ~ 100% Q_o

B = 0.2 m (x1.2)

C = 0.6 m (x1.7) : 13% $Q_o \approx z_m$

D = 1.5 m (x20) : 2% $Q_o \approx z_{eu}$

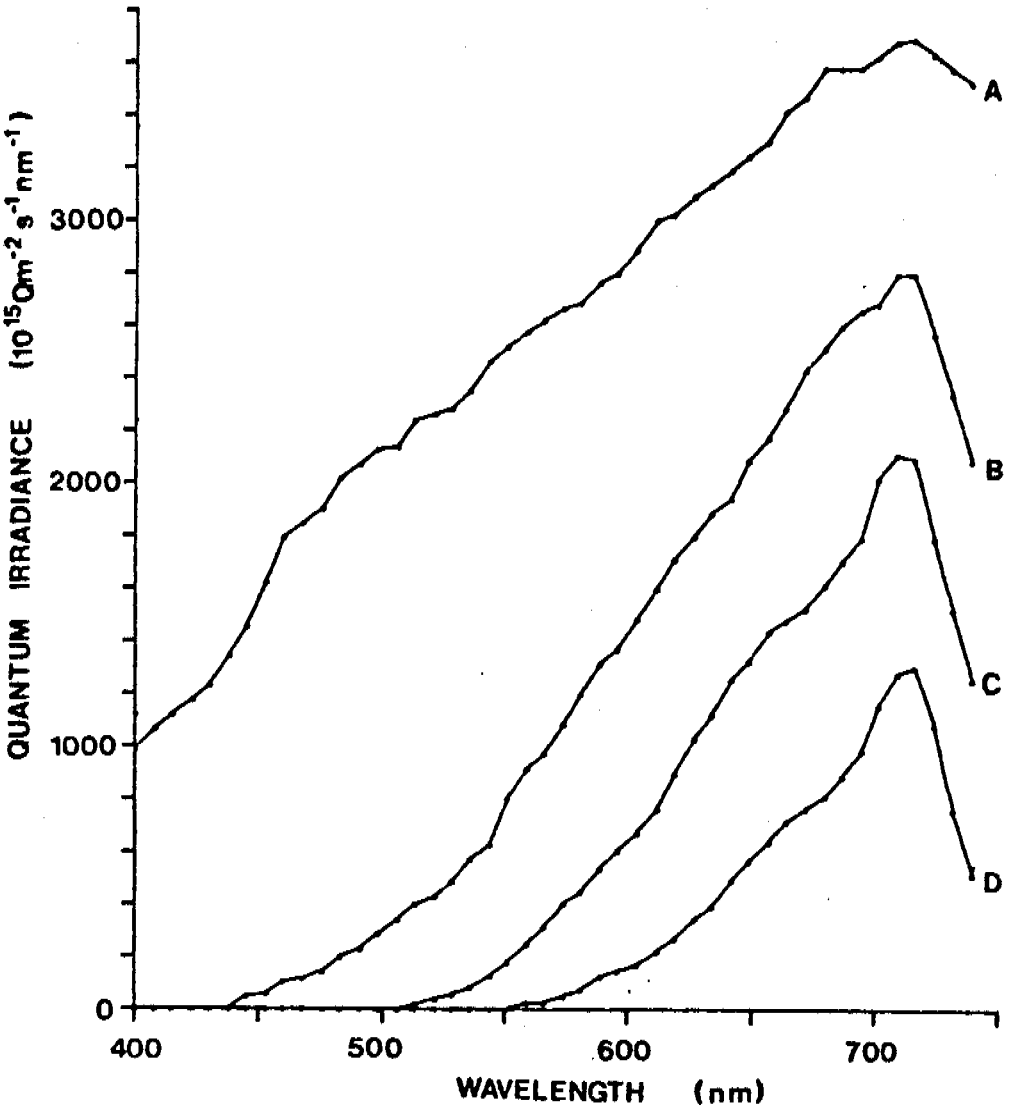

Fig. 4.8.4 *In situ* quantaspectrometric measurements at selected depths in Ja Ja billabong on 18/9/78.

A = 0.01 m : ~ 100% Q_o

B = 0.2 (x1.7) : 30% Q_o

C = 0.5 (x4) : 7% $Q_o \approx z_m$

D = 1.0 (x22) : 0.7% $Q_o \approx z_{eu}$

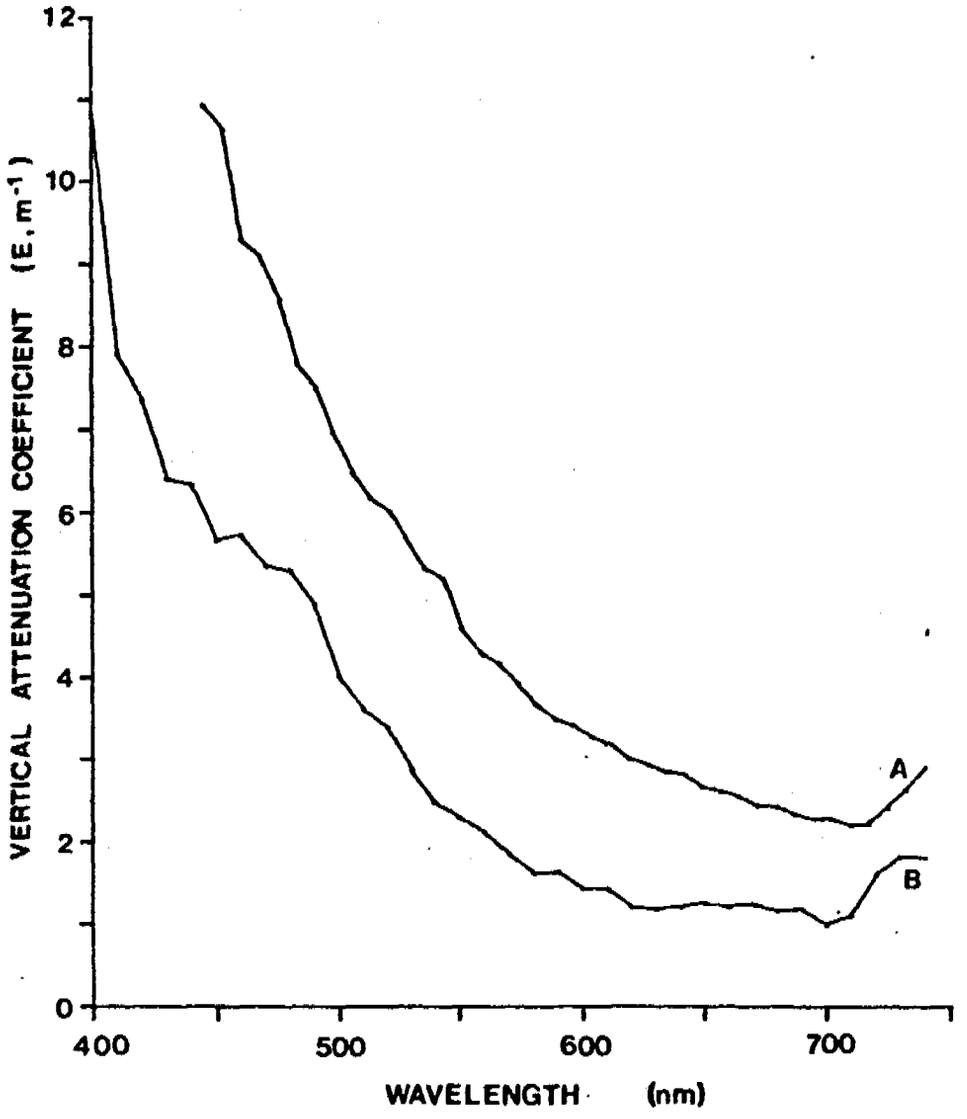

Fig. 4.8.5 The attenuation spectra of Ja Ja billabong on ١٢/١/٣٤(A) and ٢/٦/٣٤ (B).

Table 4.9A

Date	Time (hrs)	E_d (m^{-1})	z_{eu} (m)	$z_{S.D.}$ (m)
9/6/78	1320	1.44	1.4	
31/7/78	1120	2.11	0.9	
23/6/79	0945	2.33	0.9	
10/8/79	1020	5.51	0.4	0.15

Table 4.9A Optical characteristics of Goanna billabong. Symbols as for Table 4.2A.

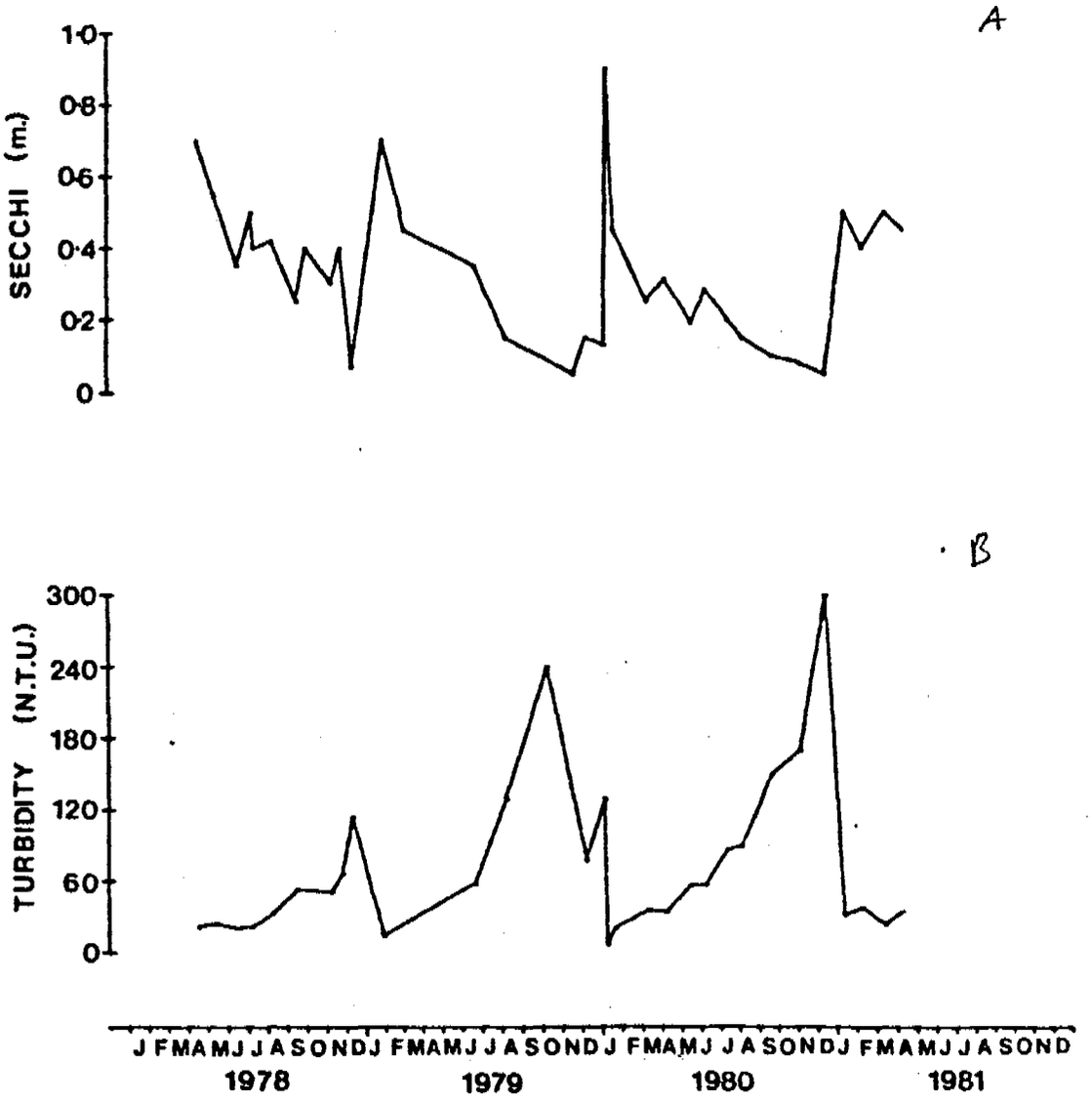

Fig. 4.9.1 Seasonal variations in Secchi transparency (A) and turbidity (B) in Goanna billabong.

transparencies may fall as low as 0.05 m. It is interesting to note that in the three successive years turbidity maxima progressively increased.

In Goanna, in contrast to Ja Ja, chlorophyll increases during the Dry then abruptly declines as the Wet commences (Fig. 4.9-2B).

The single spectral irradiance curve (Fig. 4.9-3) is similar overall to that of Ja Ja except that the transmission peak is not so far towards the red. The attenuation spectrum (Fig. 4.9-4) shows a curious maximum at 420 nm. Instrumental error is suspected.

4.10 The underwater light field in Jabiluka billabong

Although the E_d values (Table 4.10 and Fig 4.10.1) span four years those from the same months do not vary appreciably from year to year, so that together the 4 years of data give a seasonal picture. This picture, borne out by the transparency data (Fig. 4.10-2A), is one of contraction of the euphotic zone over the Dry as turbidity levels markedly increase (Fig. 4.10-2B). Each year, the Wet brings dramatic improvements in water clarity as the turbid billabong is flushed.

The maximum euphotic depth (≃ 3m) occurs at the Wet/Dry interface. However, rapid deterioration in water clarity halves the euphotic zone by June. For the next 2-3 months the euphotic depth changes little and then declines abruptly to less than 0.5 m in the late Dry, at the time of maximum turbidity. The sudden drop in turbidity values in January 1980 coincided with sudden increases in acidity of the billabong waters. This is likely to have caused flocculations (cf. Hart & McGregor, 1980). Subsequent recovery of turbidity values occurred at the first flush.

Gilvin values (Fig. 4.10-2A) are at a maximum just after the Wet/Dry interchange, fluctuate erratically during the Wet, and decline during the Dry. Chlorophyll values decreased regularly during the 1980 Dry, but fluctuated erratically in the 1981 Dry (Fig. 4.10-2B).

As with the other turbid billabongs, peak transmission occurs near

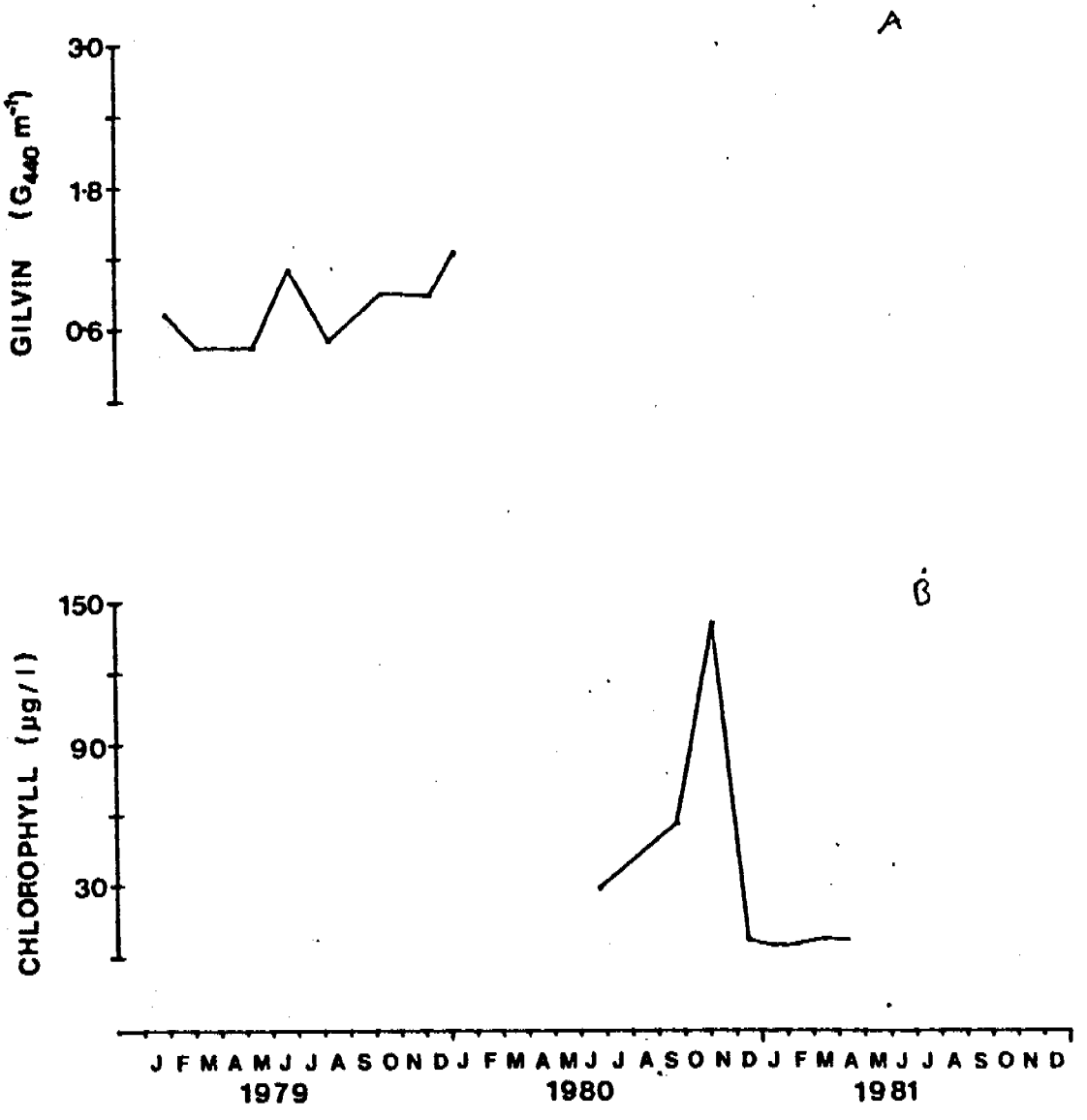

Fig. 4.9 Seasonal variations in gilvin (G440) (A) and chlorophyll (B) in Goanna billabong.

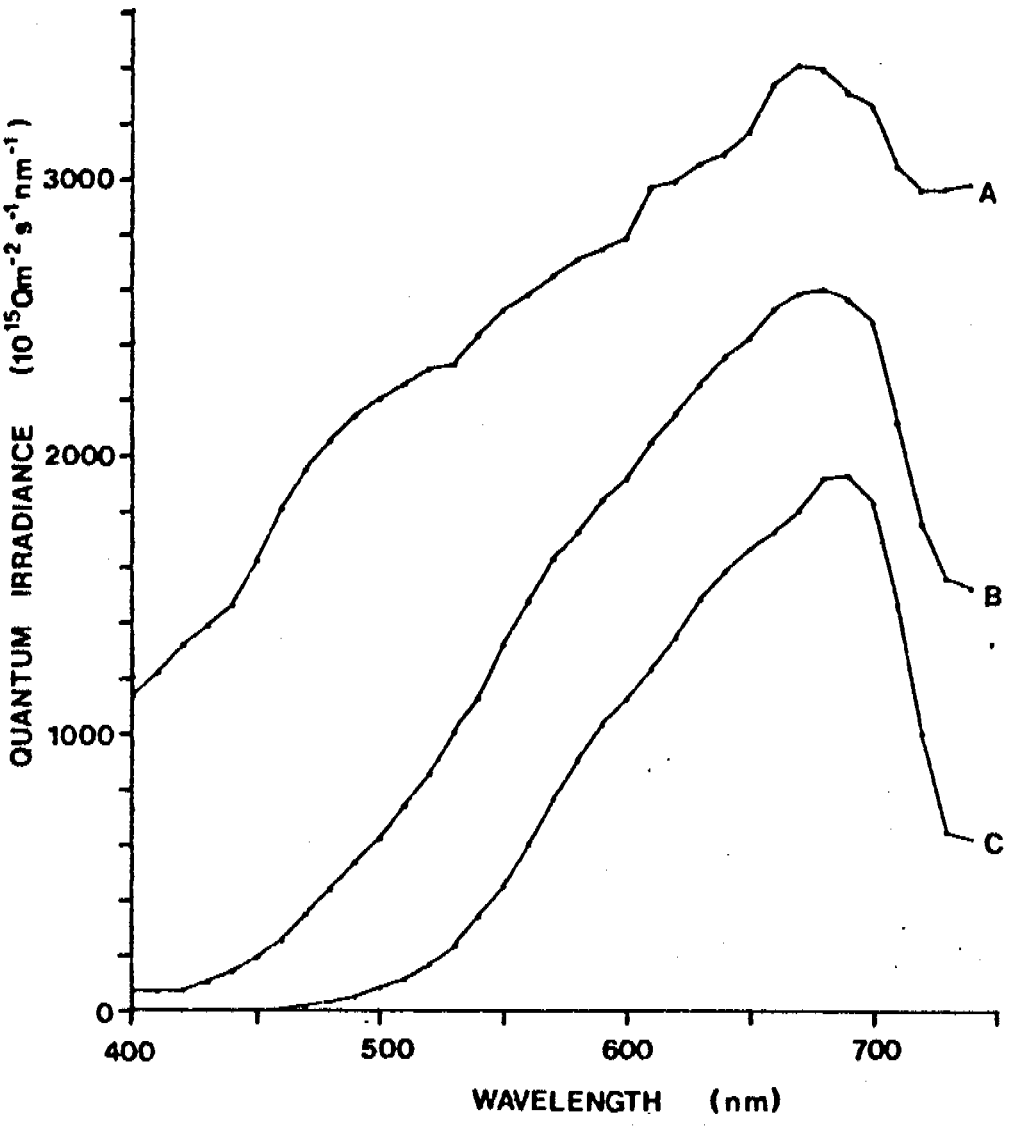

Fig. 4.9.3 *In situ* quantaspectrometric measurements at selected depths in Goanna billabong on 9/6/78 .

A = 0.025 m : ~100% Q_o

B = 0.3 m (x1.7) : 37% Q_o

C = 0.7 m (x5) : 0.9% $Q_o \propto z_m$

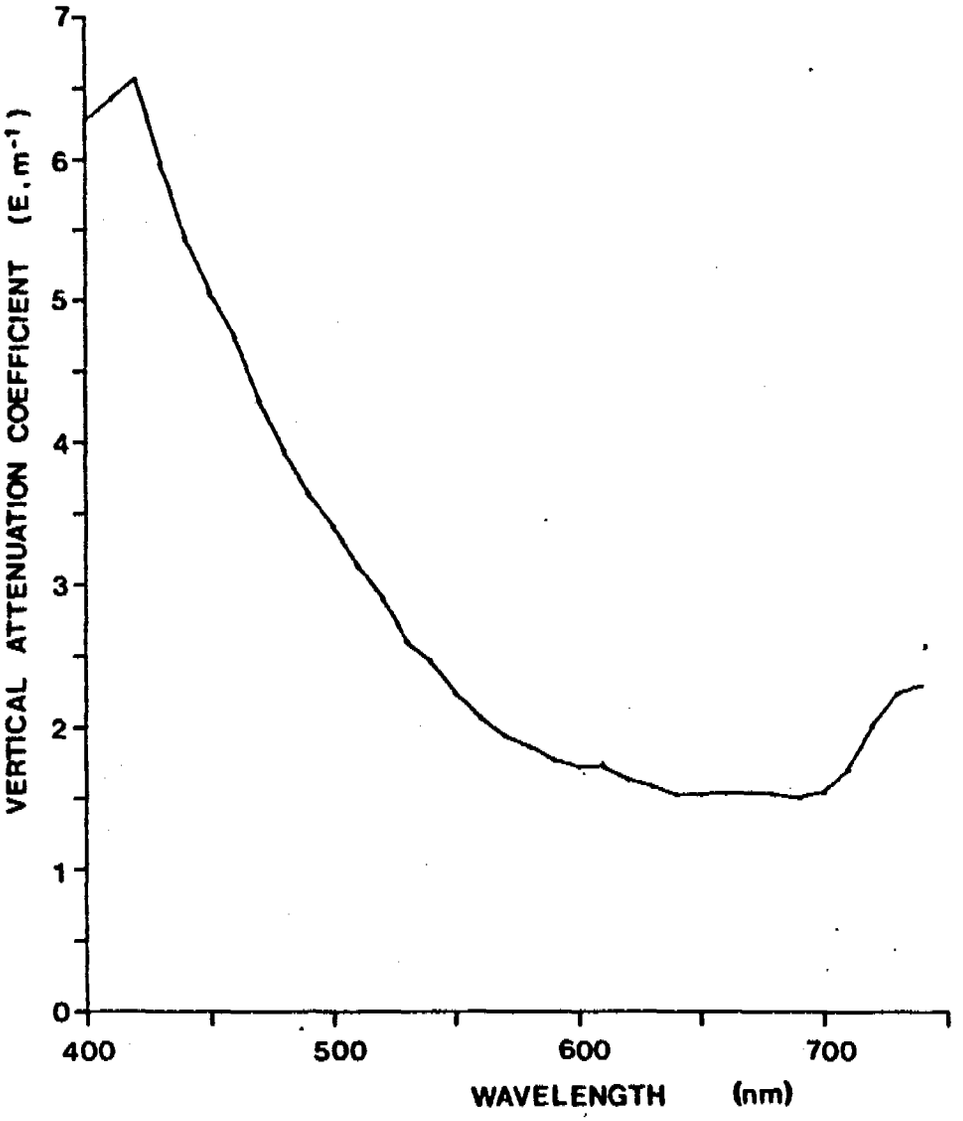

Fig. 4.9.4 The attenuation spectrum of Goanna billabong on 9/6/78.

Table 4.10A

Date	Time (hrs)	E_d (m^{-1})	z_{eu} (m)	$z_{S.D.}$ (m)
7/ 4/81	0900	0.65	3.1	2.3
28/ 5/79	1430	1.07	1.9	
11/ 7/79	0830	1.39	1.4	0.6
12/ 6/79	0840	1.41	1.4	0.45
9/ 8/79	0845	1.59	1.3	0.5
30/ 8/80	1245	1.81	1.1	0.4
24/10/80	1530	3.39	0.6	0.3
25/11/80	0820	5.09	0.4	0.08
13/11/79	1115	6.84	0.3	0.15

Table 4.10A Optical characteristics of Jabiluka billabong. Symbols as for Table 4.2A.

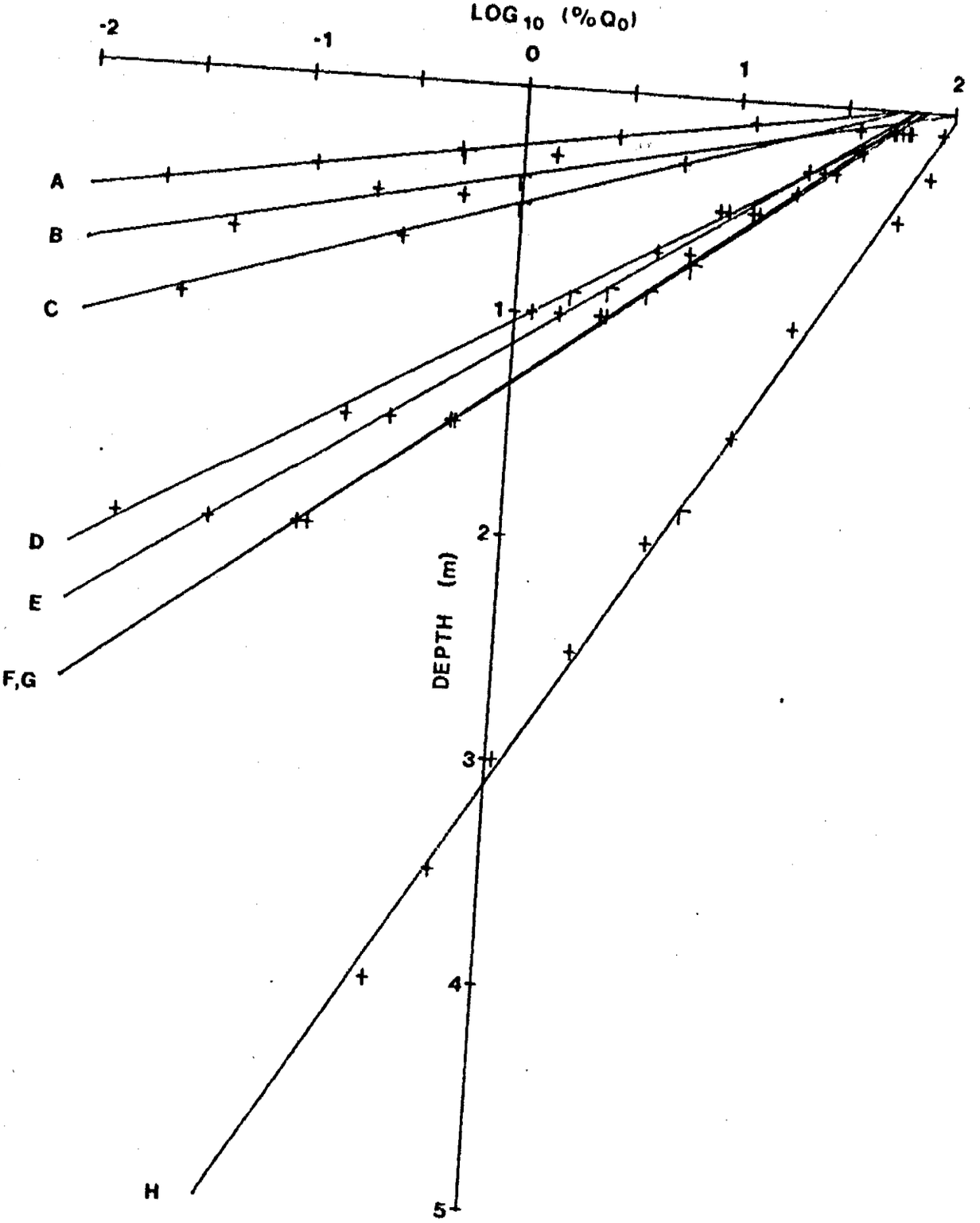

Fig 4.10-1. Vertical attenuation of downwelling PAR in Jabiluka billabong at various times of the year. The slope of the line is $-E$ (vertical attenuation coefficient) and the intercept on the y axis gives the euphotic depth ($Z_{eu} = \ln Q_0 = {}^2/_E$).

A = 13/11/79; B = 25/11/80; C = 24/10/80; D = 30/9/80;
E = 9/8/79; F = 11/7/79; G = 12/6/79; H = 27/4/81.

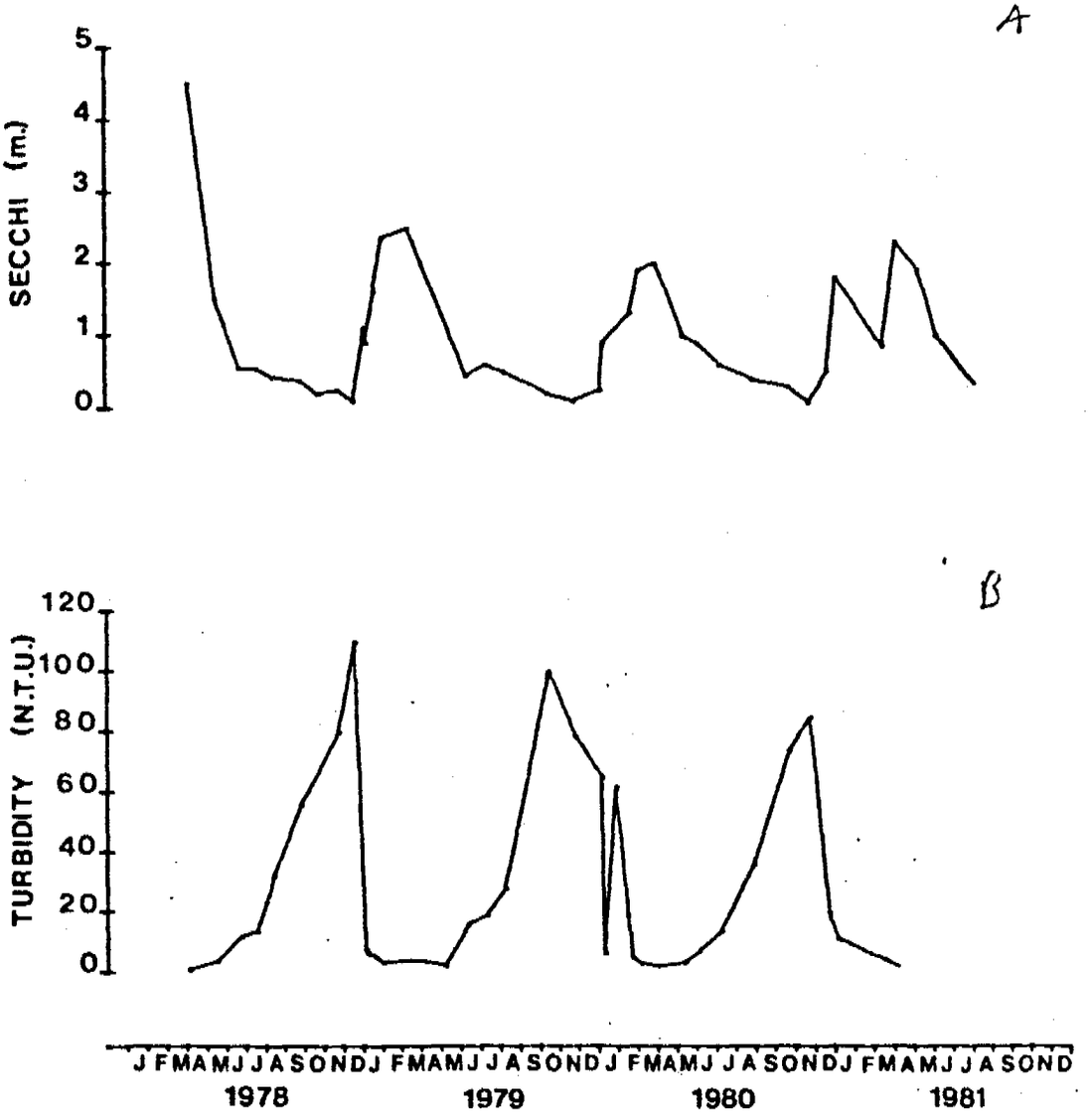

Fig. 4.10.1 Seasonal variations in Secchi transparency (A) and turbidity (B) in Jabiluka billabong.

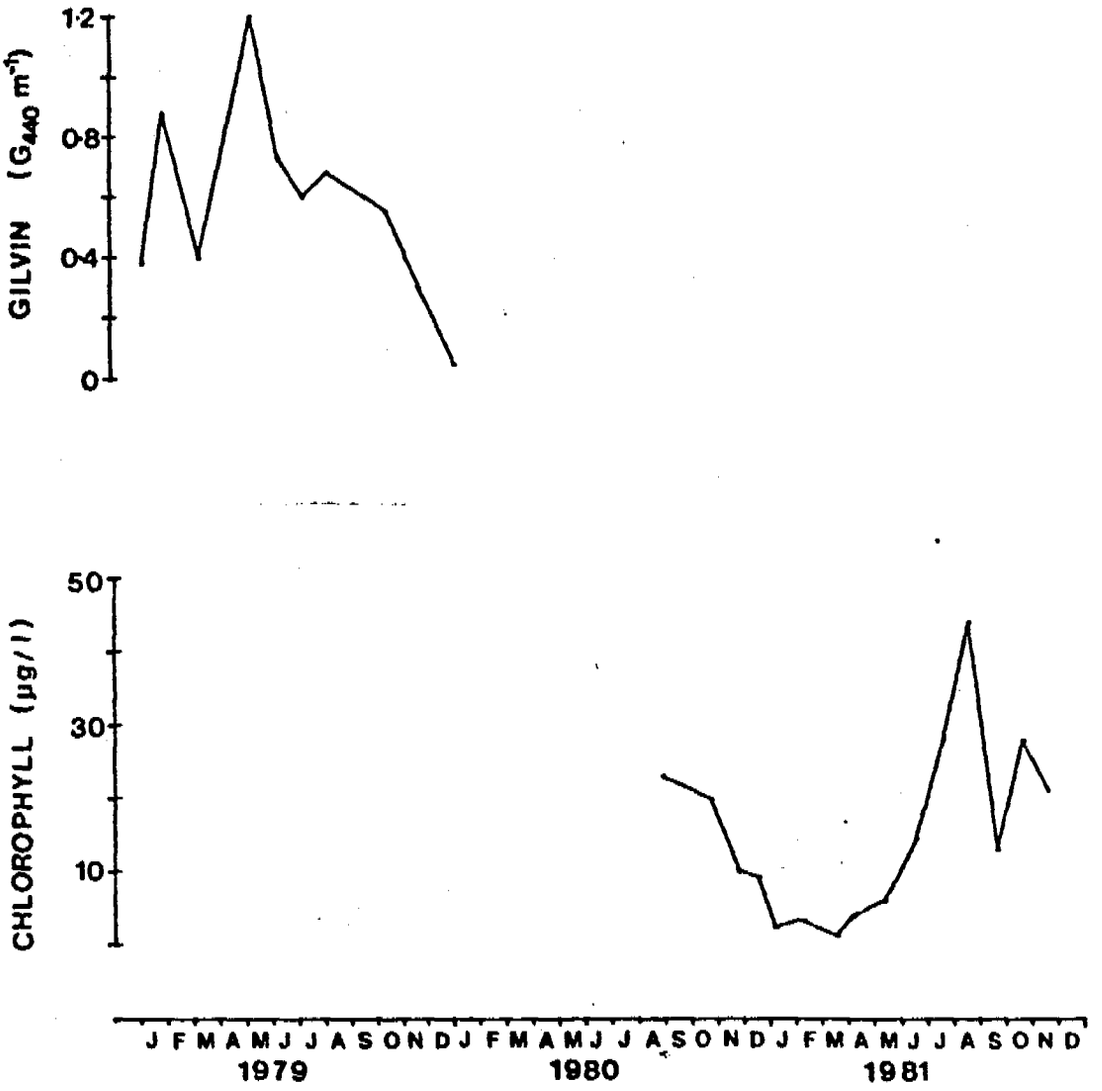

Fig. 4.10.2 Seasonal variations in gilvin (G_{440}) (A) and chlorophyll (B) in Jabiluka billabong.

700 nm (Fig. 4.10-3,4,5) with, in addition, a hint of absorption at the chlorophyll-a wavelength. The same maximum of vertical attenuation coefficient at 420 nm (Fig. 4.10-5,6) occurred as in Goanna.

4.11 The underwater light field in Nankeen billabong

The E_d value (Table 4.11), taken the day after the June profile for Ja Ja (see Section 4.8), indicated a euphotic depth (1.0 m) only half that of Ja Ja. In fact, Nankeen in June had the same euphotic depth as Ja Ja in September. This is to be expected since Nankeen in the Dry is always more turbid than Ja Ja (Figs. 4.8-1B, 4.11-1B). Correspondingly, transparency in Nankeen can fall as low as 0.05 m (Fig. 4.11-1A). As for the other turbid billabongs, water clarity rapidly drops during the Dry as turbidities markedly increase. Chlorophyll levels (Fig. 4.11-2) are at a peak in the early to mid Dry and at a minimum in Wet. The form of the irradiance spectrum at the euphotic depth (Fig. 4.11-3) resembles that of Ja Ja and Jabiluka, with a transmission peak around 700 nm and some chlorophyll-a absorption. The spectral attenuation curve (Fig. 4.11-4) resembles that for Ja Ja.

4.12 The underwater light field in Gulungul billabong

E_d values (Table 4.12) are available for the early Dry and on one occasion during the Wet. From this limited data it is apparent that a dramatic decline in euphotic depth occurs from around mid-June. After August the billabong becomes too shallow to accommodate the underwater equipment, but both transparency and turbidity data (Fig. 4.12-1A,B) indicate that the euphotic zone would be further limited. In 1979, in the three-month period following May, the euphotic depth contracted from 2.1 m to 0.4 m, i.e. to 20% of its former depth.

The basic pattern of water clarity in Gulungul is the same as for the other turbid billabongs, with maximum turbidity and minimum transparency in the Dry. However, in contrast to most billabongs, where

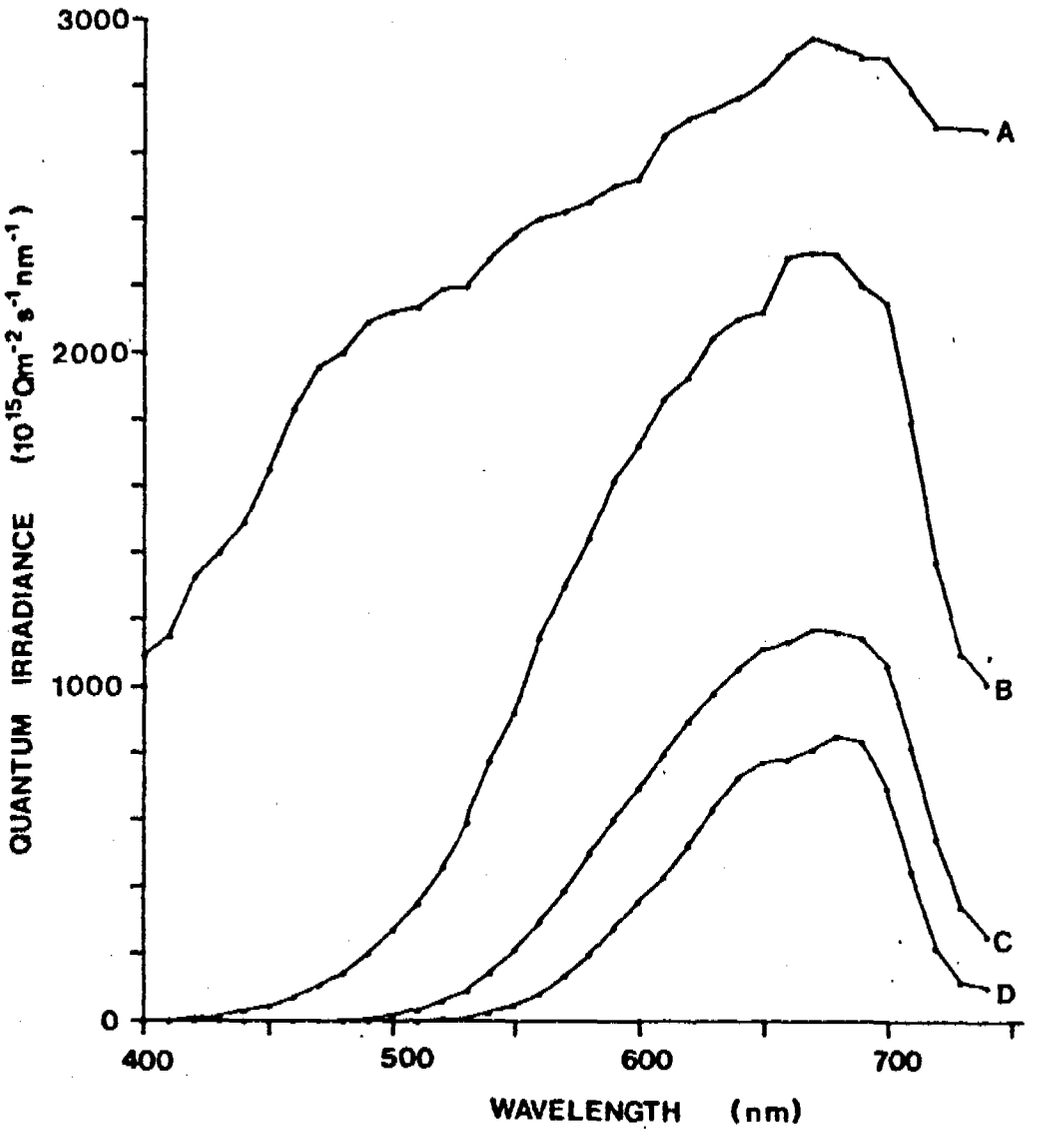

Fig. 4.10.4 *In situ* quantaspectrometric measurements at selected depths in Jabiluka billabong on 28/5/79.

A = Aerial : 100% Q_o

B = 0.5 m (x1.7)

C = 1.0 m (x1.7)

D = 2.0 m (x7)

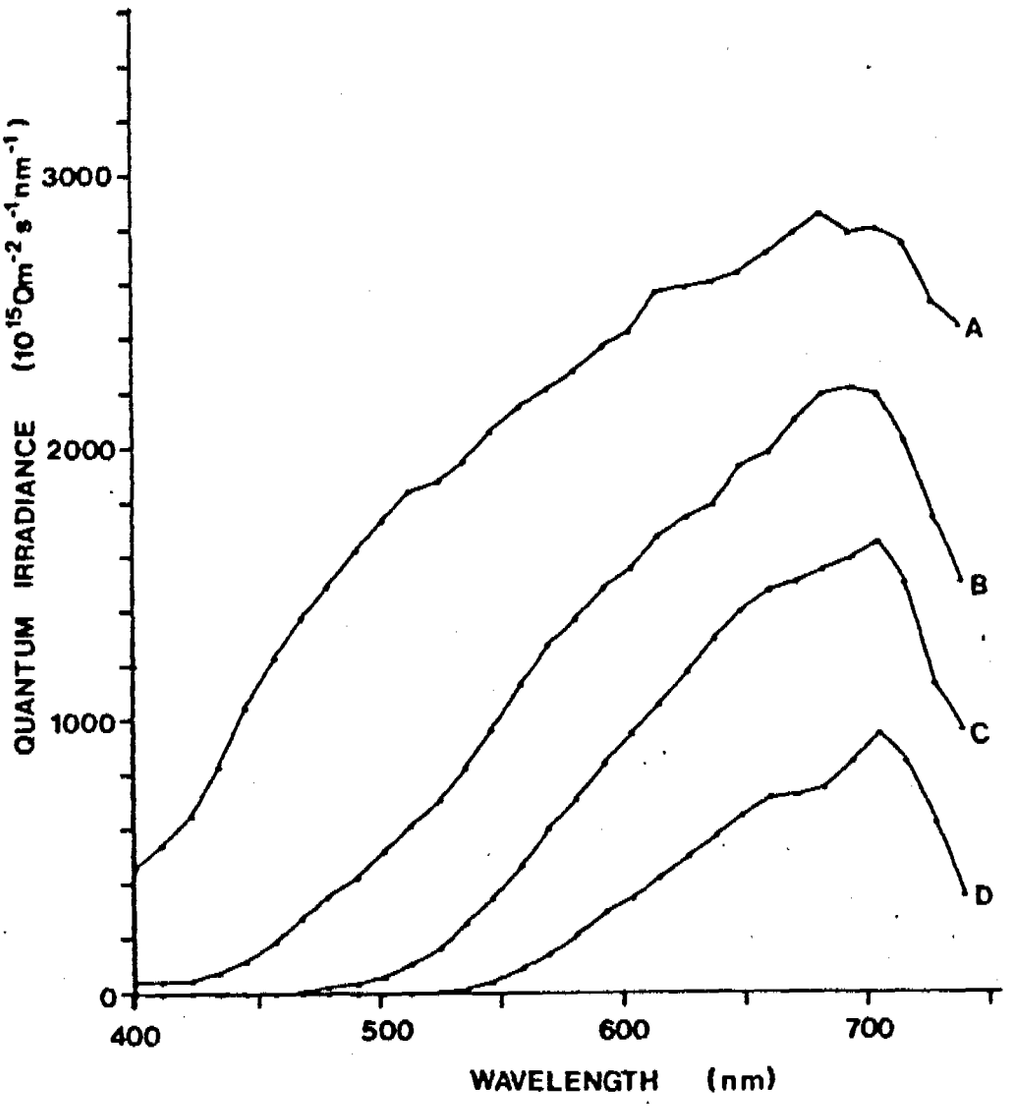

Fig. 4.10.5 *In situ* quantaspectrometric measurements at selected depths in Jabiluka billabong on 9/8/79.

A = 0.2 m : ~100% Q_o

B = 0.2 m (x1.3)

C = 0.5 m (x2.5) : 9% $Q_o \approx z_m$

D = 1.0 m (x7) : 2% $Q_o \approx z_{eu}$

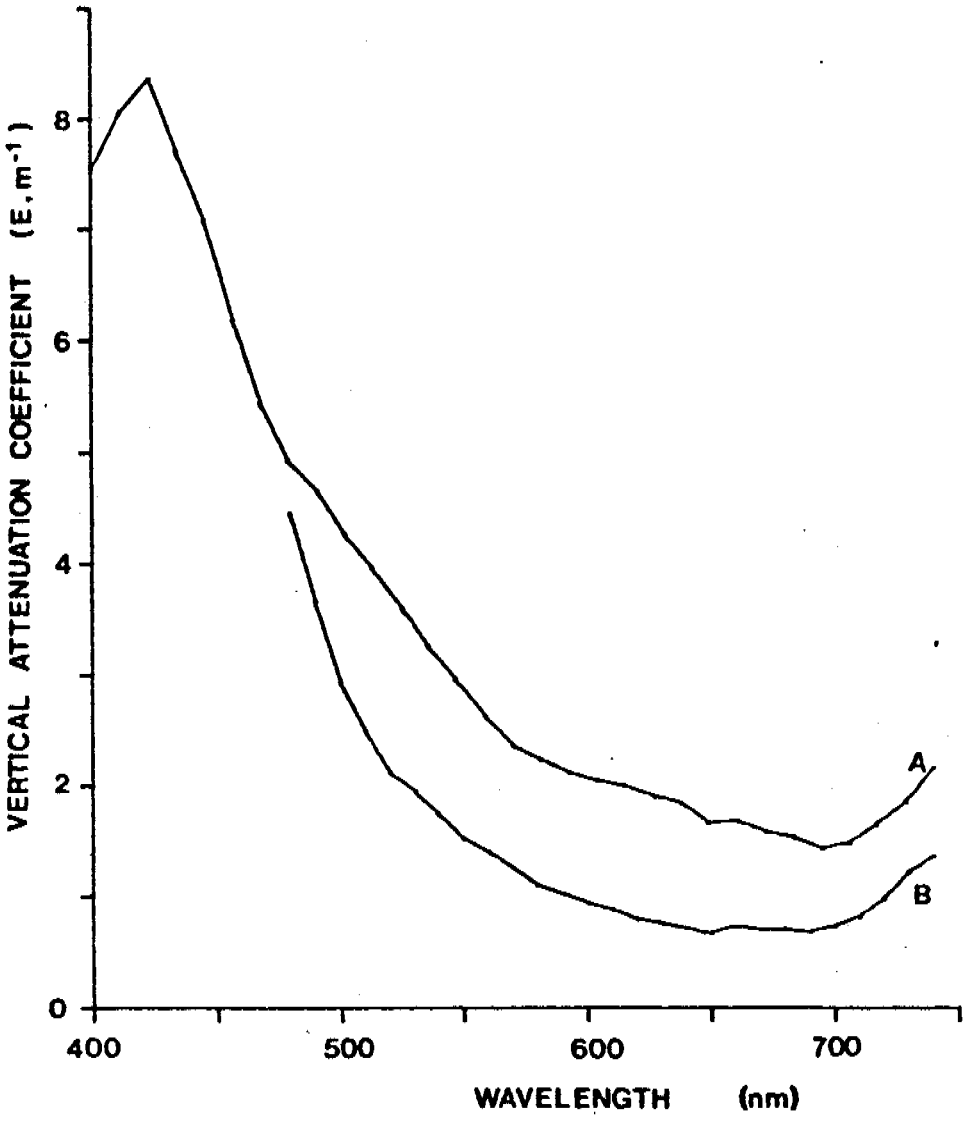

Fig. 4.10.6 The attenuation spectra of Jabiluka billabong on 9/3/79 (A) and 22/5/79 (B).

Table 4.11A

Date	Time (hrs)	E_d (m^{-1})	zeu (m)	$z_{S.D.}$ (m)
8/6/78	1230	2.05	1.0	

Table 4.11A Optical characteristics of Nankeen billabong. Symbols as for Table 4.2A.

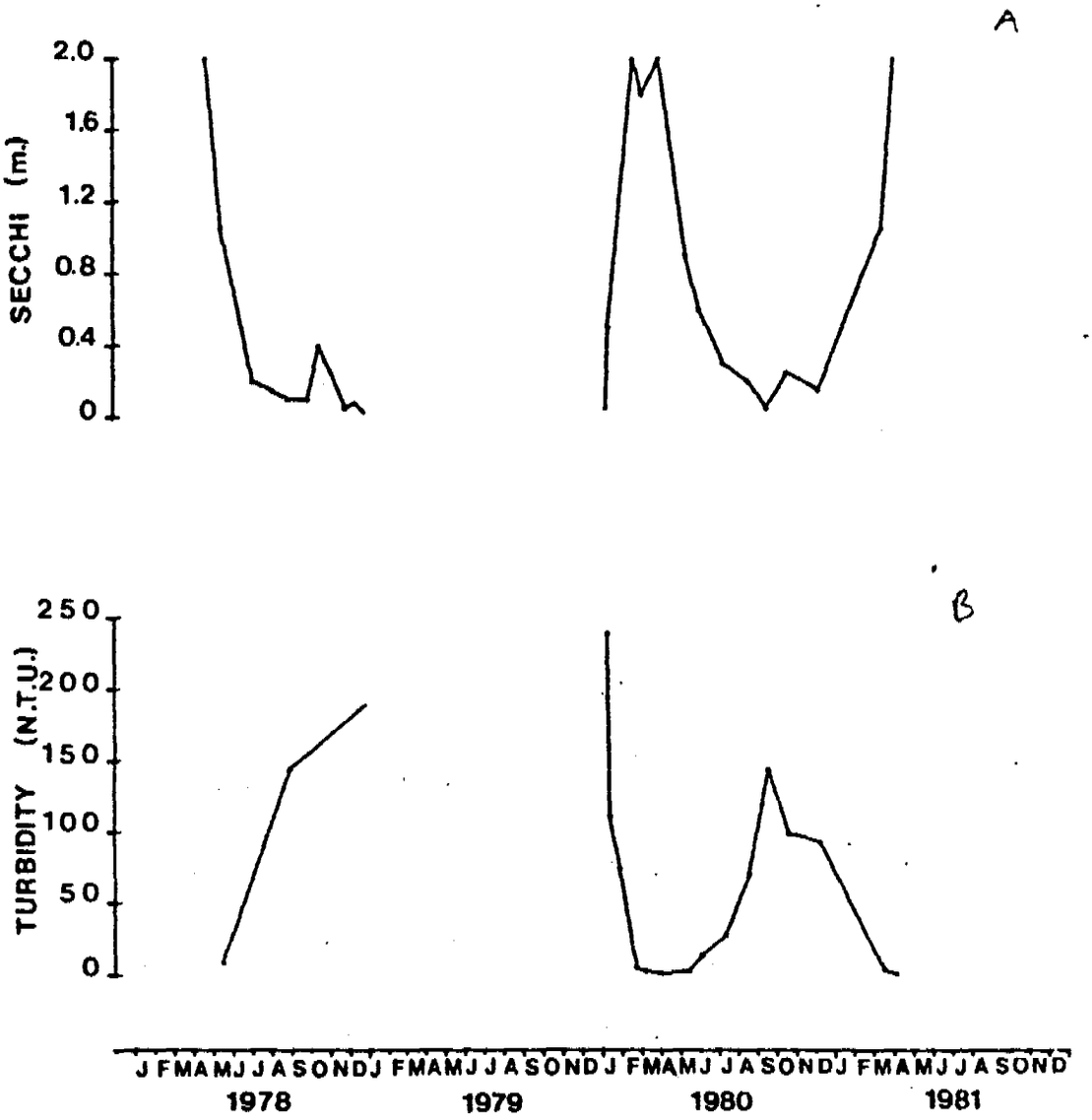

Fig. 4.11.1 Seasonal variations in Secchi transparency (A) and turbidity (B) in Nankeen billabong.

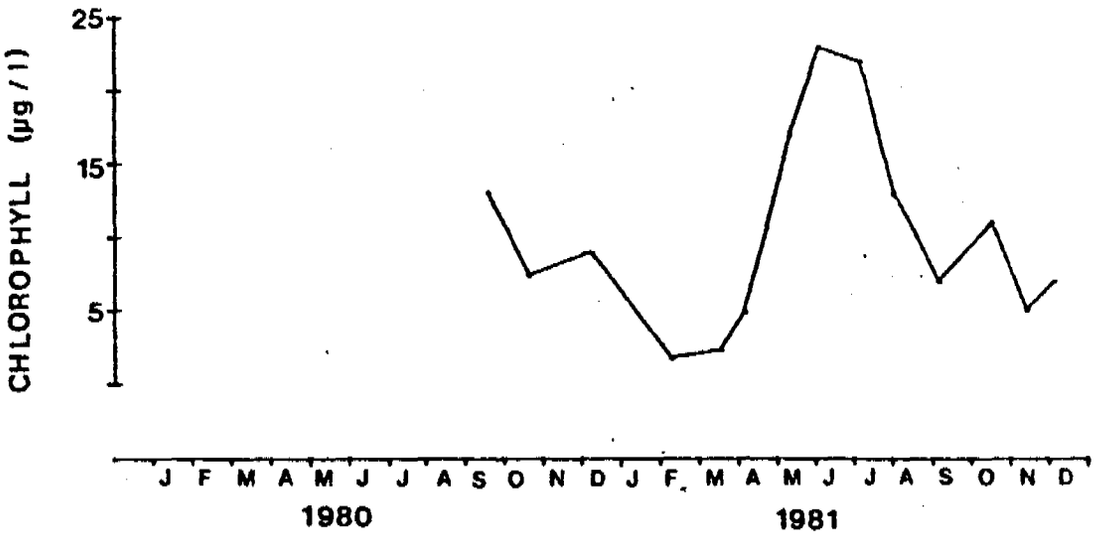

Fig. 4.11.2 Seasonal variations in chlorophyll in Nankeen billabong.

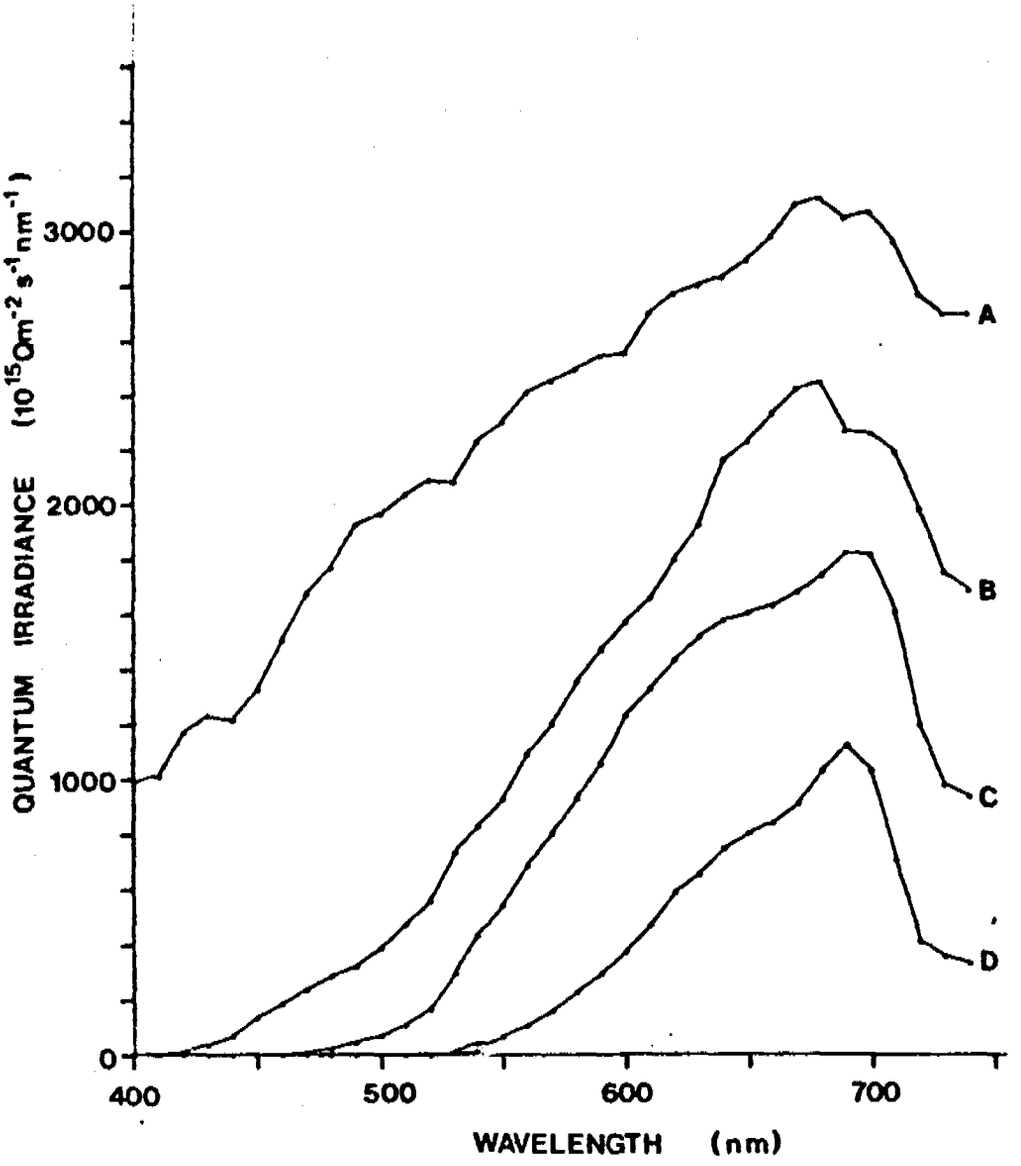

Fig. 4.11.3 *In situ* quantaspectrometric measurements at selected depths in Nankeen billabong on 8/6/78.

A = 0.2 m : ~100% Q_o

B = 0.2 m (x1.4) : 33% Q_o

C = 0.4 m (x3) : 11% $Q_o \approx z_m$

D = 0.9 m (x11) : 0.9% $Q_o \approx z_{eu}$

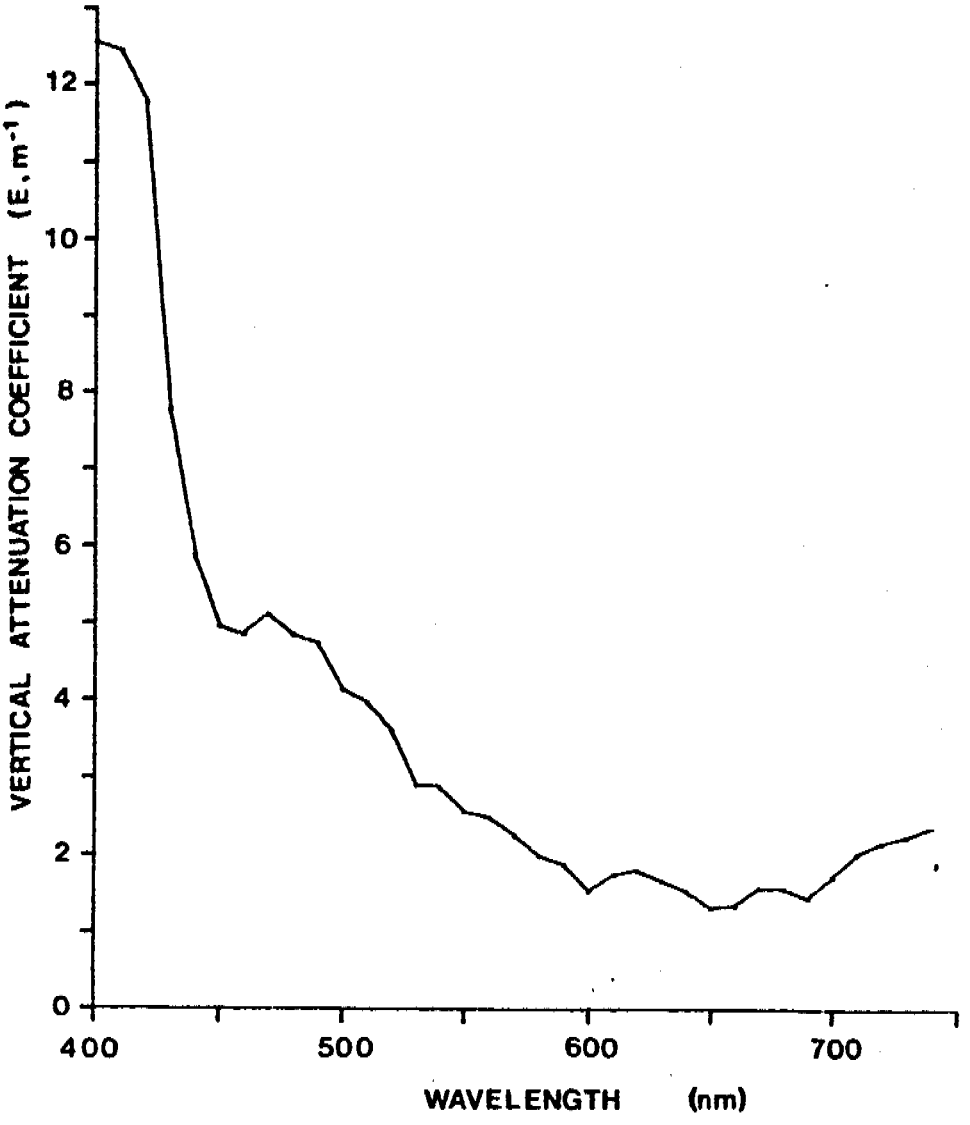

Fig. 4.11.4 The attenuation spectrum of Nankeen billabong on 8/6/78.

Table 4.12A

Date	Time (hrs)	E_d (m^{-1})	z_{eu} (m)	$z_{S.D.}$ (m)
17/2/81	1500	0.80	2.5	0.7
28/5/79	1015	0.97	2.1	0.9
16/4/81	0915	1.02	2.0	1.4
7/6/79	0930	1.06	1.9	0.85
21/5/79	1000	1.31	1.5	0.9
9/7/79	0940	2.48	0.8	0.35
30/7/79	0830	5.55	0.4	0.2

Table 4.12B Optical characteristics of Gulungul billabong. Symbols as for Table 4.2A.

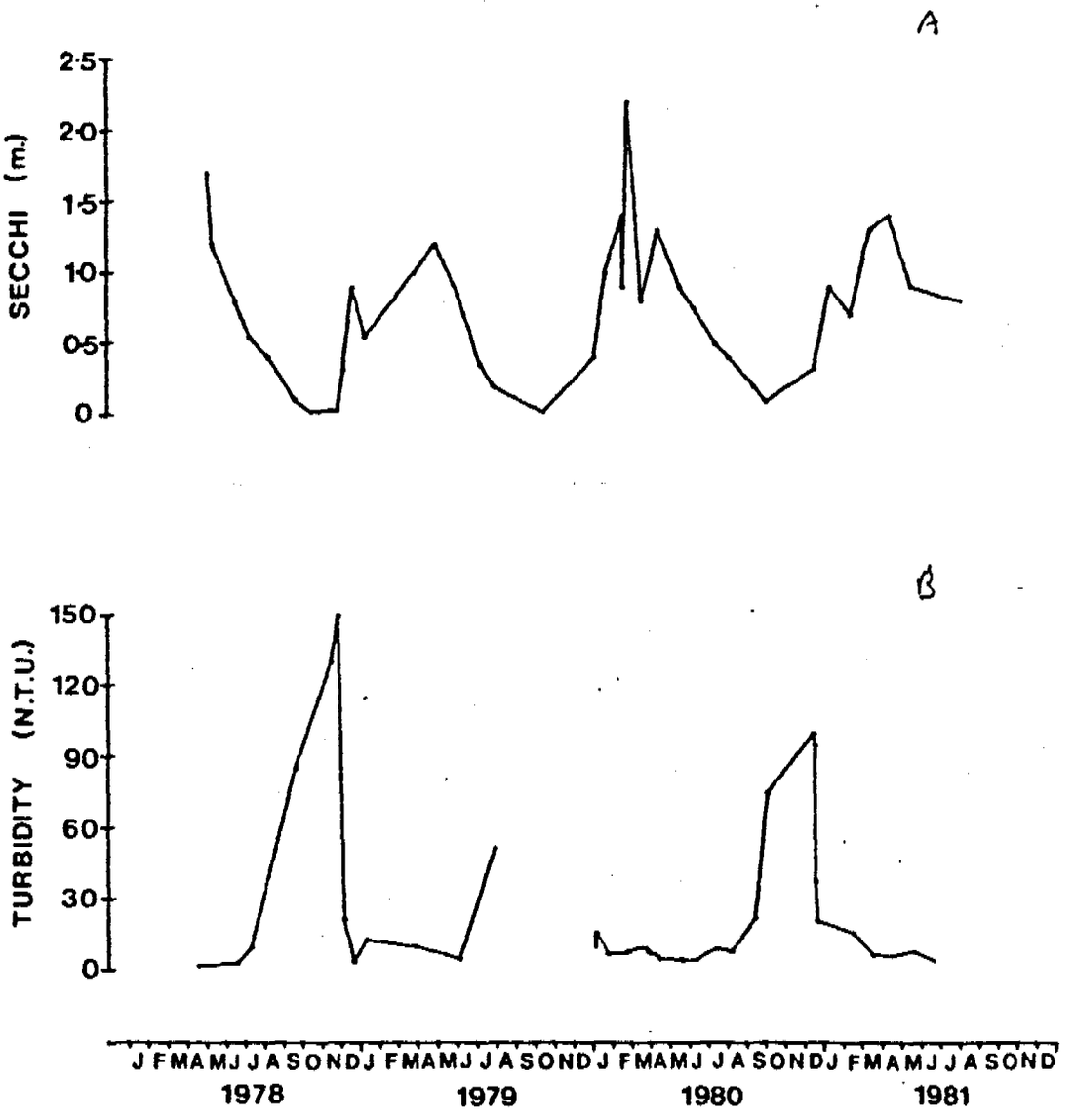

Fig. 4.12.1 Seasonal variations in Secchi transparency (A) and turbidity (B) in Gulungul billabong.

maximum transparency occurs at the Wet/Dry interchange, Gulungul may experience intermittent periods of high transparency during the Wet; the oscillation (Fig. 4.12-1A) between February and March 1980 are a case in point. The reason for this is that Gulungul is a backflow billabong, receiving intermittent inputs of flood waters from the Magela Creek, rather than continuous through-flow. Thus Gulungul, and other backflow billabongs, may be static while main Channel and flood plain billabongs are flowing.

The dramatic increases in turbidity from mid-June coincide with the death of the dense stands of *Najas tenuifolia*, permitting turbulent mixing.

The gilvin concentrations in Gulungul reached a peak in July in 1979 (Fig. 4.12-2A); doubtless the decomposition of *Najas* contributes gilvin at this time.

The only spectral data for Gulungul (Figs. 4.12-3,4) is from the early Dry while the billabong was relatively non-turbid. The broad transmission band at z_{eu} peaked around 650 nm, with hints of absorption by chlorophyll a satellite band and chlorophyll a respectively. Later in the year, a profile more like that for Ja Ja would be expected. As for Goanna and Jabiluka, there is an unexplained maximum of vertical attenuation coefficient at approximately 420 nm (Fig. 4.12-5).

4.13 The underwater light field in Georgetown billabong

This billabong rates as the "dirtiest" billabong studied in this investigation. Even by May-June, early in the Dry, when most other billabongs would be at their clearest, Georgetown has a euphotic zone of less than 1 m (Table 4.13). With pronounced seasonality, Georgetown alternates between very turbid and not quite so turbid (Figs. 4.13-1A,B). Fleetingly, it is flushed by Wet season inflows, but even then transparency does not increase beyond 0.8 m (Fig. 4.13-1A). Chlorophyll concentrations are

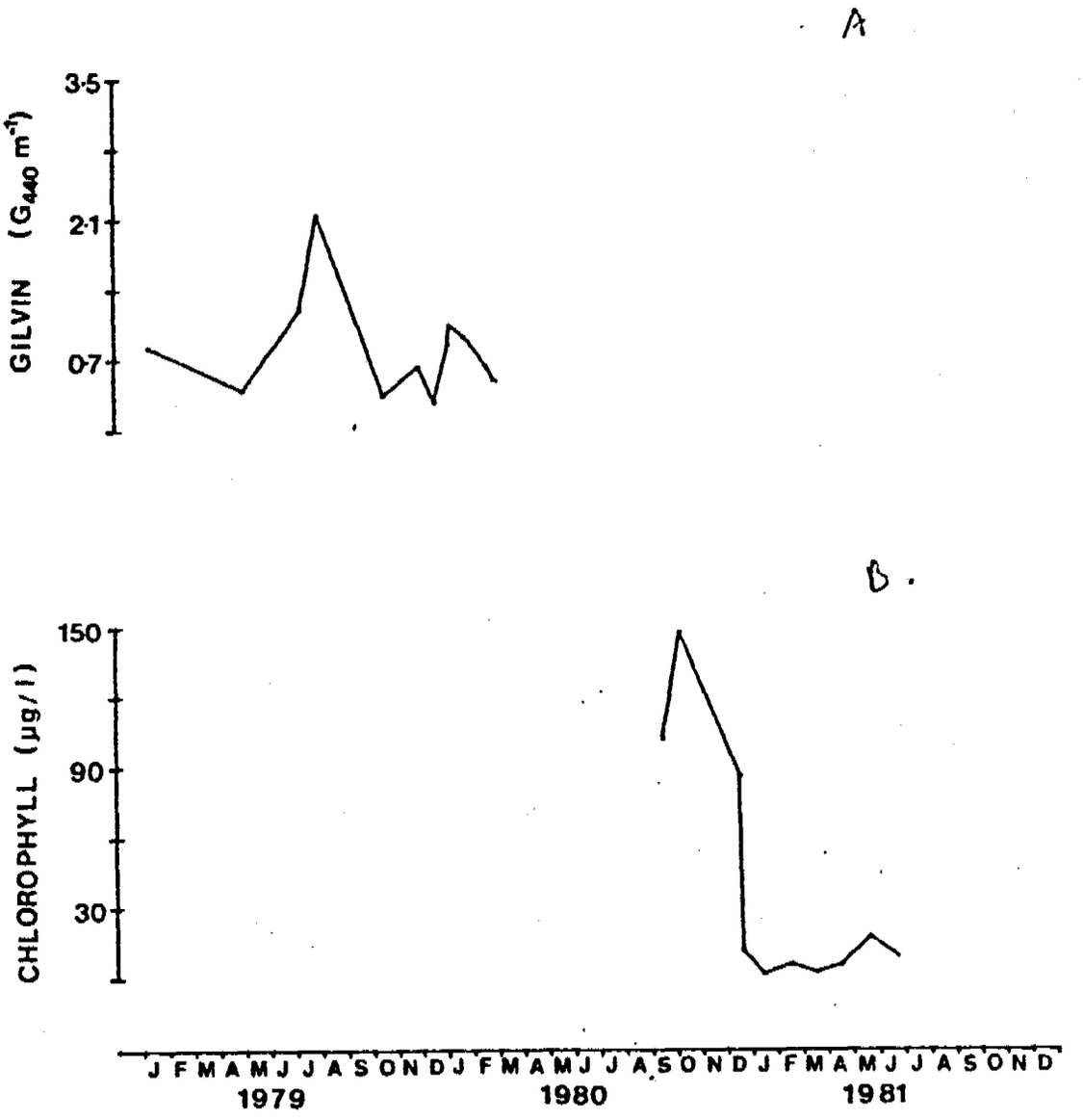

Fig. 4.12.2 Seasonal variations in gilvin (G_{440}) (A) and chlorophyll (B) in Gulungul on 28/5/79.

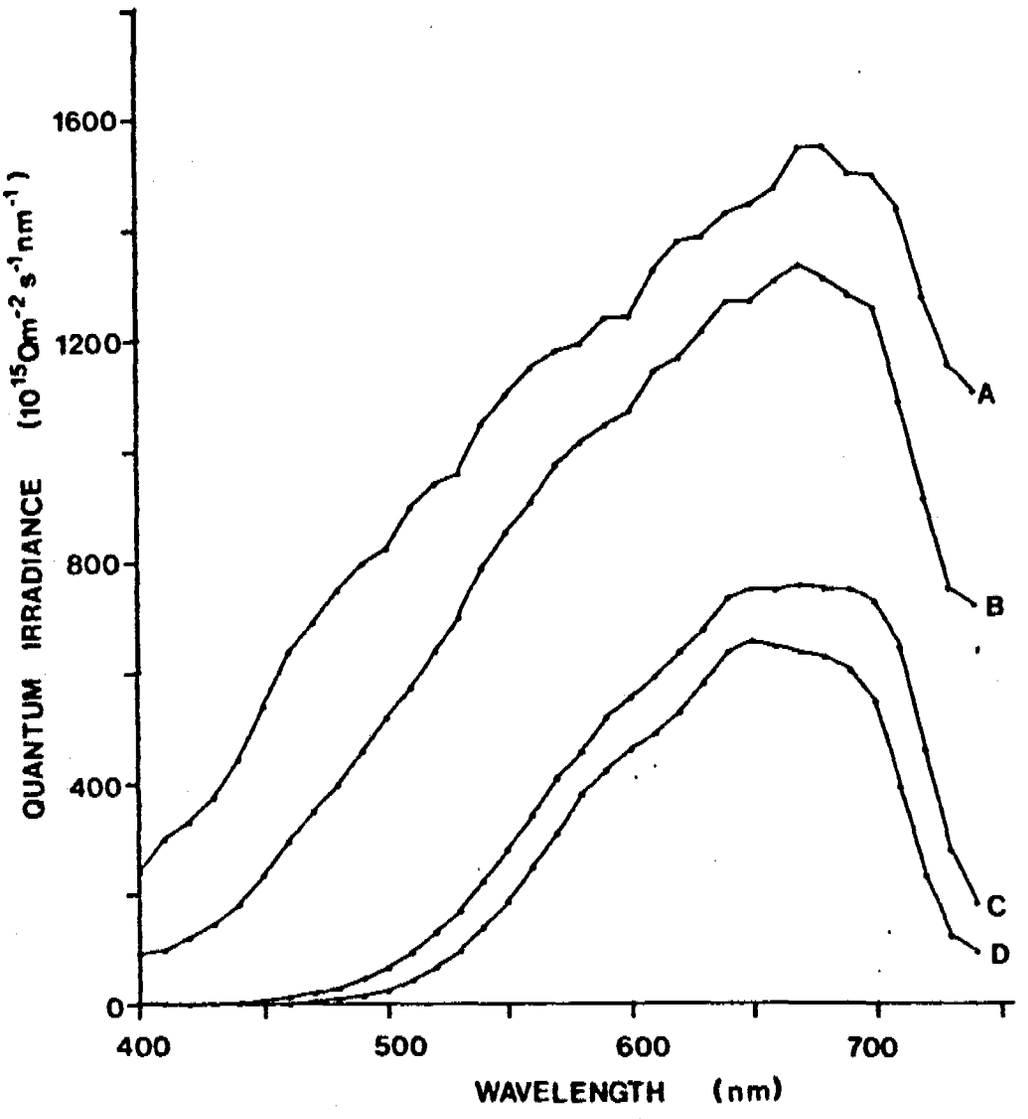

Fig. 4.12.3 *In situ* quantaspectrometric measurements at selected depths in Gulungul billabong on 28/5/79.

A = 0.1 m : 84% Q_o

B = 0.3 m

C = 1.0 m (x2) : 13% $Q_o \approx z_m$

D = 1.4 m (x4) : 5% Q_o

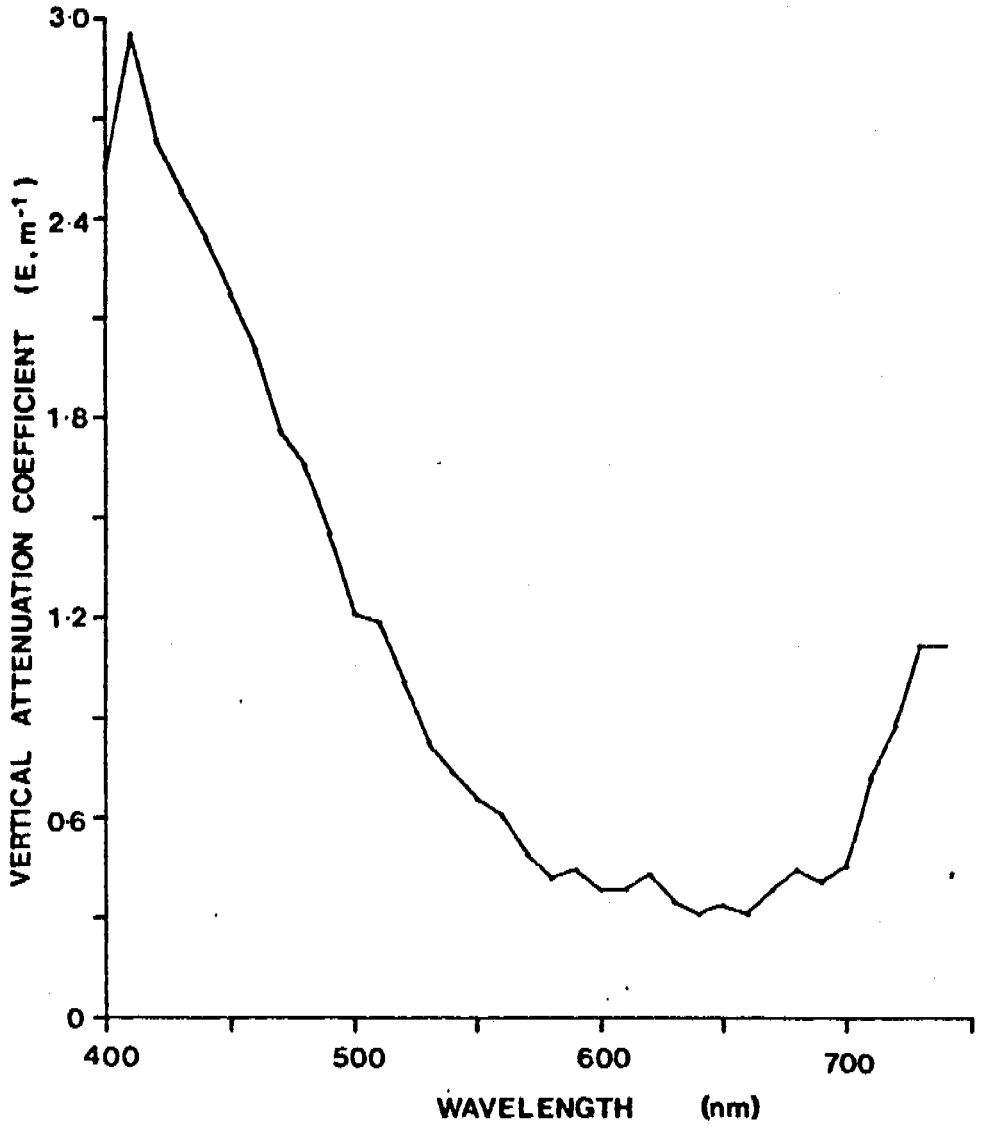

Fig. 4.12.4 The attenuation spectrum of Gulungul billabong on 28/5/79.

Table 4.13(i)

Date	Time (hrs)	E_d (m^{-1})	z_{eu} (m)	$z_{S.D.}$ (m)
1/6/78	1400	2.67	0.7	
27/5/79	1030	3.63	0.6	0.2

Table 4.13(ii) Optical characteristics of Georgetown billabong. Symbols as for Table 4.2(i).

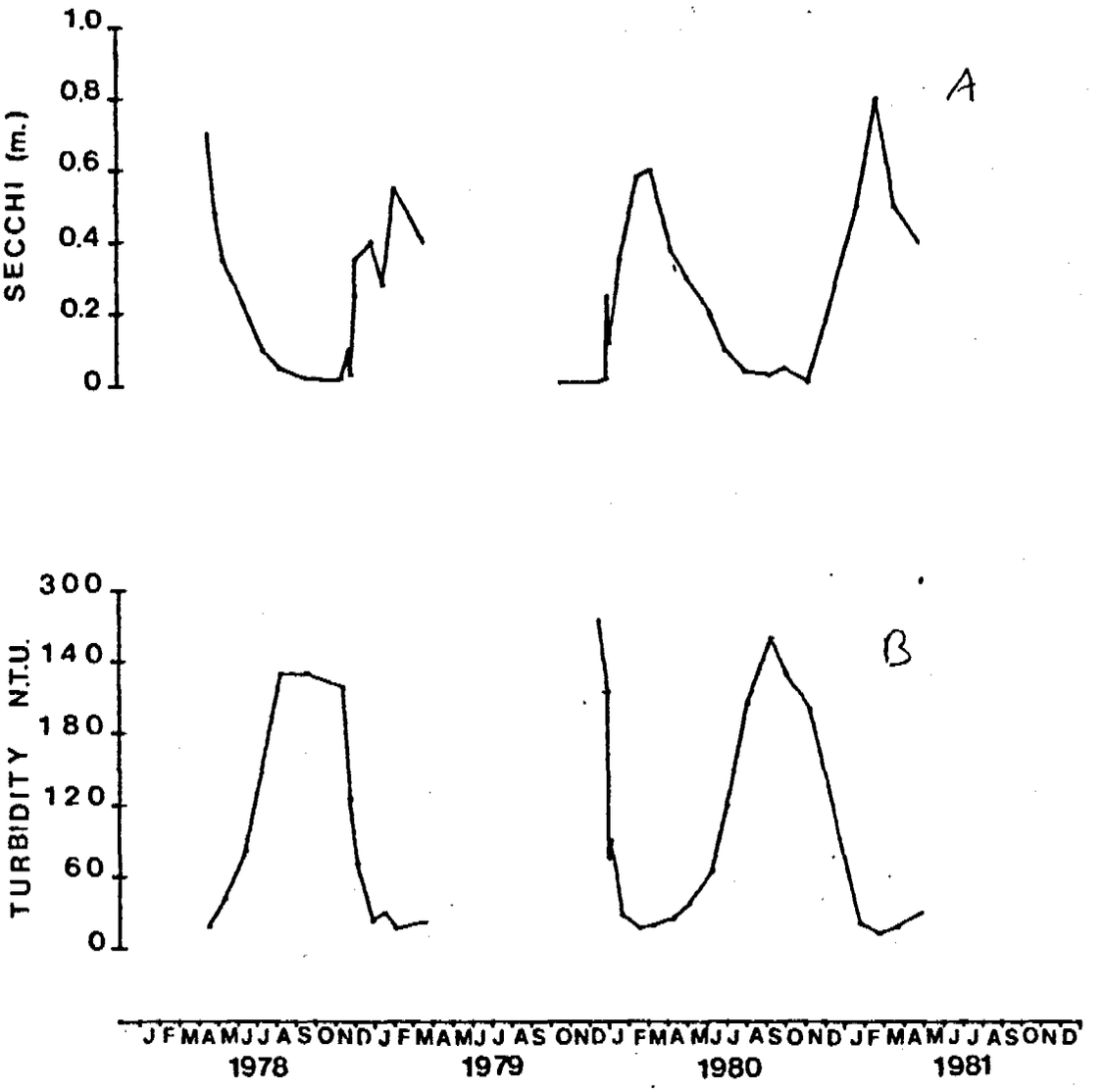

Fig. 4.13.1 Seasonal variations in Secchi transparency (A) and turbidity (B) in Georgetown billabong.

never high, but peak at the time of maximum transparency (Fig. 4.13-2).

The spectroradiometric data show strong attenuation of blue wavelengths, leaving a narrow transmission band with a peak at about 700 nm (Figs. 4.13-3,4), typical of turbid billabongs. The vertical attenuation spectrum for 27/5/79 is unusual. In addition to a peak at the blue end, noted for some other billabongs, there is an anomalous peak at 560 nm. No explanation is offered.

4.14 Principal factors of light attenuation in the billabongs

The euphotic depth is an important parameter because it determines the depth in the water column to which photosynthetic gain occurs. It is best measured by an instrument such as the Li-Cor quantameter, yielding absolute values of photosynthetically-active radiation (PAR). However, use of this instrument is time-consuming and for accurate measurements requires near-perfect field conditions. On the other hand, Secchi transparency measurements ($z_{S.D.}$) are made rapidly and simply, with acceptable precision if care is taken. Moreover, they can be made when wind and scudding clouds make Li-Cor measurements difficult, lengthy or impossible. It is stressed that a quantameter is to be preferred when conditions allow. However Secchi measurements, though often scorned for their simplicity, can give good results if used with care. The latter point is also stressed, for all too often the Secchi disk is used in a rough and ready fashion. Standardised methods should be used, with goggles or water telescope (Welch 1948), and, ideally, only one trained operator should carry out the measurements.

That the two measurements are highly correlated is shown by Figure 4.14-1, so that the Secchi transparency, for which there is abundant data, can be used confidently to investigate the principal limitations on euphotic depth. The contribution to light attenuation, and therefore the effect on euphotic depth, of the three principal

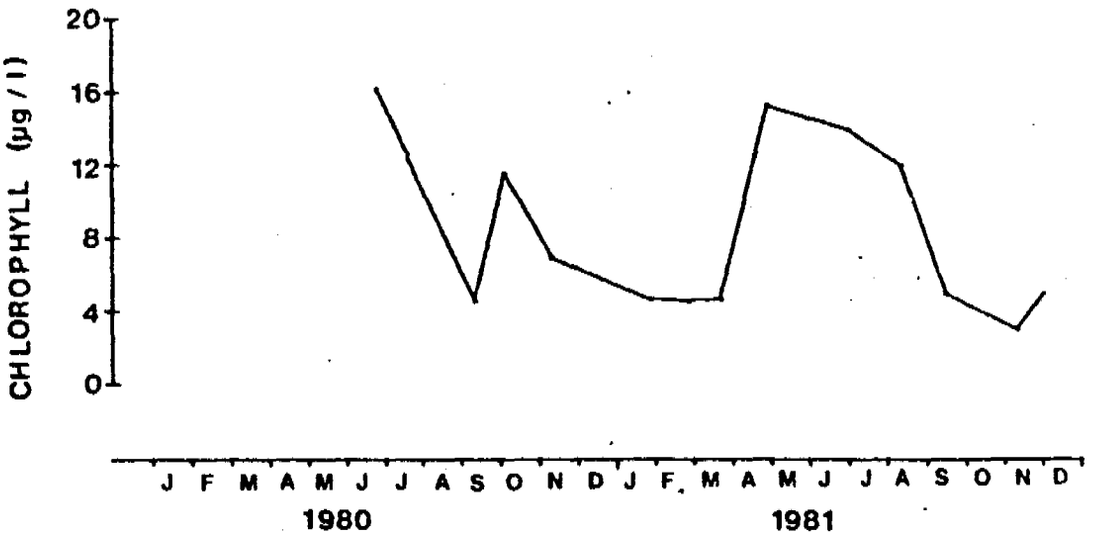

Fig. 4.13.2 Season variations in chlorophyll in Georgetown billabong.

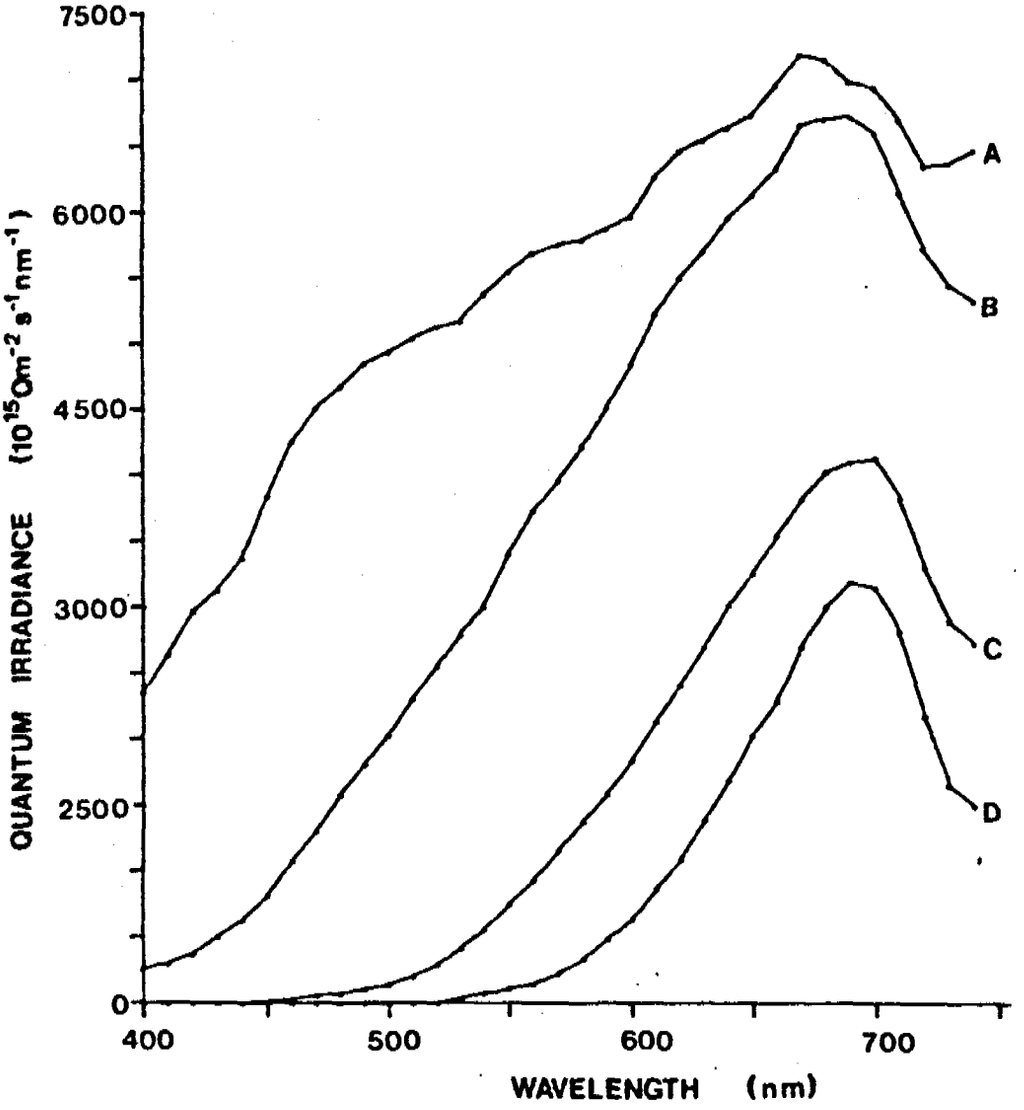

Fig. 4.13.3 *In situ* quantaspectrometric measurements at selected depths in Georgetown billabong on 1/6/78.

A = 0·02m
B = 0·2m (×2·2) : 25·2% Q_0
C = 0·4m (×5·7) : 6·2% Q_0
D = 0·6m (×11) : 1·8% $Q_0 \approx Z_{eu}$

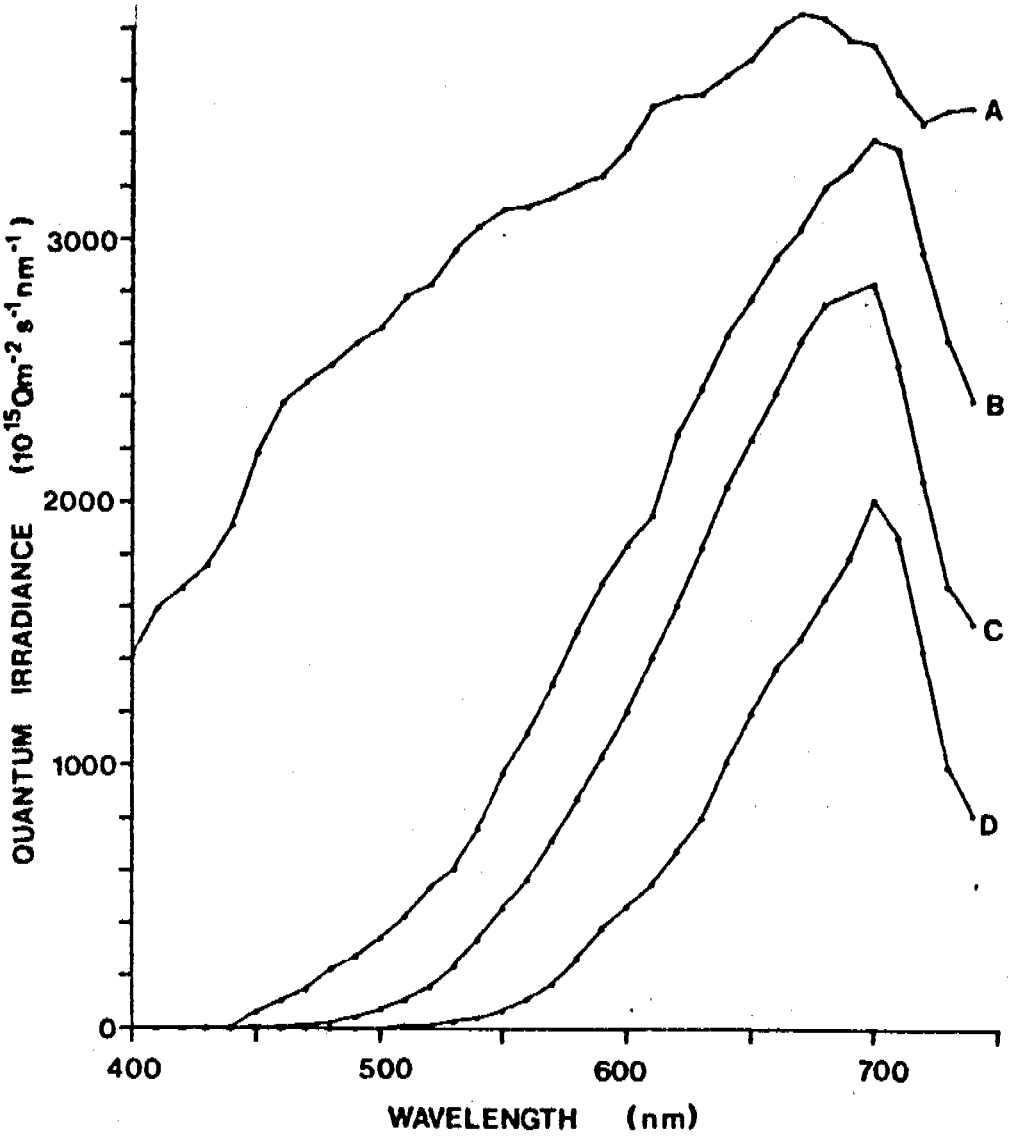

Fig. 4.13.4 *In situ* quantaspectrometric measurements at selected depths in Georgetown billabong on 27/5/79.

A = Aerial : 100% Q_o

B = 0.05 m (x4)

C = 0.2 m (x7) : 14% $Q_o \approx z_m$

D = 0.5 m (x32) : 0.9% $Q_o \approx z_{eu}$

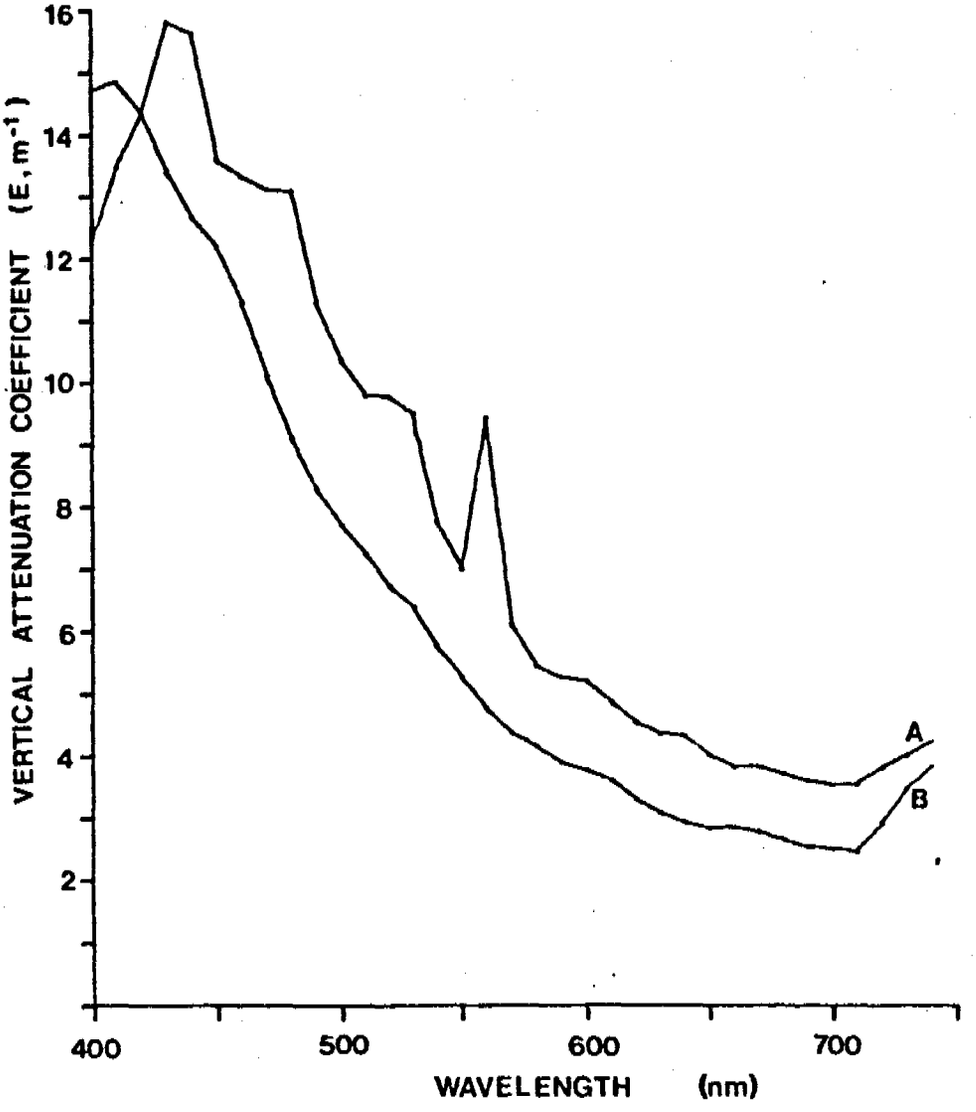

Fig. 4.13.5 The attenuation spectra of Georgetown billabong on 1/6/78 (A) and 27/5/79 (B).

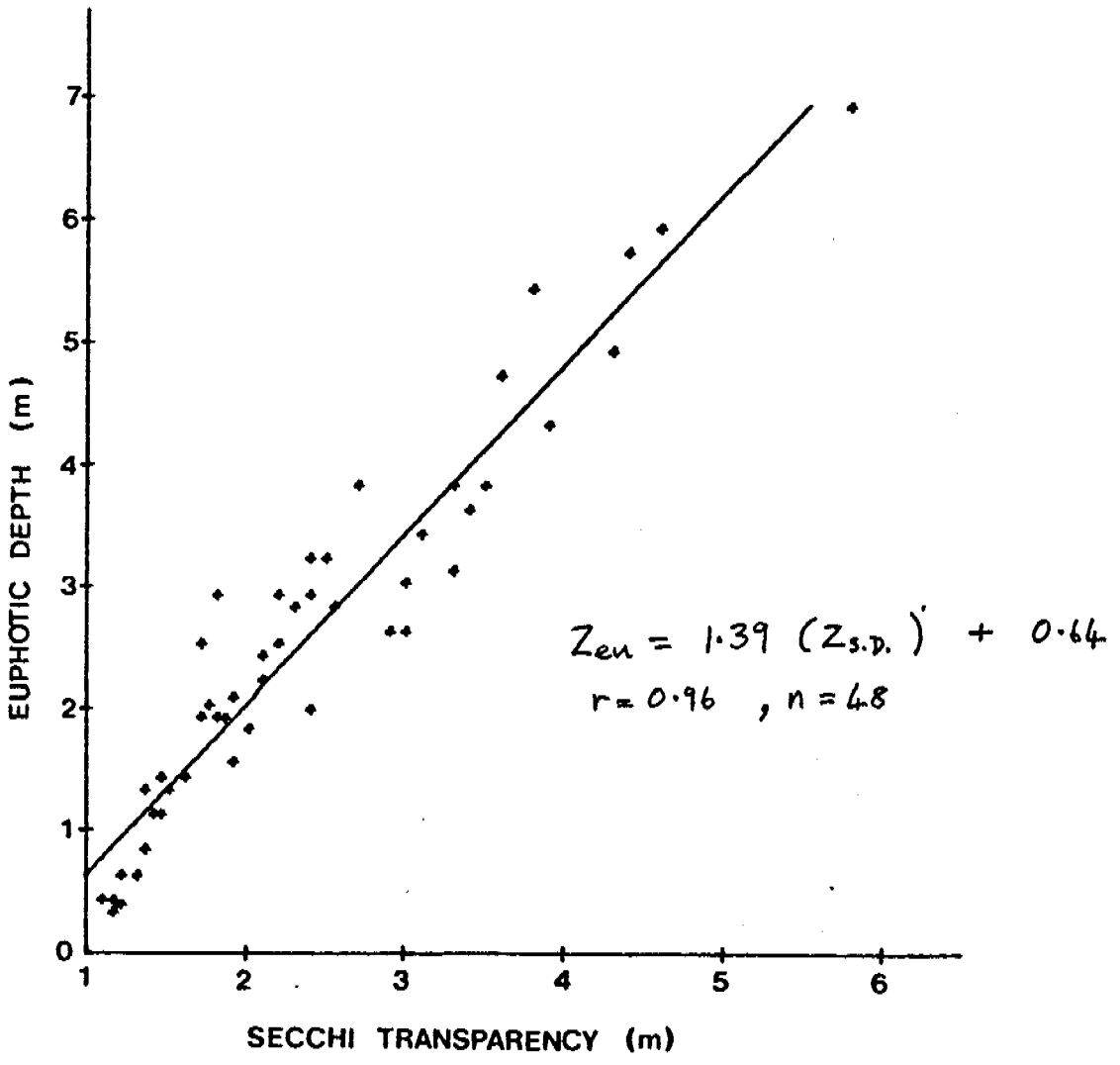

Fig. 4.14.1 Regression of euphotic depth (z_{eu}) on Secchi transparency ($z_{S.D.}$) for billabongs of the Alligator Rivers region.

scattering and absorbing components of natural waters was therefore assessed by linear regression against $1/z_{S.D.}$ (Table 4.14-1). It is clear that only turbidity has significant correlation with reciprocal $z_{S.D.}$. It can therefore be looked on as the principal determinant of euphotic depth. However, it is conceivable that at times of low turbidity, absorbing components could assume importance. For this reason equations 2 to 4 were recalculated for those occasions when turbidity was <10 NTU. The results are shown in Table 4.14-2. Again, turbidity is still the principal attenuator but there appears to be a greater relative contribution by gilvin.

Table 4.14.1

1) $z_{eu} = 1.39\ (z_{S.D.}) + 0.64.$ $r = 0.96,\ n = 48$

2) $\frac{1}{z_{S.D.}} = 0.15\ (Tn) - 0.73.$ $r = 0.78,\ n = 291$

3) $\frac{1}{z_{S.D.}} = 0.01\ (Chl.a) + 4.02.$ $r = 0.04,\ n = 103$

4) $\frac{1}{z_{S.D.}} = 3.90\ (G_{440}) + 2.21.$ $r = 0.09,\ n = 155$

Table 4.14-1 Regression equations showing relationship between $z_{S.D.}$ and various parameters. Tn = turbidity (N.T.U.). G_{440} = gilvin (m^{-1}).

Table 4.14.2

1) $\frac{1}{z_{S.D.}} = 0.11\ (Tn) + 0.32.$ $r = 0.7$ $n = 160.$

2) $\frac{1}{z_{S.D.}} = 0.00\ (Chl.a) + 0.75.$ $r = 0.05$ $n = 58$

3) $\frac{1}{z_{S.D.}} = 0.31\ (G_{440}) + 0.61.$ $r = 0.27$ $n = 108$

Table 4.14-2 Regression equations showing relationship between $z_{S.D.}$ and various parameters when turbidity was <10 N.T.U.

5.0 LABORATORY RESULTS

For one sampling, in May 1979, as well as the usual underwater and laboratory measurements, samples were sent to Canberra for further investigations on the optical characteristics of the water, particularly the contribution of particulate matter to absorption, as opposed to scattering, of light. For theoretical treatments, natural logarithms are to be preferred and in this section K_d, g_{440} and p_{440}, all based on e, are used ($K_d = 2.303 E_d$; $g_{440} = 2.303 G_{440}$).

5.1 The Optical Properties of the Water

The optical properties of the water at the May sampling are summarized in Table 5.1. At this period (beginning of the Dry) the water was of moderate turbidity (2.0-6.4 NTU), with the exception of Georgetown which was very turbid (75 NTU). As might be expected, the values of the scattering coefficient, b, calculated from the irradiance data, vary roughly in parallel with the values of nephelometric turbidity, being in the approximate range 2-6m^{-1} in the four moderately turbid billabongs measured, and 64 m^{-1} in Georgetown.

As judged by g_{440}, all the billabong waters contained low to moderate levels of gilvin, within the range previously observed for water bodies for parts of southeastern Australia (Kirk 1976, 1977, 1980), but well below values for south-west Tasmania (King & Tyler, 1981a-d). Where they differed from the water bodies of comparable turbidity in New South Wales was in the high level of particulate absorption. The spectra in Figs. 5.1.1-5.1.7 show in every case that absorption of the PAR wavelengths by the particulate fraction was approximately the same as, or a good deal higher than, their absorption by the soluble fraction. The average value of the ratio of the particulate fraction absorption coefficient

Table 5.1

lower case.

Billabong	K_d	z_{eu}	Secchi depth	$R(z_m)$	$\$_{440}$	$\$_{440}$	Chl a	T_n	b
	m^{-1}	m	m		m^{-1}	m^{-1}	mg m^{-3}	NTU	m^{-1}
Mudginberri	1.24	3.7	1.7	0.022	1.11	1.13	13.0	1.95	2.22
Noarlanga	1.34	3.4	2.1	0.031	2.46	2.69	6.4	4.75	3.36
Island	1.50	3.1	-	0.018	1.64	3.79	11.4	2.0	2.38
Leichardt	1.68	2.7	1.6	-	1.77	2.43	5.5	2.8	-
Gulungul	2.21	2.1	0.9	0.038	2.28	1.68	8.3	4.8	5.71
Jabiluka	2.46	1.9	-	-	2.33	4.79	17.8	6.4	-
Georgetown	8.50	0.5	0.2	0.143	1.99	18.00	5.4	75.0	64.3

Table 5.1 Optical characteristics of billabongs, late May, 1979. K_d is the vertical attenuation coefficient for downwelling irradiance of PAR. z_{eu} is the depth at which downwelling PAR is reduced to 1% of the sub-surface level. $R(z_m)$ is the reflectance, the ratio of upwelling to downwelling irradiance, at about the mid-point of the euphotic zone. (lower case) $\$_{440}$ and $\$_{440}$ are the values of the absorption coefficient at 440 nm, of the soluble and particulate fractions, respectively. T_n is the nephelometric turbidity, b is the scattering coefficient value calculated from the underwater irradiance measurements.

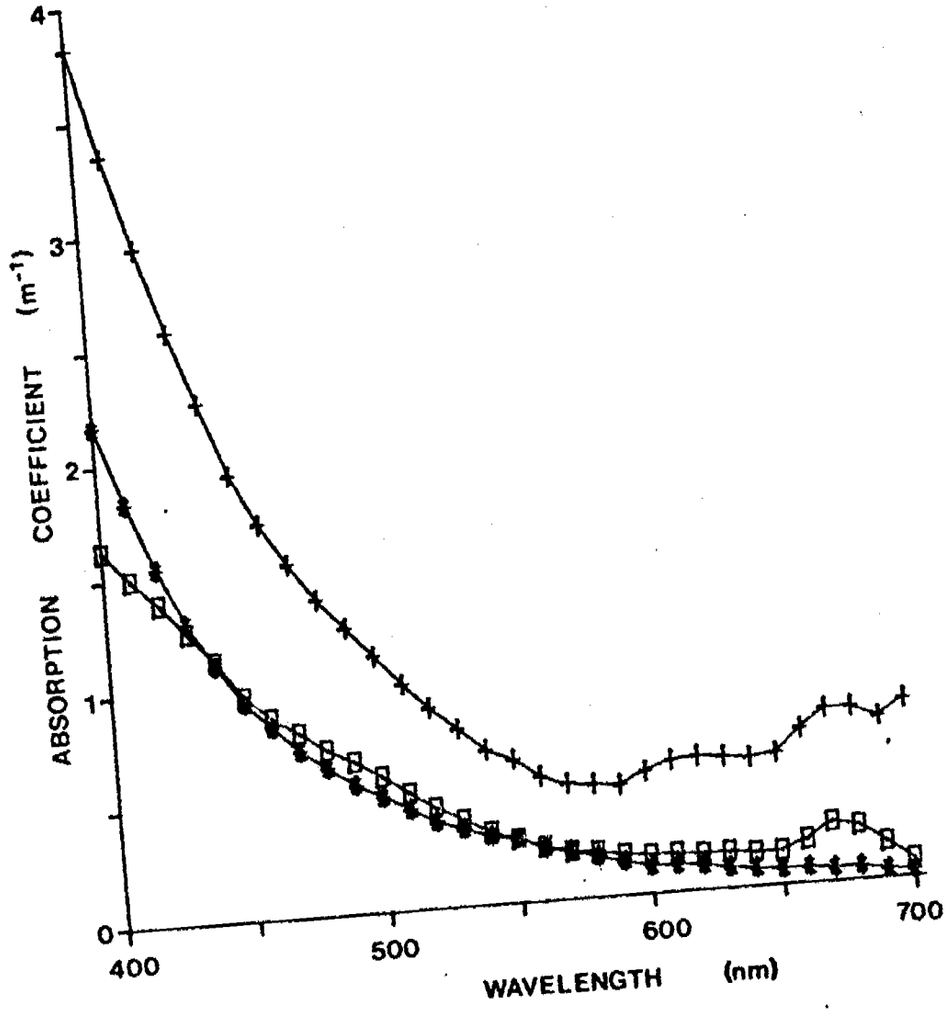

Fig. 5.1.1 Spectral absorption properties of the waters of Mudginberri billabong in May 1979.
* = Soluble fraction; □ = particulate fraction;
+ = total absorption coefficient due to all components (soluble and particulate colour and water itself).

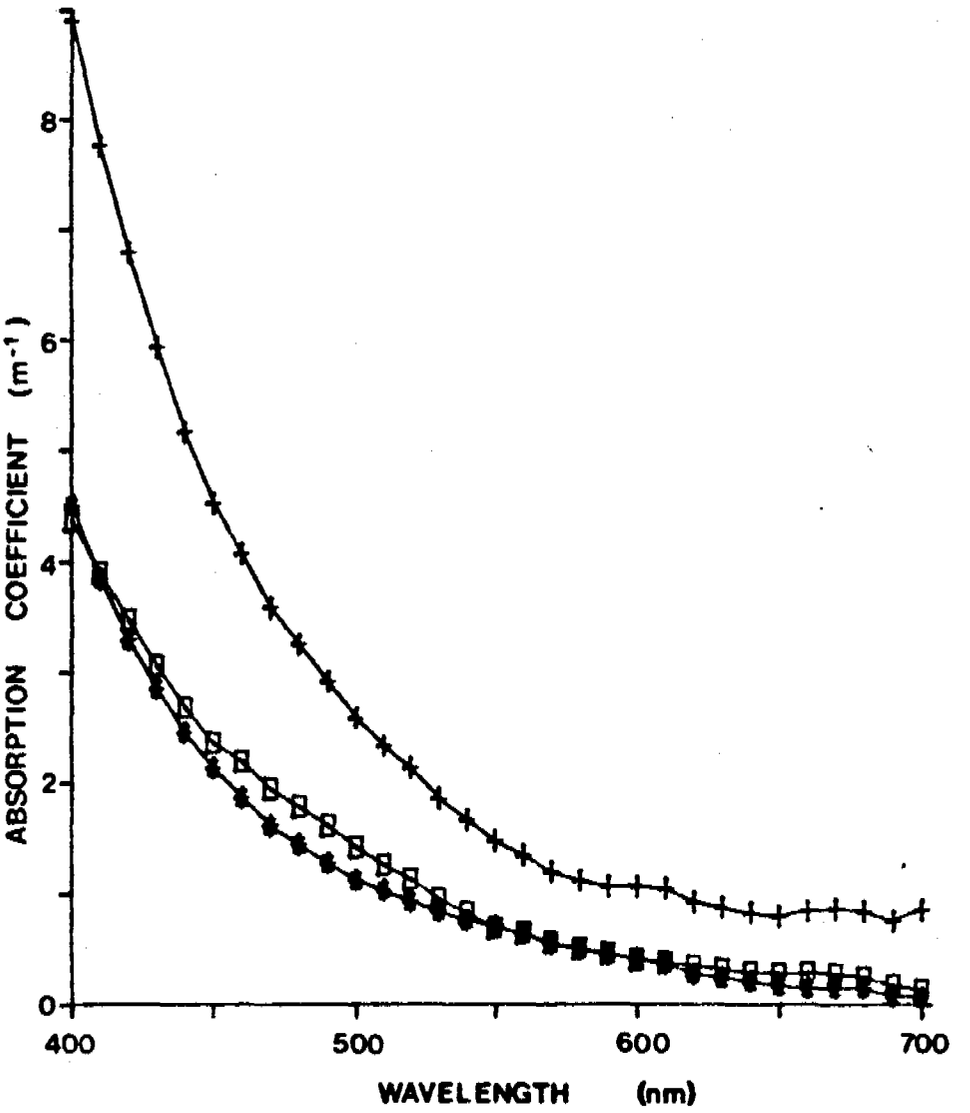

Fig. 5.1.2 Spectral absorption properties of the waters of Noarlanga billabong in May 1979. Symbols as for Fig. 5.1.1.

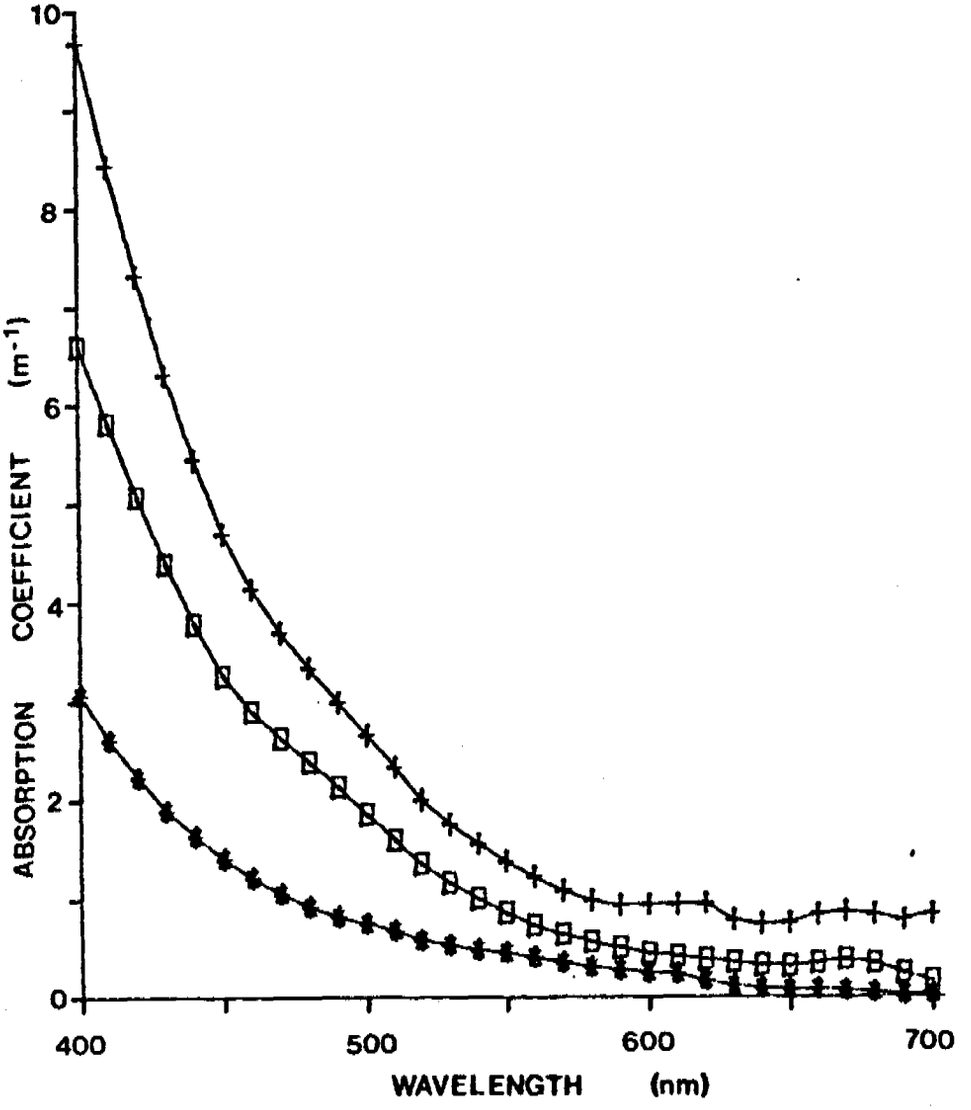

Fig. 5.1.3 Spectral absorption properties of the waters of Island billabong in May 1979. Symbols as for Fig. 5.1.1.

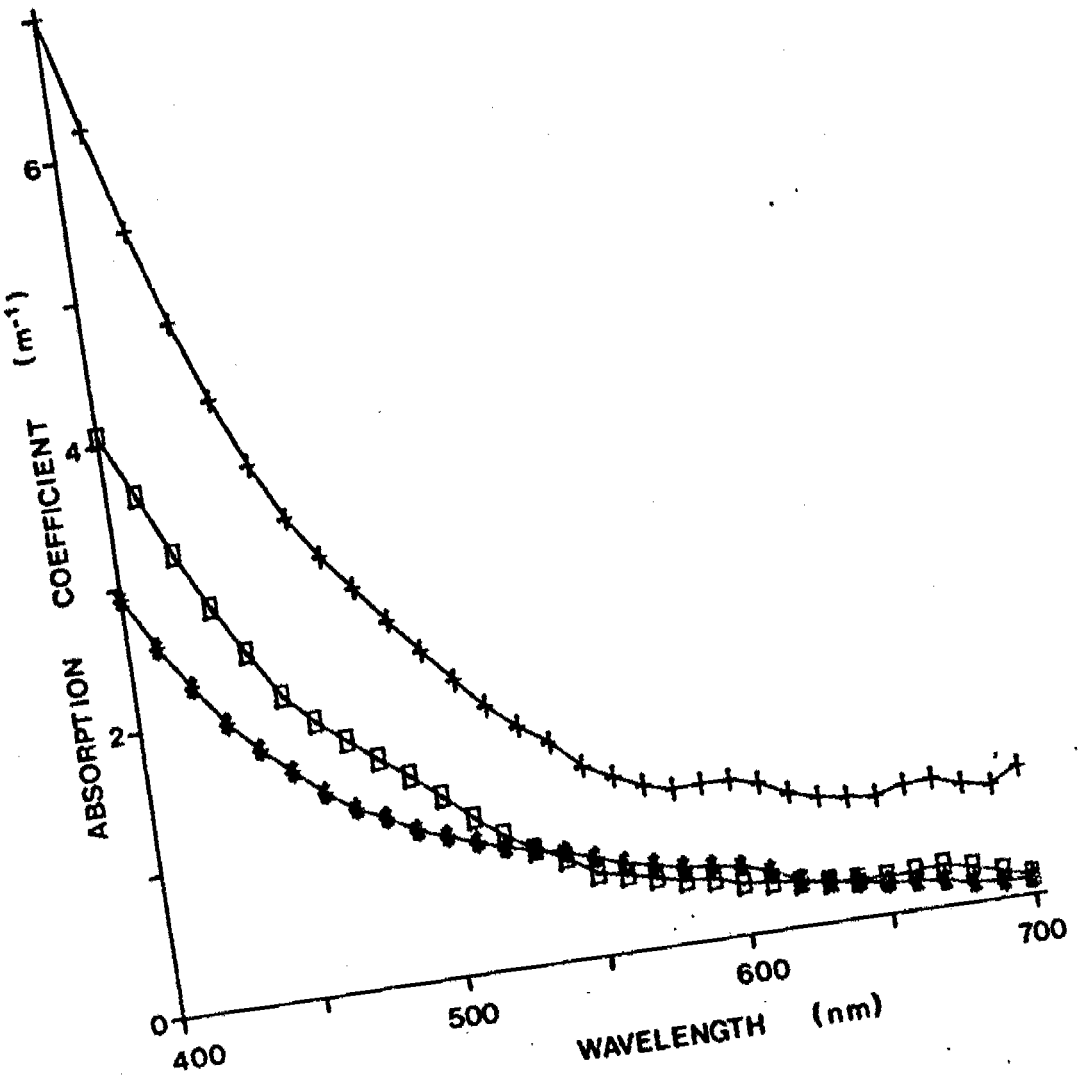

Fig. 5.1.4 Spectral absorption properties of the waters of Leichardt billabong in May 1979. Symbols as for Fig. 5.1.1.

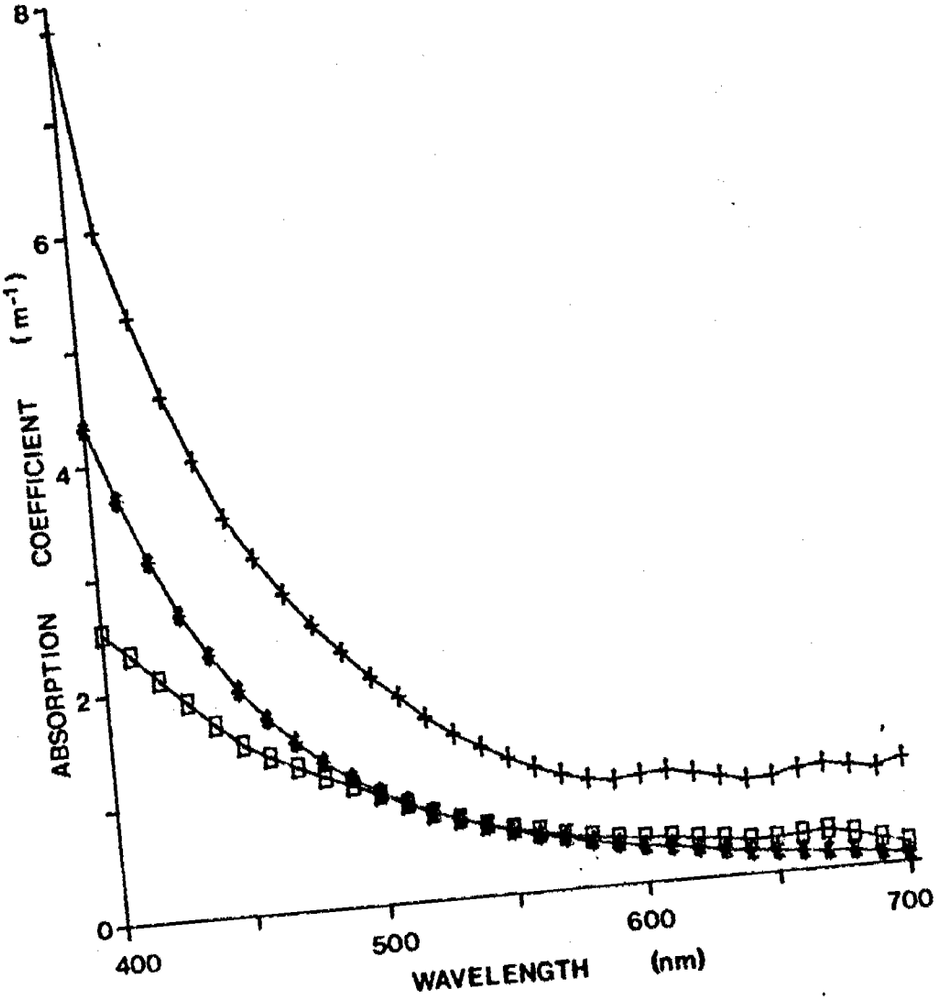

Fig. 5.1.5 Spectral absorption properties of the waters of Gulungul billabong in May 1979. Symbols as for Fig. 5.1.1.

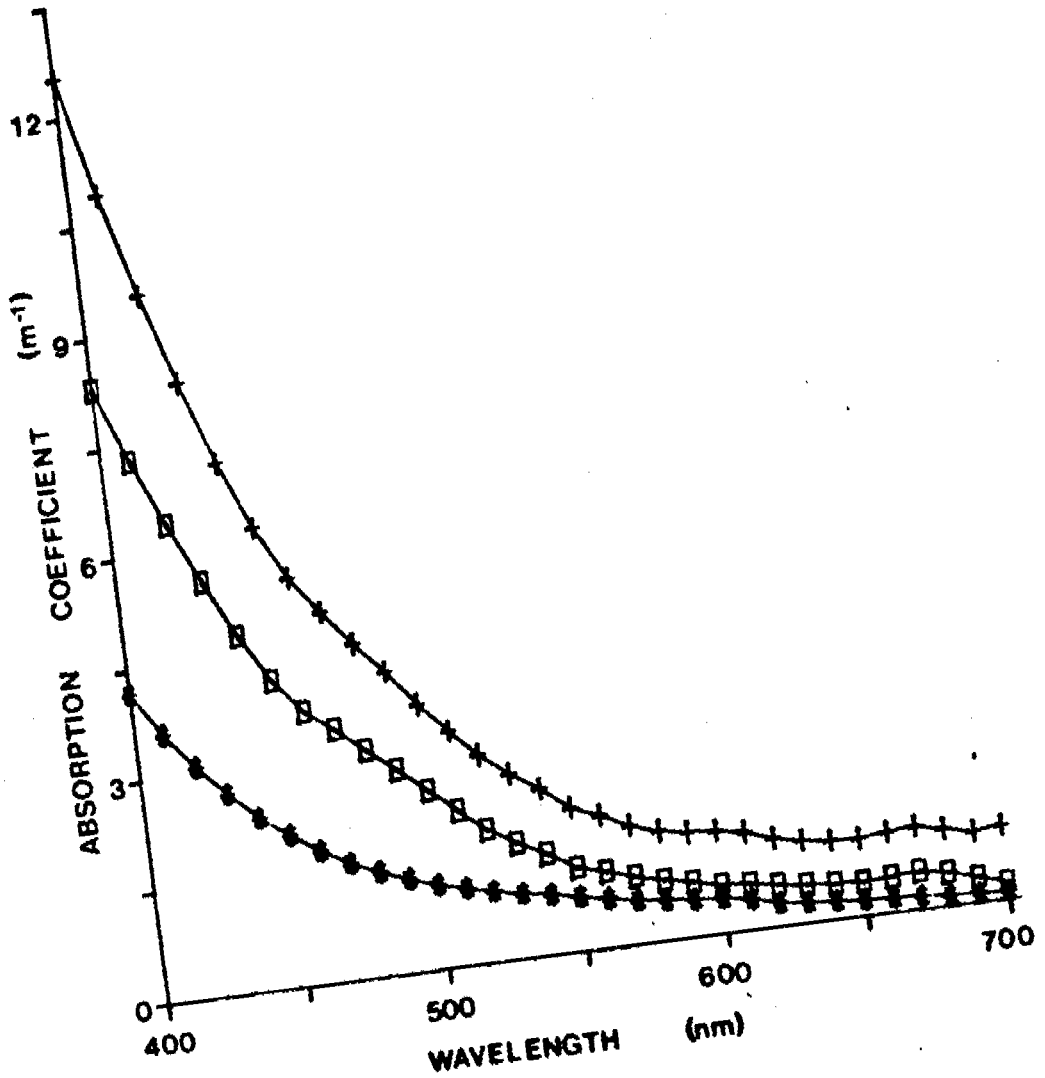

Fig. 5.1.6 Spectral absorption properties of the waters of Jabiluka billabong in May 1979. Symbols as for Fig. 5.1.1.

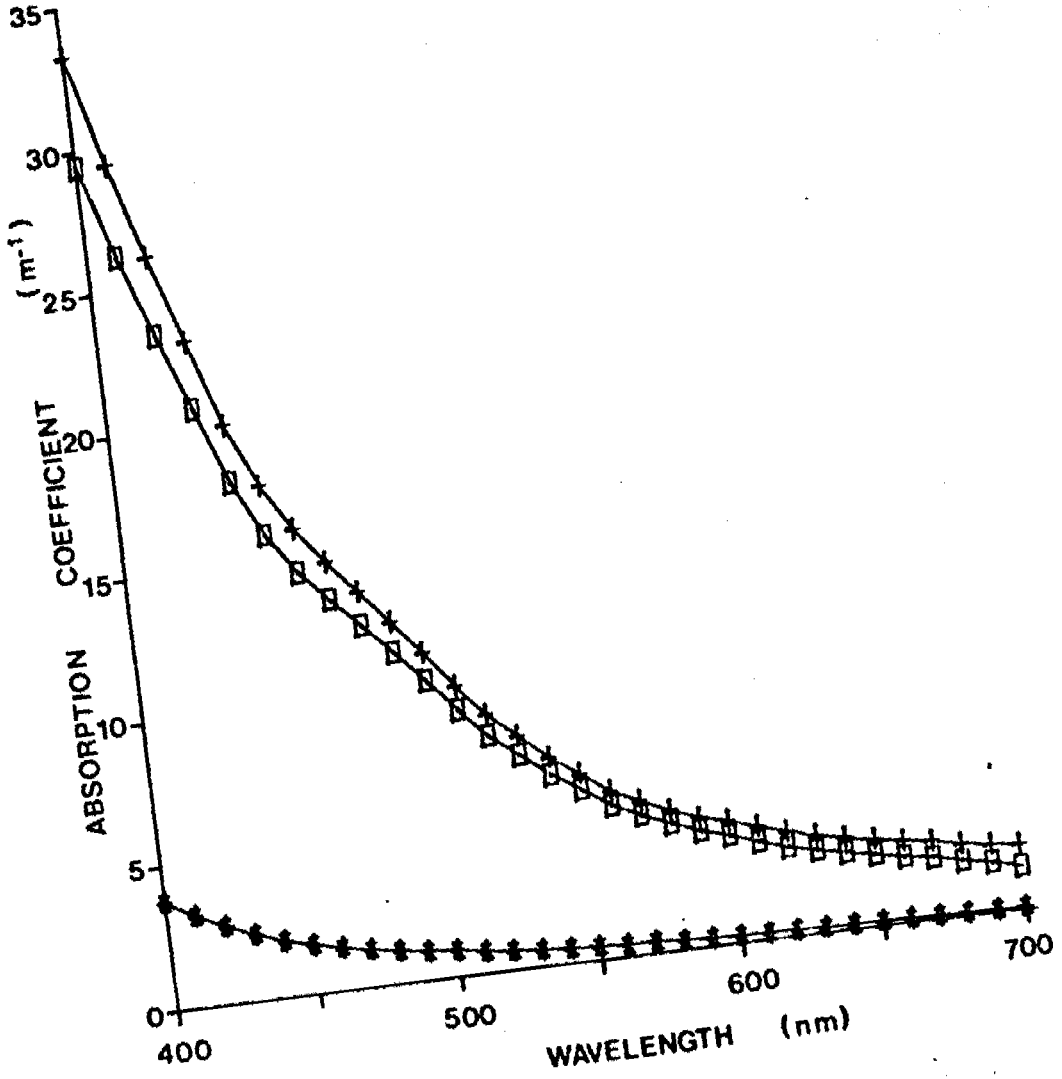

Fig. 5.1.7 Spectral absorption properties of the waters of Georgetown billabong in May 1979. Symbols as for Fig. 5.1.1.

at 440 nm (ϕ^{p}_{440}) to the nephelometric turbidity (T_n) for the seven billabongs was 0.75 ± 0.51. For seven water bodies in the southern tablelands of N.S.W./A.C.T., the corresponding mean ratio was 0.22 ± 0.13 (calculated from data of Kirk, 1980). These ratios were significantly different at the 5% level (t test).

All the billabongs, with the possible exception of Georgetown, apparently contained sufficient levels of phytoplankton for the chlorophyll a absorption peak to appear at about 670 nm in the particulate fraction spectra. Nevertheless, these spectra are dominated by the yellow-brown humic materials present in this fraction, as shown by the progressive rise in absorption with decreasing wavelength; in the blue region the absorption bands of the photosynthetic pigments are virtually undetectable against the high background absorption.

Figs. 5.1.1-5.1.7 also show the total absorption spectra of the billabong waters, due to all three absorbing fractions, the soluble and the particulate colour, and the water itself.

5.2 Contribution of the different fractions to absorption of PAR

Attenuation of light with depth is primarily due to absorption, although scattering can greatly increase the amount of absorption that takes place. The relative contribution to absorption of PAR of the different components of natural waters is best expressed as the percentage of total absorbed PAR quanta accounted for by each component (Table 5.2).

In the first six billabongs, all of moderate turbidity, the three major absorbing fractions - water, gilvin, particulate matter - all make substantial contributions to light absorption. In every billabong the particulate fraction absorbed more of the quanta than either of the other fractions, although in four cases gilvin absorbed nearly as much. This contrasts with the southern tablelands of New South Wales where in five out of seven water bodies examined the soluble colour was the major absorbing component (Kirk, 1980). When the comparison is confined to

Table 5.2

Billabong	Quanta absorbed (% of total)		
	By water	By soluble fraction[a]	By particulate fraction[b]
Mudginberri	28.9	32.8	38.3
Noarlanga	20.0	37.0	43.0
Island	20.9	24.9	54.3
Leichhardt	19.7	37.7	42.6
Gulungul	20.0	39.7	40.3
Jabiluka	15.8	29.0	55.1
Georgetown	5.9	7.5	86.6

[a] Gilvin

[b] Tripton/phytoplankton

Table 5.2 Calculated distribution of absorbed PAR quanta between the particulate fraction, soluble fraction and water itself in the euphotic zone of the billabongs.

waters of comparable turbidity, the conclusion still holds that the particulate fraction contributes more to light absorption in the Alligator Rivers billabongs than it does in the N.S.W. water bodies. In the turbid Georgetown billabong the particulate fraction accounted for nearly 90% of the absorbed PAR.

5.3 Contribution of scattering to attenuation

Scattering does not by itself extinguish photons; a photon that has been merely scattered is still available for photosynthesis. Scattering intensifies attenuation mainly by increasing the pathlength the photons must traverse, so increasing the likelihood of their being absorbed within a given depth. Backscattering of photons out of the water makes a (usually) small additional contribution to attenuation.

The reflectance values (Table 5.1) show that this is very small in the billabongs. Significantly it is an order of magnitude greater in Georgetown. The contribution of scattering to the attenuation of PAR can be assessed by calculating, on the basis of the total absorption spectrum of the water, what the value of K_d would be in the absence of scattering, and comparing this with the value of K_d measured in that water body (Kirk, 1981a; 1981c). Table 5.3 compares these two values for each of the seven billabongs. For all except Georgetown scattering increased the vertical attenuation coefficient for PAR by an average of 58%. In the turbid Georgetown billabong the increase was 111%.

Table 5.3

Billabong	K_d (calc.) (b = 0) m^{-1}	K_d(meas.) m^{-1}	$\frac{K_d(\text{meas.})}{K_d(\text{Calc.})}$
Mudginberri	0.70	1.24	1.77
Noarlanga	1.09	1.34	1.23
Island	1.00	1.50	1.50
Leichardt	1.13	1.68	1.49
Gulungul	1.16	2.21	1.91
Jabiluka	1.56	2.46	1.58
Georgetown	4.02	8.50	2.11

Table 5.3 Contribution of scattering to vertical attenuation of PAR. The values of vertical attenuation coefficient calculated from the absorption spectrum of the water K_d (calc.) assuming zero scattering (b = 0) are compared with those actually measured in the billabongs with a quanta meter K_d(meas.) .

6. DISCUSSION

Table 6.1 is a synopsis of the water clarity trends in billabongs of the Alligator Rivers Region, and of the limnological factors which determine such optical characteristics. It is apparent that the response of billabong optics to the distinct seasonality of the prevailing climatic and hydrological regimes (see Walker, Waterhouse and Tyler, 1982) varies from billabong to billabong. At the Dry/Wet interchange, whether the first flush of water through a billabong improves or reduces water clarity, depends upon the condition of the billabong just prior to the flush; a clear, non-turbid billabong will be muddied whereas a turbid one will be cleansed. Thereafter, for most billabongs, the Wet is a time of fluctuating clarity, depending primarily on the rate of flow through the billabong. At high flow periods, the tripton load in the creeks is usually high, markedly reducing billabong water clarity, but when flow is languid, a significant proportion of the tripton load may drop out and clarity improves. Back-flow billabongs such as Gulungul and Umbungbung, which are comparatively isolated from current flow, may experience annual clarity maxima during the late Wet.

In most billabongs, maximum clarity occurs at the Wet/Dry inter-change, when flow ceases, allowing sedimentation of the suspended load. In addition, at this time, the coincidence of the yearly minimum in wind strength, and maximum dry season water levels in the billabongs minimises wind-induced resuspension of bottom sediments. Phytoplankton biomass and gilvin are also low. Rapid deterioration in water clarity follows, primarily due to increasing turbidity, which has a reciprocal relationship with $z_{S.D.}$ (and z_{eu}). Thus small increases in turbidity at the time of maximum transparency result in dramatic declines in $z_{S.D.}$ and concurrent severe contraction of the euphotic zone. Further, near exponential rises in turbidity in the backflow and most floodplain billabongs during the mid to late Dry, mostly attributable to wind-disturbance of the sediments,

Table 6.1

Billabong	Turbidity (N.T.U.)	Gilvin (m^{-1})	Chlorophyll (μg/L)	$z_{S.D.}$(m) 'Wet'	$z_{S.D.}$(m) 'Dry'	z_{eu}(m) (measured)	Changes in z_{eu} over Dry
Bowerbird	0.3-30	0.07-0.33	0.9-4.3	1.6-4.0	3.2-74.9	3.8-6.9	Decreases
Noarlanga	1.2-8.8	0.02-0.80	1.8-10	0.85-1.5	1.5-3.5	3.4-5.4	Increases
Mudginberri	0.9-34	0.10-1.08	0.7-60	0.6-1.8	0.9-2.7	3.5-3.8	Decreases
Kulukuluku	1.3-6.5	0.32-0.93	2.6-25	1.5-2.3	1.1-2.1	3.6	Erratic
Nimbawah[1]	2.3-12	-	1.4-15.5	0.5-1.5	1.3-1.7	-	Erratic
Red Lily[1]	3-11.2	-	3-24	0.9-1.4	0.6-1.2	-	Erratic
Island	1.8-25	0.05-0.93	2.3-59	0.7-1.9	0.7-2.7	2.0-3.6	Erratic
Murganella Rd[1]	7-29	-	1.8-13.9	-	-	-	Erratic
Leichhardt	1.1-52	0.48-1.10	6.0-210	0.6-1.8	0.35-3.6	1.1-3.2	Decreases
Jingalla[1]	1.5-78	-	-	-	-	-	Decreases
Mine Valley[1]	3.7-82	-	-	-	-	-	Decreases
Ja Ja	2.0-140	0-1.68	4.0-44	0.6-3.5	0.05-3.9	1.0-2.0	Decreases
Goanna	7.0-300	0.4-1.30	7.3-141	0.25-0.9	0.05-0.7	0.4-1.4	Decreases
Umbungbung[1]	2.5-760	-	1.2-480	-	-	-	Decreases
Jabiluka	1.0-110	0.05-1.20	1.3-17.4	0.9-2.5	0.08-4.5	0.3-3.1	Decreases
Nankeen	1.3-250	0.27-1.63	1.8-86	0.5-2.0	0.03-2.05	1.0	Decreases
Gulungul	1.9-150	0.35-2.15	2.0-148	0.4-2.2	0.02-71.9	0.4-2.5	Decreases
Georgetown	12-230	0.18-2.80	4.6-55	0.2-0.8	0.02-0.7	0.6-0.7	Decreases

[1] Although these billabongs are not discussed in the body of the report, since they were never subject to investigation by quantum or quanta spectrometric equipment, relevant data is included for comparison. Seasonal trends in z_{eu} can be inferred from the $z_{S.D.}$ data.

Table 6.1 Some characteristics and related optical properties of Alligator Rivers billabongs.

but also influenced by wallowing buffaloes, may restrict the euphotic zone to 0.3 metres or less.

In Noarlanga, by contrast, water clarity improves after the Wet, with the euphotic depth maximal late in the Dry. This is due to both the steady reduction of turbidity and to lower gilvin values, which decline from their early Dry peak. For five non-turbid billabongs, no discernible trend in water clarity through the Dry is obvious.

Comparative data for a number of national and international lakes is given in Table 6.2. Comparison with Table 6.1 suggests that the billabongs encompass nearly all water types - non-turbid to very turbid, and oligotrophic to eutrophic (based on chlorophyll concentrations). The exceptions are that there is no very clear billabong at any time of the year (cf. Tahoe Lake) and gilvin concentrations are never high (cf. Sulphide Pool). Although the seasonal range of euphotic depth in the billabongs is often large, it does not approach that recorded for McConaughy Reservoir, Nevada, which varies within a thirty-four fold range (0.4-12.5, Table 6.2).

The strong correlation between Secchi transparency and euphotic depth indicates that the former, simple measurement can, if carefully carried out, give a fair indication of the depth of the euphotic zone. Various conversion factors, which set the photic depth at 2-5 times the Secchi depth, have been published (Bindloss, 1976). The commonly used relationship of Poole and Atkins, which gives the euphotic depth as 2.7 times the Secchi transparency, and which has been accepted as being generally applicable where detailed light profiles are unavailable (Idso & Gilbert, 1974), would be an overestimate for the Alligator River billabongs. There, $z_{eu} = 0.64 + 1.39\ z_{S.D.}$ so that the factor ranges between 1.5 and 2.0 for the depths of billabongs encountered. Rawson (1950) also found that the factor decreased as $z_{S.D.}$ increased.

Numerous authors have examined the relationship between light attenuation (indicated by Secchi transparency, vertical attenuation

Table 6.2

Lake	Turbidity (N.T.U.)	Gilvin (m^{-1})	Chlorophyll (ng/l)	$z_{S.D.}$ (m)	z_{eu} (m)	Source
L. Tahoe, California	-	-	-	19-38	55	Smith et al. 1973
L. Siikajarvi, Finland	-	0.45	1.9	6.5	10.2	Eloranta, 1978
Loch Leven, Scotland	-	0.4-1.2	0-240	0.2-3.8	1.2-7.4	Bindloss, 1976
Loch Neagh, N.Ireland	-	1.6-3.0	4-75	-	1.85-3	Jewson, 1977
55 Florida Lakes	1.1-30	0.18-25	1.4-87	0.22-6.15	-	Brezonik, 1978
McConaughy Res.Nebraska	-	-	-	-	0.4-12.5	Roemer and Hoagland, 1979
L. George, Uganda	-	-	263-1077	-	0.2-0.6	Ganf, 1974
Rust der Winter Dam,S .Africa	4.7-28	-	4.1-30.6	0.5-1.9	1.3-5.8	Walmsley et al., 1980
Lindeyspoort Dam,S.Africa	2.6-220	-	0.4-25.8	0.05-3	-	Walmsley, 1978
Roodeplaat Dam, S.Africa	-	-	4-477	0.4-6.9	0.7-10.4	Walmsley et al., 1978
L.Burley Griffin, A.C.T.	2.6-69	0.71-3.04	1.6-16.9	-	0.9-3.7	Kirk, 1977a; 1980a
Clyde River estuary, N.S.W.		0.28	2.2	-	6.5	Kirk, 1977a
Lake Tooms, Tas.	10-15	0.5	-	1.5-2	-	Croome & and Tyler, 1972
Sulphide Pool, Tas.	1.4-3.6	6.30-12.08	18-163	0.8-1.3	0.8-1.1	King and Tyler, 1981b; 1982b
L. St. Clair, Tas.	0.1-0.34	<0.38	-	9.3-13.3	8.7-12.0	Steane and Tyler, unpubl.

Table 6.2 Some characteristics and related optical properties of lakes from various parts of the world.

coefficient, or euphotic depth) and three parameters determining the extent of light penetration in natural waters - turbidity, water colour, and chlorophyll. A strong reciprocal relationship between $z_{S.D.}$ and turbidity has been often demonstrated (Brezonik, 1978; Walmsley, 1978; Walmsley et al., 1980). Water colour is also potentially a dominant attenuator (cf. Eloranta, 1978; King and Tyler, 1980; Kirk, 1976), and in some lakes chlorophyll absorption is highly significant (Bindloss, 1976; Ganf, 1974; Jewson, 1977). However, in situations where one parameter is normally the light attenuator, other parameters may become significant when the principal attenuator is in low concentrations (cf. Jewson, 1977). Thus, in the Alligator Rivers Region, though turbidity of surface waters is the principal light attenuator, gilvin may have some effect at low turbidities.

No relationship between $z_{S.D.}$ and chlorophyll could be demonstrated for the billabongs. This invalidates any use of the Secchi disk as an index of trophic status in the Alligator Rivers Region. Elsewhere, various indices have been developed (e.g. Brezonik, 1978; Carlson, 1977) to link transparency and trophic status, and large eutrophication programmes have been based upon the use of the Secchi disk by untrained personnel (Vollenweider, Shapiro et al. 1975). This approach has been severely criticised (Megard *et al.*, 1980) as frequently leading to wrong conclusions and inappropriate management strategies.

The billabongs are particularly characterized by the great contribution to absorption of light by the particulate materials. In the turbid waters, absorption is dominated by the tripton fraction. Visual examination of particulate fractions from these waters suggests that they are more organic in nature, and of a deeper brown hue, than particulate matter from water bodies in the southern tablelands of N.S.W. Hart & Thomas (1981) have shown that billabong sediments do indeed have a high organic

content. Although the specific absorption coefficients (absorption per unit mass) for this material have not been measured, it seems likely on the basis of its appearance, and of the ratios of β_{440} to nephelometric turbidity, that these coefficients in the blue region would be higher than those reported for water bodies in the southern tablelands (Kirk, 1980). The presence of such strongly absorbing particulate material in the waters of the billabongs is presumably determined in some way by the vegetation and soils of the catchment. In this regard the heavy macrophyte crops of the late Wet and early Dry may be of significance.

For seven billabongs in May, 1979, the average ratio of turbidity to the estimated scattering coefficient (b, m^{-1}) was 1.03±0.23, in agreement with the ratio of 1.09±0.14 obtained from a number of waters in the southern tablelands of N.S.W. (Kirk, 1981a; 1981b). This is despite the very different nature of the waterbodies concerned. In all seven billabongs, scattering increased the value of the vertical attenuation coefficient substantially beyond that expected on the basis of absorption alone. It should be realised that a given value of the scattering coefficient does not always produce the same increase in K_d. The more strongly coloured the water, the less the effect that scattering has; the photons tend to be absorbed before their angular distribution has been much altered by scattering. In Georgetown billabong, with a high concentration of (mainly particulate) colouring matter ($\beta_{440} + {}^{g}\beta_{440} = 20.0\ m^{-1}$). The very high scattering ($b \simeq 64\ m^{-1}$) approximately doubled K_d. In Lake George, N.S.W., on the other hand, a water body of roughly comparable turbidity but lower colour ($\beta_{440} + {}^{g}\beta_{440} = 4.5\ m^{-1}$), a somewhat lower scattering coefficient ($b \simeq 55\ m^{-1}$) increased K_d about three-fold (Kirk, 1981a).

The quantaspectrometric data show that, for most billabongs, not only is there severe attenuation of total PAR but also that there is strong selective attenuation of blue wavelengths. Thus, the prevailing underwater light climate is one of low intensity red light. The laboratory studies show that, except when turbidity was low, this preferential extinction of blue light results from absorbance by the tripton rather than the gilvin, and as such the greater the turbidity, the shallower the euphotic zone and the redder the light. Georgetown is the prime example of this condition. Only in the clearest billabongs, such as Bowerbird, does blue light penetrate to the same extent as the red.

Comparison of the quantaspectrometric data for Georgetown and Ja Ja, for example, with the scant data from elsewhere, suggests that the available PAR will always be red if the waters are turbid. Thus the Georgetown spectrum has the same characteristics as that for Tooms Lake, Tasmania (Fig. 6.1) and that for Lake Burley Griffin, A.C.T. (Kirk, 1979). Significantly, these spectra do not differ in any great way from the spectra for non-turbid, but highly coloured waters such as many in Tasmania (Fig. 6.2 and King & Tyler, 1981a, b; 1982a, b). In sharp contrast, non-turbid, non humic waters, such as the ocean and oligotrophic lakes, have a spectrum closer to that predicted by laboratory measurements of absorption coefficients for monochromatic light in pure water. Typically, in clear natural waters, the most penetrating wavelength is in the yellow, at about 580 nm, and the euphotic depth is considerable. This is shown by the data for Bateman's Bay (Kirk, 1979) and Lake St. Clair, Tasmania (Fig. 6.3; Table 6.2). Of the Alligator Rivers billabongs, only Bowerbird has this sort of spectrum (Fig. 4.2.3).

Inasmuch as ~~that~~ success in photosynthesis depends not so much on how much PAR is present but on how much can be absorbed by the pigment array of the phytoplankters, it seems logical that those species whose photosynthetic action spectrum has strong components in the red, will be more

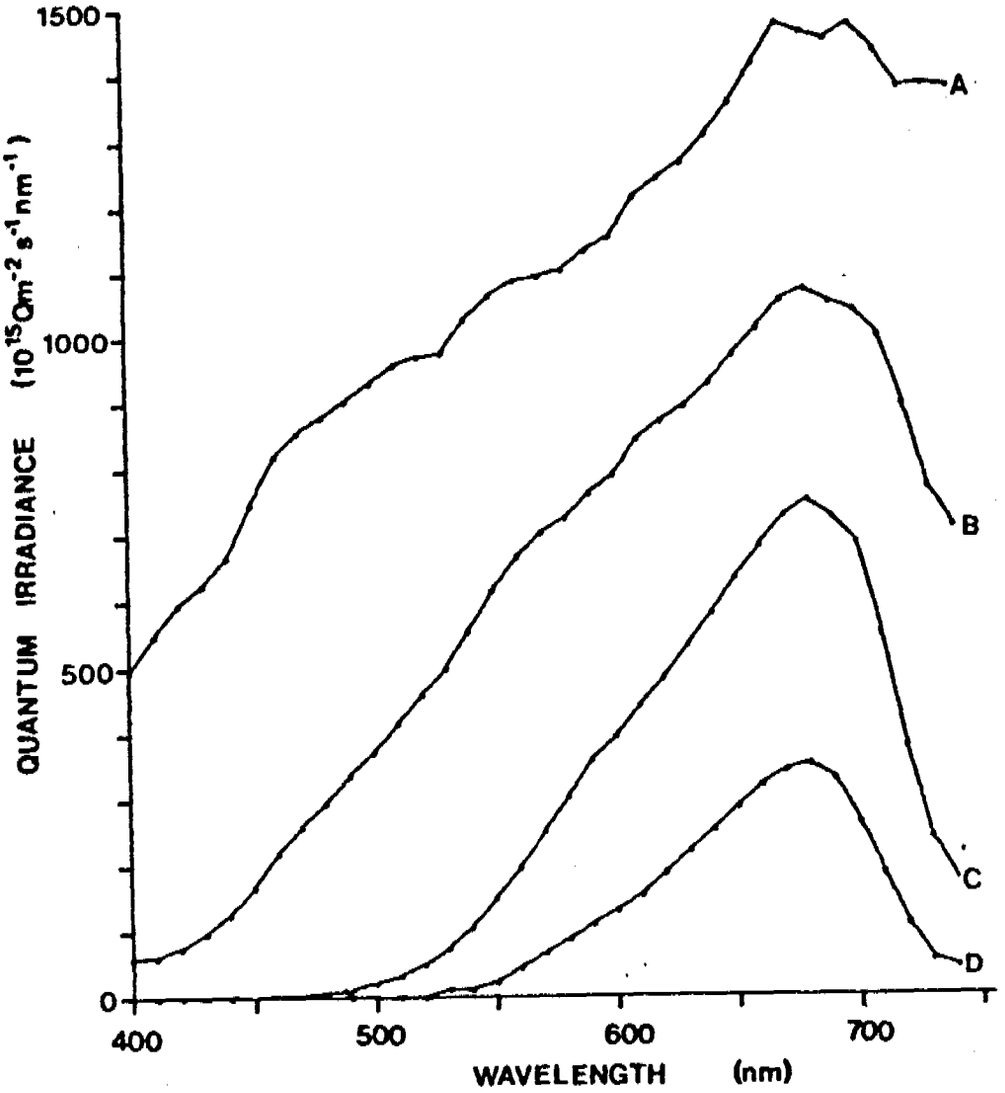

Fig. 6.1 *In situ* quantaspectrometric measurements at selected depths in Tooms Lake, Tasmania (source : Steane and Tyler, unpubl.).

A = 0.01 m AERIAL : 100 % Q_0

B = 0.2 m

C = 1.0 m : 7 % $Q_0 \approx Z_m$

D = 2.0 m. : 0.9 % $Q_0 \approx Z_{eu}$

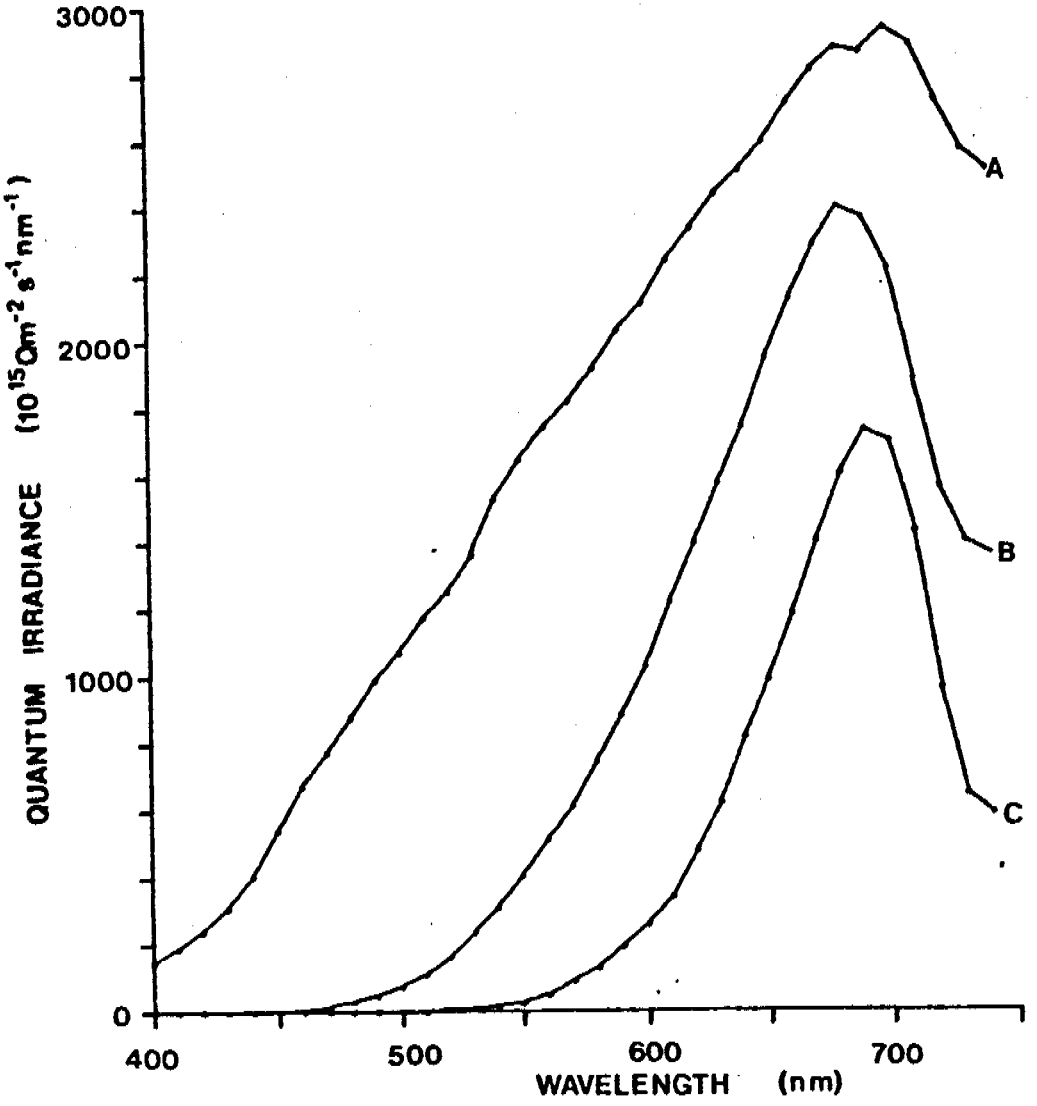

Fig. 6.2 *In situ* quantaspectrometric measurements at selected depths in ~~Lake Fidler~~ Sulphide Pool, Tasmania, (source: Bowling and Tyler, unpubl.).

A = 0.1m : 53% Q_0

B = 0.5m : 11% Q_0 ≈ 2m

C = 1.2m : 1% Q_0 = 2cm

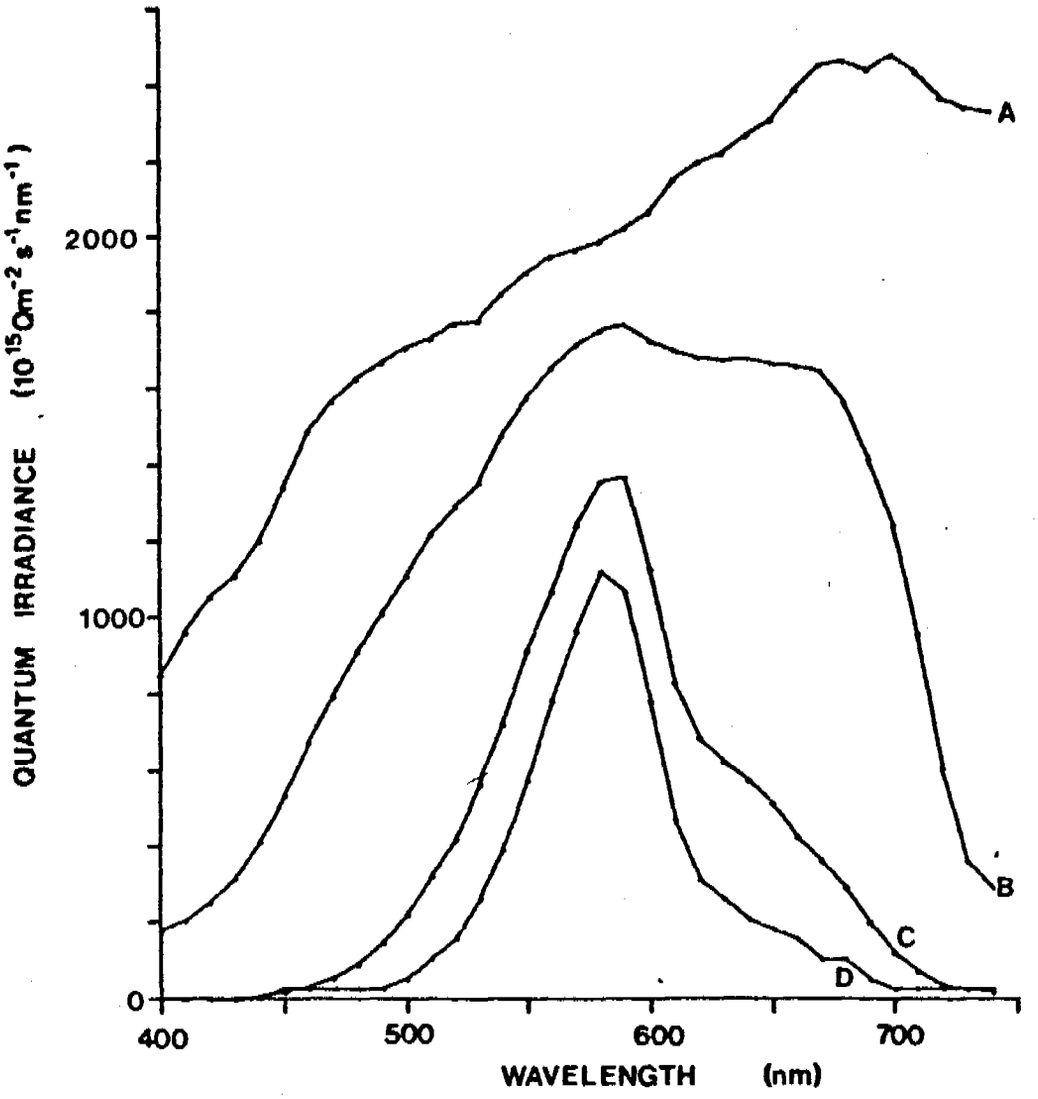

Fig. 6.3 *In situ* quantaspectrometric measurements at selected depths in Lake St. Clair, Tasmania (source: Steane and Tyler, unpubl.).

A = Aerial: 100% Q_0

B = 1.0 m : 63% Q_0

C = 6.0 m : 8% $Q_0 \approx Z_m$

D = 10.0 m : 0.82 $Q_0 \approx Z_{eu}$

successful in the turbid billabongs than those which lean heavily on the blue.

Acknowledgements

We thank Jill Kessell, Hugh King, Janet Waterhouse and Hank van der Wiele who, at various times, gave assistance in the field, and Lee Bowling, the late Michael Steane and Rosemaree Wickham who assisted in the laboratory. John Ferris wrote the computer programmes.

9. REFERENCES.

N.B. Underlining → Italics

Anon (1975). Standard Methods for the Examination of Water and Wastewater. 13th Ed. American Public Health Association.

Brezonik, P.L. (1978). Effect of organic colour and turbidity of Secchi disk transparency. J. Fish. Res. Bd. Can., 35, 1410-16.

Bindloss, M.E. (1974). The light climate of Loch Leven, a shallow Scottish lake, in relation ot primary production by phytoplankton. Freshwat. Biol., 6, 501-18.

Carlson, R.E. (1977). A trophic state index for lakes. Limnol. Oceanogr., 22, 361-369.

Cox, C.S. (1974). Refraction and reflection of light at the sea surface. *In* Jerlov, N.G. and Steemann-Nielsen (eds.): Optical Aspects of Oceanography. Academic Press, London.

Croome, R. and Tyler, P.A. (1972). Physical and chemical limnology of Lake Leake and Tooms Lake, Tasmania. Arch. Hydrobiol., 70, 341-354.

Eloranta, P. (1978). Light penetration in different types of lakes in Central Finland. Holarct. Ecol., 1, 362-366.

Ganf. G.G. (1974). Incident solar irradiance and underwater light penetration as factors controlling the chlorophyll content of a shallow equatorial lake (Lake George, Uganda). J. Ecol., 62, 593-609.

Halldal, P. and Halldal, K. (1973). Phytoplankton chlorophyll and submarine light conditions in Kings Bay, Spitsbergen, July 1971. Norw. J. Bot., 20, 99-108.

Hart, B.T. and McGregor, R.J. (1980). Flocculation of Retention Pond Water. Caufield Institute of Technology, Water Studies Centre, Technical Report No. 16. 8pp.

I.A.P.S.O. (1979). Sun Report. Prepared by working group on symbols, units and nomenclature in physical oceanography. 99p.

Idso, S.B. and Gilbert, R.G. (1974). On the universitality of the Poole and Atkins Secchi disk-light exctinction equation. J. Appl. Ecol., 11, 399-401.

Jeffrey, S.W. and Humphrey, G.F. (1975). New spectrophotometric equations for determining chlorophylls a,b,c, and c_2 in higher plants, algae, and natural phytoplankton. Biochem. Physiol. Pffanzen Bd., 167(5), 191-194.

Jerlov, N.G. (1970). Light. General introduction. In Otto Kinne (ed.) Marine Ecology : a Comprehensive, Integrated Treatise on Life in Oceans and Coastal Waters. Wiley-Interscience, New York.

Jerlov, N.G. (1976). Marine Optics. Elsavier Oceanography Series 14. Elsevier Sci. Publ. Co., Amsterdam.

Jewson, D.H. (1977). Light penetration in relation to phytoplankton content of the euphotic zone of Lough Neah, N. Ireland. Oikos, 28(1), 74-83.

King, R.D. and Tyler, P.A., (1981a). Limnology of Perched Lake, South-west Tasmania. Aust. J. Mar. Freshwater Res., 32, 501-15.

King, R.D. and Tyler, P.A., (1981b). Meromictic lakes of South-west Tasmania. Aust. J. Mar. Freshwater Res., 32, 741-56.

King, R.D. and Tyler, P.A. (1982a). Lake Fidler, a meromictic lake in Tasmania. Arch. Hydrobiol., (in press).

King, R.D. and Tyler, P.A., (1982b). Sulphide Pool and Lake Morrison, meromictic lakes of South-west Tasmania. Arch. Hydrobiol., (in press).

Kirk, J.T.O. (1975). A theoretical analysis of the contribution of algal cells to the attenuation of light within natural waters. New Phytol., 75, 11-20.

Kirk, J.T.O. (1976). Yellow substance (gelbstoff) and its contribution to the attenuation of photosynthetically active radiation in some inland and coastal south-eastern Australian waters. *Aust. J. Mar. Freshwater Res.*, 27, 61-71.

Kirk, J.T.O. (1977a). Use of a quanta meter to measure attenuation and underwater reflectance of photosynthetically active radiation in some inland and coastal south-eastern Australian waters. *Aust. J. Mar. Freshwater Res.*, 28, 9-21.

Kirk, J.T.O. (1977b). Attenuation of light in natural waters. Aust. J. Mar. Freshwat. Res., 28, 497-508.

Kirk, J.T.O. (1979). Spectral distribution of photosynthetically active radiation in some south-eastern Australian waters. Aust. J. Mar. Freshwater Res., 30, 81-91.

Kirk, J.T.O. (1980a). Relationship between nephlometric turbidity and scattering coefficients in certain Australian waters. Aust. J. Mar. Freshwat. Res., 31, 1-12.

Kirk, J.T.O. (1980b). Spectral absorption properties of natural waters : contribution of the soluble and particulate fractions to light absorption in some inland waters of south-eastern Australia. Aust. J. Mar. Freshwater Res., 31, 287-96.

Kirk, J.T.O. (1981a). A Monte Carlo study of the nature of the underwater light field in, and the relationships between optical properties of, turbid yellow waters. Aust. J. Mar. Freshwater Res., 37, 513-32.

Kirk, J.T.O. (1981b). Estimation of the scattering coefficient of natural waters using underwater irradiance measurements. Aust. J. Mar. Freshwater Res., 32, 533-9.

Kirk, J.T.O. (1981c). Light and photosynthesis in aquatic ecosystems. Proceedings 5th International Photosynthesis Congress (Greece, 1980). (in press).

Megard, R.O; Settles, J.C; Boyer, H.A. and Coombs, W.S. Jr. (1980). Light, Secchi disks, and trophic states. Limnol. Oceanogr., 25(2), 373-87.

Morel, A., and Prieur, L. (1977). Analysis of variations in ocean colour. Limnol. Oceanogr., 22, 709-22.

Rawson, D.S. (1950). The physical limnology of Great Slave Lake. J. Fish. Res. Bd. Can., 8, 1-66.

Roemer, S.C. and Hoagland, K.D. (1979). Seasonal attenuation of quantum irradiance (400-700nm) in three Nebraska reservoirs. Hydrobiologia, 63(1), 81-92.

Shapiro, J; Lundquist, J.B. and Carlson, R.E. (1975). Involving the public in limnology - an approach to communication. Verh. Internat. Verein. Limnol., 19, 866-74.

Smith, R.C; Tyler, J.E. and Goldman, C.R. (1973). Optical properties and colour of Lake Tahoe and Craker Lake. Limnol. Oceanogr., 18(2), 189-99.

Steane, M. (1979). Light penetration and stratification in Tasmanian lakes and reservoirs. Hons. Thesis, University of Tasmania.

Strickland, J.D.H. (1958). Solar radiation penetrating the ocean. A review of requirements, data and methods of measurement, with particular reference to photosynthetic productivity. J. Fish. Res. Bd. Can., 15(3), 453-93.

Talling, J.F. (1969). *In* Vollenweider, R.A. (Ed.). Primary Productivity in Aquatic Environments. Blackwell, Oxford.

Thomas, P.A. and Hart, B.T. (1981). Textural Characteristics and Trace Metal Concentrations in Billabong Sediments from the Magela Creek System, Northern Australia. Caufield Institute of Technology, Water Studies Centre, Technical Report No. 18. 38pp.

Walker, T.D., Waterhouse, J.,and Tyler, P.A. (1982). Thermal stratification and the distribution of dissolved oxygen in billabongs of the Alligator Rivers Region, Northern Territory. Office of the Supervising Scientist, Australian Government Publishing Service (in press).

Walmsley, R.D. (1978). Factors governing turbidity in a South African reservoir. Verh. Internat. Verein. Limnol., 20,1684-1689.

Walmsley, R.D., Toerien, D.F., and Steijn, D.J. (1978). An introduction to the limnology of Roodeplaat Dam. J. Limnol. Soc. Sth. Afr., 4(1),35-52.

Walmsley, R.D; Butty, M; Van der Piepen, H. and Grobler, D. (1980). Light penetration and the interrelationships between optical parameters in a turbid subtropical impoundment. Hydrobiologia, 70,145-157.

Welch, P.S. (1948). Limnological Methods. McGraw-Hill, New York.